# Oxford Brookes University

## PhD Thesis

**RADIATION-INDUCED CHROMOSOME INSTABILITY AND INTERCELLULAR COMMUNICATION: THE ROLE OF DOSE RATE AND IMPLICATIONS FOR CARCINOGENESIS**

Author:

Eman Mohammed Ahmed Elbakrawy

A thesis submitted in partial fulfilment of the requirements of Oxford Brookes University for the degree of Doctor of Philosophy

September 2017

# Acknowledgements

First and foremost all the praises and thanks be to Allah, the most beneficent, the most merciful, and peace be upon his Prophet Mohammad (PBUH). I would like then to thank the Egyptian government for funding my PhD project. I am also grateful to Oxford Brookes University and the Gray Institute for Radiation Oncology & Biology, University of Oxford, for providing all the high quality facilities used to undertake my project.

I would like to express my sincere gratitude to my supervisor, Professor Munira Kadhim, for her tremendous support, guidance and help during my PhD journey and allowing me to grow as a research scientist. As she always says, failure is not an option! I am also indebted to the Genomic Instability Research Group, in particular, Deborah Bowler and Kim Chapman for being a source of support as well as good advice and collaboration. A huge thank-you has to be extended to Dr Ammar Al-Mayah and Dr Scott Bright for the technical training and help from day one until I finished my project. In addition, I am very appreciative of Brittany Almond, Jessica Horsburgh and Raheem Al-Abedi for being such supportive colleagues.

I am very grateful to my second supervisor Dr Mark Hill (University of Oxford) for his great support, help and supervision during the course of my PhD and I thank him for his valuable comments and guidance. I am also indebted to his team, in particular Dr Jamie Thompson and Luke Bird for their help in experiments and general lab questions.

A huge thank-you has to go to all my friends for their continuous spiritual and practical support, and for being my family in Oxford. In no particular order, John Leake who is always my source of advice and help and my lovely brother in humanity. I really appreciate his endless guidance in different areas of life. Helen for her helpful suggestions and guidance in every aspect of living in Oxford. And Heidi Gastall, a wonderful and generous friend who has been through a lot with me and I am blessed to have you as a friend, hun! I have been learning a lot from you all, my lovely friends! Finally yet importantly, I would like dedicate this thesis to my beloved father's soul (blessed be his soul). Your prayers for me were what sustained

me this far! I would like also to express my sincere gratitude and appreciation to my family, in particular Mum for her continuous support and courage.

# Abbreviations

| Abbreviations | Description |
|---|---|
| AO | Acridine orange |
| ATM | Ataxia telangiectasia-mutated |
| BE | Radiation induced-bystander effects |
| BN | Binucleate cells |
| BSA | Bovine serum albumin |
| °C | Degrees Celsius |
| CBMN | Cytokinesis-block micronucleus assay |
| cGy | Centigray (1 centigray = 0.01 gray) |
| CHO | Chinese hamster ovary cell line |
| CIN | chromosomal instability |
| DDREF | Dose and dose rate effectiveness factor |
| $dH_2O$ | Distilled water |
| DHE | Dihydroethidium |
| DIOC6 | 3, 3′-dihexyloxacarbocyanine iodide |
| DMSO | Dimethyl sulfoxide |
| DNA | Deoxyribonucleic Acid |
| DPBS | Dulbecco's phosphate-buffered saline |
| DSBs | DNA double strand breaks |
| EDTA | Ethylenediaminetetraacetic |
| ERK | Extracellular signal-related kinase |
| FCS | Foetal calf serum |
| GI | Radiation induced-genomic instability |
| Gy | Gray |
| h | Hour |
| HDR | High dose rate |
| HR | Homologous recombination |
| ICCM | Irradiated cell conditioned medium |
| ICRP | International Commission on Radiological Protection |
| iNOS | Inducible nitric oxide synthase |
| IR | Ionizing radiation |

| Abbreviations | Description |
|---|---|
| KCl | Potassium chloride |
| LDR | Low dose rate |
| LET | Linear energy transfer |
| LNT | Linear-no-threshold |
| M | Molar |
| MAPK | Mitogen-activated protein kinase |
| MEM | Minimum essential medium |
| MEFs | Mouse embryonic fibroblast cells |
| MN | Micronuclei |
| mg | Milligram |
| mGy | Milligray |
| miRNA | MicroRNA |
| ml | Millilitre |
| mm | Millimetre |
| mM | Millimolar |
| mRNA | Messenger RNA |
| µg | Microgram |
| µl | Microlitre |
| µm | Micrometre |
| NaCl | Sodium chloride |
| NaOH | Sodium hydroxide |
| NPBs | Nucleoplasmic bridges |
| NHBE | Normal human bronchial epithelial |
| NHEJ | Non-homologous end joining |
| NHLF | Human lung fibroblasts |
| NTE | Non-targeted effects |
| nm | Nanometre |
| NO | Nitric oxide |
| NOS | Nitric oxide species |
| OH | Hydroxyl group |
| P | P-value |
| PBS | Phosphate buffered saline |
| PCR | Polymerase chain reaction |

| Abbreviations | Description |
|---|---|
| PD | Population doubling |
| PI | Propidium iodide |
| PO | Peroxidase |
| P53 | Protein 53 |
| qRT-PCR | Real-time reverse transcription polymerase chain reaction |
| RIGI | Radiation-induced genomic instability |
| RNA | Ribonucleic acid |
| ROS | Reactive oxygen species |
| RT | Room temperature |
| SBs | DNA single strand breaks |
| SCE | Sister chromatid exchanges |
| SDS | Sodium dodecyl sulphate-polyacrylamide running buffer |
| SEM | Standard error of the mean or the median |
| SOD | Superoxide dismutase |
| SR | Synchrotron radiation x-ray exposure |
| TBST | A mixture of 8 g NaCl, 2.4 g Trizma HCl, and 800 ml distilled water, then pH adjusted to 7.6 using HCl, 1 ml Tween 20 |
| TGF-β | Transforming growth factor-beta |
| TNF-α | Tumour necrosis factor-alpha |
| UV | Ultra-violet |
| v | Volts |
| v/v | Volume per volume |
| w/v | Weight per volume |

# Abstract

The biological risks associated with low dose and low dose rate (LDR) radiation exposures are not yet well characterised. Experimental studies indicate that in addition to biological effects resulting from direct DNA damage, a variety of non-DNA targeted effects (NTE) including radiation-induced genomic instability (RIGI), genomic instability being a known enabling characteristic of cancer, may crucially contribute to the overall outcome. RIGI can induce delayed mutations, chromosomal damage and micronucleus formation in the progeny of cells many generations after the original radiation event.

The work presented explores the role of dose and dose rate, as well as radiation quality, on RIGI. For low-LET x-rays, the induction of RIGI in normal primary human fibroblast (HF19) cells was investigated as a function of dose and dose rate and as a function of dose for high-LET alpha-particles. An additional aim was to investigate the potential role of reactive oxygen species (ROS), tumour necrosis factor-alpha (TNF-α) and transforming growth factor-beta (TGF-β1) in the induction of DNA damage and GI in HF19 cells following 0.1 and 1 Gy high dose rate (HDR) and low dose rate (LDR) x-ray irradiation. The x-ray data clearly show early DNA damage and RIGI many population doublings (PD) after exposure, not only after high dose and high dose rate exposures, but also at similar levels following low dose and low dose rate exposures. 0.1 Gy and 1 Gy LDR x-ray groups suggested more damage compared to the corresponding HDR groups. However, at 20 PD the HDR groups suggested higher induction of DNA damage compared to the equivalent LDR x-ray irradiation groups. A higher induction of ROS following 0.1 and 1 Gy LDR and HDR x-ray was also demonstrated providing a potential mechanism for induction of DNA damage and RIGI.

The alpha-particle results indicate significant induction of early DNA damage and RIGI at 10 and 20 PD at doses down to 0.001 Gy, reducing at lower doses. At these low doses, not all cells would be traversed, but those that were traversed would receive significant energy deposition by the traversing particle. To conclude, our investigations have demonstrated that HF19 cells are susceptible to the induction of early DNA damage and RIGI, not only after a high dose and high dose rate exposure to low LET and high LET, but also following low dose, low dose rate exposures. The

results suggest that the mechanism of radiation induced RIGI in HF19 cells can be correlated with the induction of ROS levels following exposure to 0.1 and 1 Gy LDR and HDR x-ray irradiation.

# Table of Contents

# Table of Figures

# Table of Tables

# Chapter 1.
# Introduction

## 1.1 Ionising radiation

Ionising radiation (IR) is ubiquitous in our surroundings; it can come from cosmic rays, the food we eat, the air we breathe, the buildings we live in, and the Earth we live on (Hughes *et al.*, 2005). In addition, people can receive radiation from diagnostic procedures and medical x-rays (Hughes *et al.*, 2005). Ionising radiation was discovered at end of the 19th century and since that time has been used extensively in cancer treatment (Brenner, 2012). However, despite claims that IR cures more than half of cancer patients when used in radiotherapy treatment, it is well known that it can also cause cancer. Therefore, IR has been considered a double-edged sword and the extent of its full effects and its mechanism of action are still controversial (Brenner, 2012). Despite the fact that people are exposed every day to various types of low-dose radiation, little is known about the biological impacts of these low exposures. One of the methodologies towards fully understanding these impacts on human health is by examining the biological impacts of low-dose radiation through experimental studies (Rühm *et al.*, 2015).

Ionising radiation is highly energetic (sufficient energy to ionise an atom), and causes changes to the structures of biological samples due to the deposition of energy in those structures. IR includes sparsely ionising electromagnetic radiation (x- and gamma-rays) and densely ionising radiation (α-alpha- particles). Both sparsely and densely IR characteristics are based on the average energy transfer per unit length of track (LET: linear energy transfer) (Hall and Giaccia, 2006; Kadhim, 2003). Low LET radiation is composed of photons and has scattered, sparse energy deposition patterns due to its winding path in biological samples. In comparison, high LET radiation (for example, neutrons, alpha-particles, protons and other heavy, charged particles) produces an insult comprising a relatively small number of densely ionising, straight tracks which leads to a dense energy deposition path (Shikazono *et al.,* 2009). Exposure to naturally occurring radioactive Radon gas and its resulting alpha-particle emitting progeny dominates human exposure and is now known to be the second largest cause of lung cancer after smoking (BEIR VI, 1999).

Ionising radiation can directly or indirectly interact with biological specimens and living tissue. Direct IR interaction refers to the interaction of IR with cellular components such as DNA molecules or proteins directly, instigating chromosome damage, mutation and cell death (Hall and Giaccia, 2006; Nais, 1998; Scully and Xie, 2013). However, indirect interactions of IR are explained by interactions with cellular water molecules, producing free radicals (highly reactive atoms or molecules with a single unpaired electron). These free radicals can interact with DNA and other macromolecules leading to cell damage (Hall and Giaccia, 2006; Lehnert and Iyer, 2002).

In addition to conventional radiation-induced effects (chromosome damage, mutation and cell death), IR also induces genomic instability (GI) which is defined as an increased rate of accumulation of genomic alterations, which may appear at delayed time-points in the progeny of the irradiated cells. These alterations include ongoing new changes in chromosomes, gene mutations and enhanced cell death (Kadhim *et al.,* 2013). These responses are one of the most prominent enabling characteristics of cancer (Hanahan and Weinberg, 2011).

## 1.2 Low LET and high LET radiation

Ionising radiation is divided into two types according to the density of ionisation: low and high LET emissions. It has long been known that high LET irradiation has a greater biological impact compared to low LET (for the same absorbed dose), with a wide variety of biological effects. This difference between low and high LET is mainly due to the radiation track structure deposited over a biologically relevant scale (Goodhead, 1999). Low LET forms of radiation are composed of photons (for example x-rays or gamma-rays) and have scattered, sparse energy deposition patterns leading to isolated lesions. In comparison, high LET radiation forms (for example neutrons, alpha-particles, protons and other heavy, charged particles) produce an insult comprising a relatively small number of densely ionising, straight tracks which lead to a dense energy deposition path. As a result clustered damage would be produced as shown in figure 1.1 A (Shikazono *et al.*, 2009). High LET particles induce damage in DNA molecules in a number of positions when the ionising tracks traverse the interphase chromatin of 30 nm fibre and large and bigger loop structures.

This can induce a greater induction of DNA fragments across a large number of bases (≈0.1 kbase-Mbase). The overall number of double-strand-breaks (DSBs) produced per unit dose of high and low LET irradiation has a low dependency on the type of LET due to the balance between the number of particles and the elevation of the local ionisation density. However, the degree of DSB complexity rises with increasing LET (Goodhead, 1999). For example, 70 % of DSBs produced by high LET contain three or even more breaks (Goodhead and Nikjoo, 1997). This induction of complex DNA damage shows the relationship between the LET and the resulting biological effects. The more complex the components of the initial damage, the more severe final biological damage appears due to the less rapid working of the cell's repair system. Thus the deposition of high LET radiation in cells results in a greater number of unrepaired DSBs (Delara *et al*., 1995). The difference in the structure of the track of high and low LET is not only restricted to the DNA scale but it is also significant at the cell and tissue scale as well. With low LET radiation (e.g. x-ray), the energy of 1 Gy is delivered as sparsely ionising tracks with approximately 1000 tracks/cell, homogeneously distributed across the cell, and all cells receive the same dose of radiation. This produces approximately 20 – 40 DSBs and 20 % complex DSBs (figure 1.1). When reducing the dose to less than 1 mGy, all cell populations are irradiated with a decreased energy/dose. However, the high LET (alpha particles) has a heterogeneous energy deposition pattern with a highly densely ionising track. 1 Gy high LET produces approximately 3-4 ionising tracks (dependent on cell morphology) leading to approximately 30-40 DSBs and 70 % complex DSBs (figure 1.1) (Kadhim *et al.,* 2006). Additionally, high LET alpha-particles induce more GI/chromosomal instability in mouse and human bone marrow cells compared to x-ray at an iso-effective dose killing (Kadhim *et al*., 1992; Kadhim *et al.*, 1994).

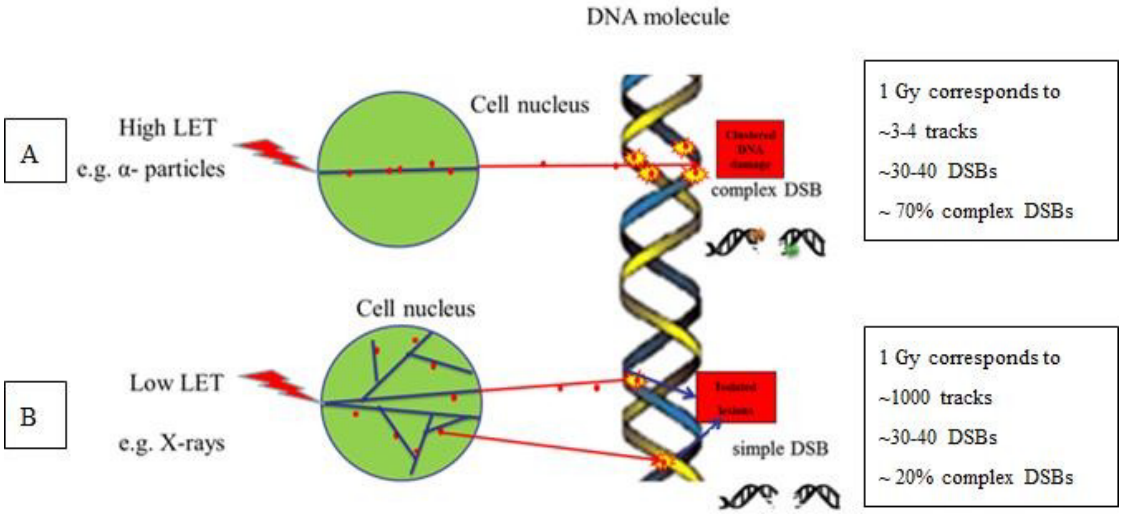


Figure 1.1: Schematic of high and low LET ionising radiation tracks through a cell nucleus. [**A]** represents the tracks of high LET radiation such as alpha -particles. [**B]** displays the tracks of low LET radiation such as gamma rays or x -rays. Adapted from Kadhim *et al.* (2006).

For example, exposure to 2.5 Gy from either $^{56}$Fe or $^{28}$Si charged particles (high LET radiation) causes greater prolonged defects in the proliferation and the contribution of club progenitor cells to the maintenance of the airway epithelium than the relative equivalent 5 Gy of low LET gamma-rays (McConnell *et al.*, 2016). This understanding of the difference in the damage induced following exposure to high and low LET radiation is crucial for therapeutic development (heavy-ions) and risk assessment of tissue damage following radiation exposure or radiotherapy (McConnell *et al.,* 2016). Recently, Werner *et al*. (2017) have stated that high LET (heavy-ions) was more effective compared to low LET (x-ray) at induction of micronucleus formation, a marker of genomic instability. Micronucleus induction levels in mouse bronchial epithelial cells receiving 1 Gy were higher in the progeny of cells irradiated with heavy- ions (nucleon iron, nucleon silicon, and oxygen heavy ions) compared to x-ray irradiated cells at 7 days following irradiation (Werner *et al.,* 2017).

## 1.1 Biological Effects of Ionising Radiation

### 1.3.1 Classical radiation biology dogma

The classical dogma in the radiobiology field affirms that the biological effects of radiation are due to the deposition of radiation energy in the cell nucleus (Morgan, 2012). The biological effects of IR can be either due to direct interaction between IR and DNA or due to indirect interaction through radiolysis products (Hall and Giaccia, 2006; Scully and Xie, 2013). These ROS are a number of reactive molecules and free radicals derived from water molecules, most notably the OH radical which has a diffusion distance of ≈4nm within the reactive environment of the cell, as shown in figure 1.2 (Roots and Okada, 1975). Thus, all types of ionising radiation induce single-strand breaks and single-base damage (Goodhead, 1999). Clustered DNA damage is produced even with low LET irradiation as a result of the nearby cluster of ionisations produced from many low energy secondary electrons (e.g 0.1-1 keV). Thus, DNA DSBs can be produced due to direct or indirect (nearby OH) ionisation or a combination of direct and OH ionisations. However, the level of DSB complexity significantly increases with LET (Goodhead, 1999). Thus, the biological consequences are unchanged through one or two cell generations/population doublings (Sawant *et al.*, 2002). According to this theory, IR can produce DNA damage during irradiation or immediately after irradiation (Ward, 1999; Ward, 2002). Since radiation deposits its energy along highly structured tracks, the resulting patterns of ionisation and excitation events are highly efficient at producing correlated sites of damage to DNA. Radiation, therefore, not only produces single-strand- breaks (SSB) or base damage but combinations of these within a few base pairs, leading to the production of not only DSBs but also complex SSBs (SSBs which have additional base or strand breaks) (Bohm *et al.*, 2010).

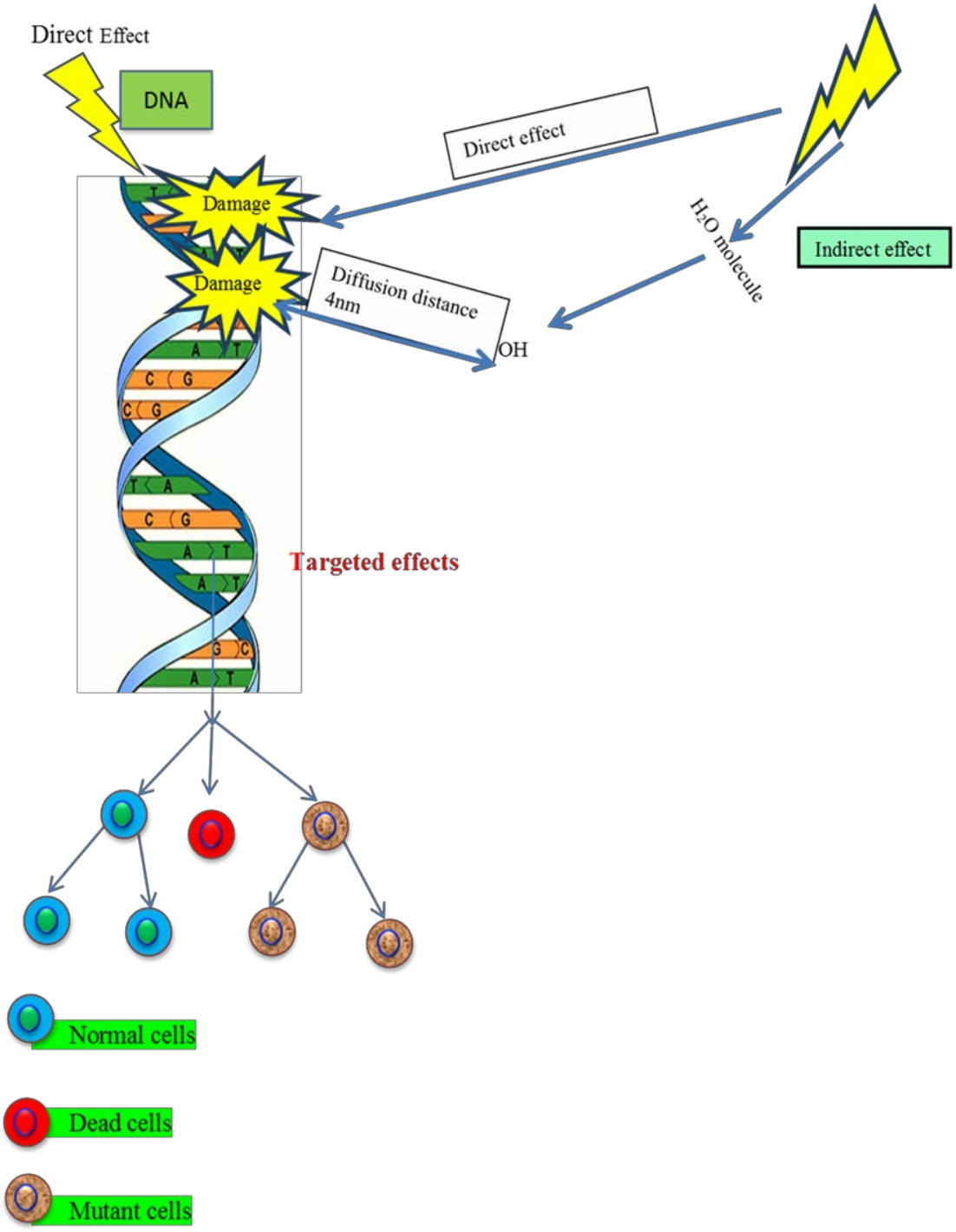


Figure 1.2: Targeted effects of ionising radiation. Targeted effects of IR can be induced directly or indirectly. Direct effects are caused when the IR hits the DNA directly, whilst the indirect effects occur when the IR interacts with water molecules leading to the production of free radicals, which then can lead to DNA damage. Adapted from Kadhim and Hill (2015) and Hall and Giaccia (2011).

### 1.3.2 Non-targeted effect of ionising radiation

In the last two decades, there has been a shift in the classical paradigm describing IR effects. Much evidence has demonstrated that radiation can also induce non-targeted effects which include genomic instability (GI) (figure 1.3) and bystander effects (BE) (figure 1.4) (Morgan, 2012; Kadhim *et al.*, 2013; Kadhim and Hill, 2015). GI is thought to be a critical step in the onset and progression of cancer (Kadhim *et al.*, 1992; Kadhim *et al.*, 1994; Hanahan and Weinberg, 2011).

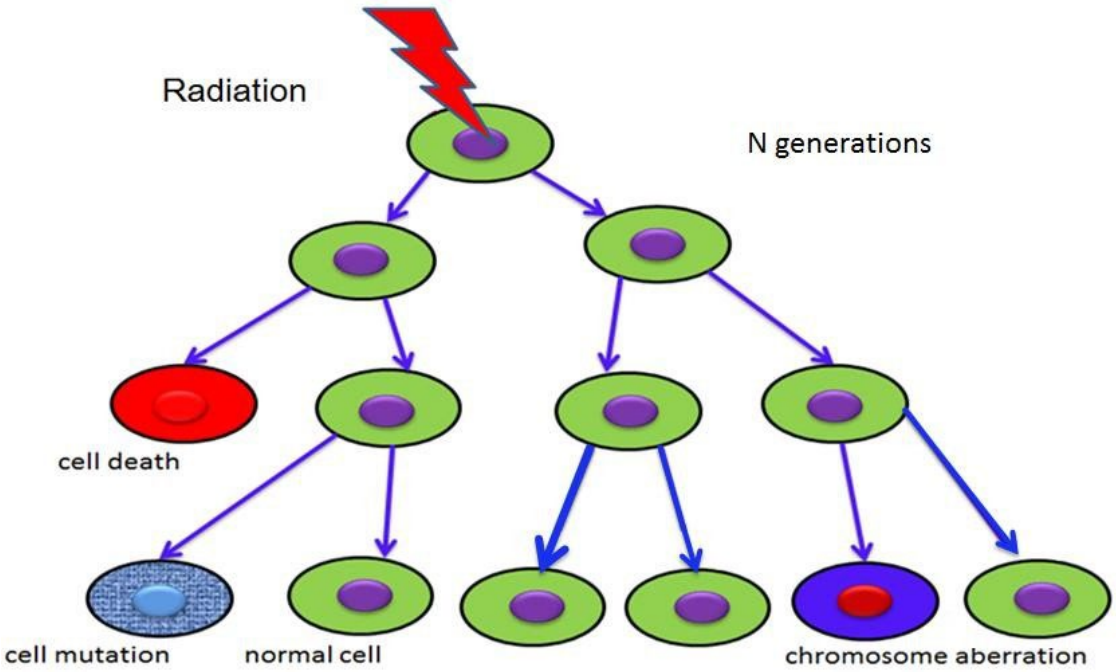


Figure 1.3: A schematic diagram illustrating the process of radiation-induced genomic instability. The progeny of irradiated cells, showing delayed chromosomal instability, mutations, and cell death. Adapted from Kadhim and Hill (2015).

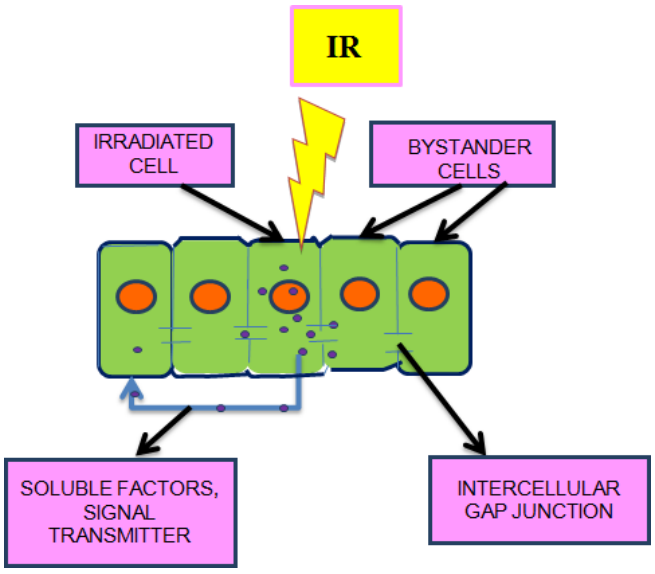


Figure 1.4: A schematic diagram showing bystander effects (BE) through both intercellular gap junction and soluble factors. The deleterious effects of radiation are found in cells that have not been irradiated but are in the vicinity of the irradiated cells. Adapted from Lam *et al.* (2015).

### *1.3.2.1 Genomic instability (GI)*

Radiation-induced GI can be defined as an increased tendency to develop alterations in the genome during the life cycle of the cell following radiation. When IR passes through biological tissue, some progeny of the surviving irradiated cell population exhibit delayed and transmissible GI responses as shown in figure 1.2 (Morgan, 2012). These responses (instabilities) are manifested as chromosomal alterations, changes in a number of sets of chromosomes, micronucleus formation, gene mutations and amplifications (Morgan *et al.*, 1996; Wright, 1998; Little, 2000; Kadhim *et al.*, 2013).

There are several factors which influence the induction of GI; these include genetic predisposition, cell type and radiation quality. Several studies have concluded that the relationship between GI response and genetic background might be due to the modification of proteins responsible for conserving genomic integrity or changing oxidative metabolism (Kadhim, 2003). Furthermore, it has been shown that the rate at which a radiation dose is delivered has an important effect on the induction of GI at late cell division. For example, micronucleus (MN) formation was used to measure the DNA damage after 7 days in both high and low dose rate irradiated mouse

lymphocytes cells. The frequency of micronucleus induction in the high dose rate population cells was higher compared to the equivalent low dose rate population cells following *in vivo* exposure to 0–4.45 Gy x-rays (Turner *et al.*, 2015).

Baverstock has suggested that due to the observed high frequency of instability and the deficiency of sharp proof of participation of DNA double-strand-breaks in the initiation of instability, it could rather be due to the modification in the expression leading to a disruption in cellular homoeostasis (Baverstock, 2000). Additionally, chromosome instability can be induced by complex cytokine-like signal transduction processes within the progeny of the surviving irradiated cells (Moore *et al.*, 2005; Natarajan *et al.*, 2007). Morgan has also hypothesised that deposition of radiation in DNA starts a series of genomic events which can lead to an increased rate of mutation and chromosomal changes in the progeny of irradiated cells that survived the initial radiation insult. Although the multiple phenotypes which result from irradiation are comparatively well characterised, the molecular, biochemical and cellular events that initiate and sustain instability remain unknown (Morgan, 2012). Genomic instability can be produced by the traversal of the cell by only a single alpha-particle track (Kadhim *et al.*, 2001). Kadhim *et al.* (2001) have observed a significant elevation in formation of aberrant cells in immobilised human T- lymphocytes at 12-13 population doublings following high LET irradiation using microbeam technology (Kadhim *et al.*, 2001). Limoli *et al.* (1997) have observed that the DNA lesions do not necessarily result in chromosomal instability. However, the complexity or quality of DNA SBs plays a significant role in initiating this phenotype (Limoli *et al.*, 1997). On the other hand, Azzam's studies have shown that genetic damage can be exhibited not only in directly irradiated cells but also other cells in their vicinity (Azzam *et al.*, 2001).

#### *1.3.2.1.1* In vivo *evidence*

Radiation-induced genomic instability has been observed *in vivo* (Watson *et al.*, 2000). A significant induction of chromosome aberrations in the haemopoietic system of CBA/H mice was observed at 24 months following a whole body exposure to high (neutron) and low (x-ray) LET irradiation (Watson *et al.*, 2001). Watson *et al.* (2000) reported the first evidence of *in vivo* chromosomal instability induced by a bystander mechanism. A mixture of irradiated and labelled un-irradiated bone marrow cells of

CBA/H mouse transplanted into female recipients displayed a significant induction of chromosome aberrations in the labelled un-irradiated cells (Watson *et al.*, 2000). Numerous studies have reported that whether *in vivo or in vitro* (animal or human) the expression of GI in irradiated cells depends on their genotype (Kadhim *et al.*, 1994; Ponnaiya *et al.*, 1997; Watson *et al.*, 1997). Moreover, radiation-induced chromosomal instability (CIN) (dicentric or centric chromosomes and micronuclei) was observed by Tanaka *et al*. (2008). The induction of micronuclei in spleen and bone marrow cells were shown after continuous gamma-ray exposure at dose rates of 20 mGy/day to 200 mGy/day, with differences in the level of micronucleus formation observed between dose rates (Tanaka *et al.*, 2008). Additionally, Salomaa *et al*. (1998) have observed an increase in chromosomal instability in long-term cultures (lymphocytes) of donors after a whole body exposure to gamma-ray $^{137}$Cs with different doses and dose rates (3, 1, 0.5 Gy) (Salomaa *et al.*, 1998).

IR and a number of chemical mutagens can induce the phenomenon of transgenerational GI which can be defined as an increase in the induction of instability in the nonirradiated offspring of irradiated parents that may affect offspring's mutation rates (Dubrova, 2003). The induction of instability due to exposure to IR in the germline of irradiated parents could affect offspring mutation rates, cancer predisposition and other characteristics (Morgan, 2003). Koturbash *et al*. (2006) have observed transgenerational GI in the thymus tissue of the offspring following combined parental exposure. The offspring revealed profound changes in DNA methylation and a significant accumulation of DNA SBs in thymus tissue which in turn could result in GI and serve as a precursor for transgenerational carcinogenesis (Koturbash *et al.*, 2006).

Additionally, exposure to low doses and low dose rates of IR could lead to transgenerational GI. Suman *et al*. (2017) have found that exposure to clinically relevant low doses of x-ray induced transgenerational intestinal tumorigenic effects in mice (6 to 8 weeks old APC$^{1638N/+}$). This was observed in the offspring of male and female direct parent irradiated groups and male parent irradiated groups (25 cGy x-ray irradiation) (Suman *et al.*, 2017). Grygoryev *et al*. (2013) have studied the effect of transgenerational exposure to low dose rate (2.4 and 21 mGy/day) gamma-ray irradiation in the liver and muscle tissue of the Japanese medaka fish. An

increase in the level of unrepaired 8- hydroxyguanine and DSB in muscle and liver tissue was observed over four generations with different patterns based on the radiation dose rates. This suggests that the initial exposure to radiation generates GI as the generations progress (Grygoryev *et al.*, 2013).

### *1.3.2.2 Biological implications of genomic instability*

The best definition of the stochastic delayed effects of IR is the multi-step processes that lead to carcinogenesis (Fearon and Vogelstein, 1990). Many experiments have demonstrated that cancer develops through a long series of mutation steps including colorectal cancer (Fearon and Vogelstein, 1990). The increase in delayed effects of ionising radiation can lead to an increase in GI, which is believed to be the most distinct enabling characteristic of cancer (Hanahan and Weinberg, 2011). Moreover, GI phenomena can increase the mutation frequency, which can lead to a second or third mutation in an individual. Although the mutation frequency is often very low even following irradiation, GI would enhance the multi-step process of mutation by a factor from 10 to 10,000 (Pichierri *et al.*, 2000). The individual who has a genetic predisposition to increased radiosensitivity has been shown to have a higher cancer risk associated with GI (Pichierri *et al.*, 2000). In order to estimate and understand the delayed stochastic effects of IR in general and the mechanism of carcinogenesis in particular, a thorough assessment of the mechanisms of how GI is elicited after radiation exposure is required (Streffer, 2000).

### *1.3.2.3 Mechanisms of GI*

Some studies have suggested a number of mechanisms involved in the induction of GI. These include epigenetics and inflammation, in addition to factors such as microRNAs and reactive oxygen species (Fenech, 2006; Aypar *et al.*, 2011; Filkowski *et al.*, 2010). For example, the biological changes associated with GI could be due to epigenetic factors that include changes in DNA methylation, RNA-associated silencing and histone modification (Kovalchuk and Baulch, 2008). The deficiency in DNA methylation and its mediators could lead to misregulation of multiple cell cycles, silencing of tumour suppressor genes, and changes in DNA repair and chromosome stability genes. These changes are eventually involved in GI induction of various human diseases, including cancer (Meng *et al.*, 2015). Several studies have investigated the possibility of DNA methylation being involved in the

mechanism of GI induction (Kovalchuk and Baulch, 2008; Kovalchuk *et al.*, 2004; Gaudet *et al.*, 2003). Dodge *et al*. (2005) have observed that DNA hypomethylation in mouse embryonic fibroblast cells (MEFs) due to the Dnmt3b-deficiency revealed an increase in chromosomal breaks, aneuploidy, polyploidy and fusions. These findings suggest that GI could be induced by the DNA hypomethylation which in turn results in spontaneous immortalization or premature senescence of Dnmt3b-deficient MEFs (Dodge *et al.*, 2005). The changes in DNA methylation and accumulation of DNA SBs in offspring of combined parental radiation exposure can also induce transgenerational GI in the thymus tissue. This, in turn, could result in GI and could serve as a precursor for transgenerational carcinogenesis (Koturbash *et al.*, 2006). Other studies performed by Kaup *et al*. (2006) indicated the persistence of dysregulation of CpG methylation in the surviving progeny of a human keratinocyte cell line, up to 20 population doublings following irradiation. This was observed from both directly and bystander irradiated cells, using an arbitrarily primed methylation sensitive PCR (Kaup *et al.*, 2006). Additionally, Holm *et al.* (2016) have reported that aberrant methylation in subsets of basal-like breast cancer can lead to the induction of GI (Holm *et al.*, 2016). Moreover, Mauro *et al*. (2016) have observed the persistence of methylation changes in V79 cells and human HaCaT keratinocytes for many cell generations in the absence of further arsenic treatment following an initial arsenic exposure. These DNA methylation changes most likely contribute to long-lasting arsenic-induced GI (Mauro *et al.*, 2016).

The process of inflammation can also be involved in radiation-induced GI. There is much evidence relating to the inflammatory responses, which occur post irradiation. These include macrophages that are activated and secrete cytokines that cause non-targeted effects (Mukherjee *et al.*, 2013; Lorimore *et al.*, 2008; Lorimore *et al.*, 2011). Lorimore *et al.* (2011) have suggested that inflammation can play a role in mediating and sustaining the effects of IR and the induction of GI in bone marrow cells. The bone marrow cells showed an increase in the induction of chromosomal instability at 1 hour and for up to 3 months following exposure to 4 Gy gamma-ray whole body irradiation (Lorimore *et al.*, 2011). Gudkov *et al.* (2011) have stated that the chronic inflammation, which is commonly observed in various tissues of older mammals results in general suppression of p53 function. This would help in understanding the increased risk of cancer detected in ageing animals and humans

(Gudkov *et al.*, 2011, p.53). Additionally, adding the inflammatory cytokines (IL-1β, IFN-γ and tumour necrosis factor alpha (TNF-α)) to three human cholangiocarcinoma cell lines (*in vitro*) produces ROS which in turn lead to the generation of nitric oxide (NO) in inflamed tissues by inducible nitric oxide synthase (iNOS). These findings indicated that activation of iNOS and the increased NO production in response to inflammatory cytokines caused DNA damage and inhibited global DNA repair activity by 70 % (Jaiswal *et al.*, 2000). Lorimore *et al.* (2008) found that IR induced chromosomal instability as a consequence of proinflammatory cytokine signalling. A macrophage (which secreted a major proinflammatory cytokine TNF-α) obtained from the bone marrow of the whole body irradiated CBA/Ca mice (4000 mGy gamma irradiation) displayed a high induction of chromosomal instability (Lorimore *et al.*, 2008). Proinflammatory cytokines (TNF-α) at certain concentrations which are not cytotoxic could play a role in the initiation of genomic instability through free radical generation following exposure to 0.1, 1 or 2 Gy low LET irradiation (Natarajan *et al.*, 2007). Recently, Usman *et al.* (2017) observed that chronic inflammation in a childhood obesity, case–control study in a cohort of obese and healthy weight 11–15-year-olds, could generate a harmful microenvironment that in turn caused damage to the DNA (Usman *et al.*, 2017). There is also much evidence relating to oxidative stress as a causative agent of radiation- induced GI (RIGI) (Clutton *et al.*, 1996; Limoli and Giedzinski, 2003; Limoli *et al.*, 2003). The persistent generation of ROS has been observed in cells for days and months following irradiation (Petkau, 1987). The major cellular sources of ROS associated with RIGI are the mitochondria. These ROS inductions can induce single or double-strand breaks of the DNA backbone as they contain an unpaired electron and are extremely reactive. Therefore, this damage may result in loss of fundamental genetic information if not properly repaired (Cooke *et al.*, 2003). Wei *et al.* (2015) have reported that ROS induced inflammation in hematopoietic stem and progenitor cells. These ROS are related to insulin resistance and hyperglycemia in the bone marrow microenvironment that generate genomic instability and activation of adaptive oncogenic pathways in the cells (Wei *et al.*, 2015). The low-dose fractionated radiation with 0.01 Gy/fraction or 0.05 Gy/fraction x-ray for 31 days exposure is able to induce an increase in mitochondrial ROS and a reduction in cellular levels of the antioxidant glutathione in normal human fibroblast cells. The excess of ROS resulted

in disruption of normal negative feedback control of AKT/cyclin D1 signalling which in turn led to growth retardation, cellular senescence and genomic instability in low-dose fractionated irradiated cells (Shimura *et al.*, 2016).

#### *1.3.2.4 Bystander effects (BE)*

Radiation-induced bystander effects is the phenomenon where the biological effects occur in cells that are not hit directly by radiation but communicate with irradiated cells through gap junction communications and/or secreted signals (bystander signals) from neighbouring irradiated cells (Figure 1.4). Bystander effects would magnify the biological impact of the radiation dose given, which can lead to DNA damage, GI, chromosome mutation and cell death. BE indicate that the IR effects are greater than those present in directly irradiated cells because they encompass a cluster of cellular responses in cells that are not hit directly by radiation (Morgan, 2012; Kadhim *et al.*, 2013). Several studies have demonstrated that the important feature of BE is the rise in the effects at low IR doses with little or no uplift at higher IR doses (i.e. plateau-type dose responses) (Goodhead, 2010).

Morgan has reported that understanding of non-targeted effects is still in its infancy mainly because the majority of information we have obtained are from *in vitro* studies. Moreover, the significant impact of non-targeted effects on human health is still to be explained (Morgan, 2012). The BE are a vital factor in radionuclide therapy as in addition to direct damage of radiation to target cells, BE occur in non-hit neighbouring cells. Therefore, healthy cells can also express some radiation-induced damage. There is still little knowledge about the assessment of whether and to what extent BE are involved in radiation-induced damage in the human organism (Widel, 2017).

#### *1.3.2.5 The mechanisms of BE*

The main factors that induce BE in non-irradiated cells are types of cellular communications. BE are thought to occur as a result of receiving signals from irradiated cells via gap junction communications or by soluble diffusible factors, which are predominant in sparsely populated cultures (Widel, 2016; Al-Mayah *et al.*, 2015; Marín *et al.*, 2014; Butterworth *et al.*, 2011; Boyd *et al.*, 2006).

These types of communications induce transmissible signals that are produced by irradiated cells, including reactive oxygen species (ROS) (Kashino *et al.*, 2007), nitric oxide species (NOS)(Shao *et al.*, 2006) and cytokines (Banaz-Yasar *et al.*, 2008) that can migrate to bystander non-irradiated cells either through media (Lehnert *et al.*, 1997; Mothersill and Seymour, 1998) or gap junctions (Azzam *et al.*, 1998; Azzam *et al.*, 2001). Hei has suggested that irradiated cells generate cytokines and prostaglandin E2 which eventually play a vital role in activating signalling pathways (Hei *et al.*, 2011).

Furthermore, recent studies suggested that microvesicles and exosomes are involved in radiation-induced bystander signalling (Al-Mayah *et al.*, 2012; Jella *et al.*, 2014). Production of ROS, reduction in cell viability and calcium influx were observed after the addition of irradiated cell conditioned medium (ICCM) to unirradiated cells. However, these effects, especially the production of ROS (key mediators of radiation-induced BE), were abrogated in unirradiated cells treated with ICCM in which exosomes were removed. Interestingly, similar effects in ICCM such as the production of ROS, reduction in viability and calcium influx were observed in unirradiated cells following the addition of isolated exosomes from ICCM (Jella *et al.*, 2014). BE and GI are seen both *in vitro* and *in vivo*. It has been found that the bystander signals are not produced by all cell types and also that not all cell types respond to bystander signals (Mothersill and Seymour, 1997; Hagelstrom *et al.*, 2008). The variation in genetics and epigenetics (change in gene expression without any change in DNA sequences), as well as radiation types/doses and activation times after exposure to the signals, can play an essential role in changing these processes. Mothersill has observed that medium from irradiated human epithelial cells might decrease the survival of un-irradiated cells. However, this did not happen in the case of human fibroblasts (Mothersill and Seymour, 1997). In addition, BE can be affected by two factors: firstly, cell density at the time of irradiation; secondly, analysis time (Lyng *et al.*, 2000). There is much evidence to suggest that the experimental and biological system, biological endpoints, radiation type and dose, time of analysis following irradiation, and system analysis should be taken into consideration when interpreting different experimental approaches (Kadhim *et al.*, 2013).

### *1.3.2.6 The interlink between GI and BE*

Much evidence has demonstrated that GI has been observed in the progeny of irradiated and bystander populations (Bowler *et al.*, 2006). Lorimore *et al*. (2003) have reported that there is a link between BE and GI (Lorimore *et al.*, 2003). Several *in vitro* and *in vivo* studies using different experimental approaches have confirmed such a link. For example, from a grid shielding experiment, Lorimore *et al*. (1998) have documented that although an unshielded cell's viability was greatly reduced, there was no significant difference in the level of chromosome instability induction in the progeny of the shielded and the unshielded groups (+ grid and – grid respectively) (Lorimore *et al.*, 1998). These results suggest that the majority of cells presenting chromosomal instability were not directly irradiated, indicating that intercellular communication between the directly irradiated and unirradiated cells produced the cell damage (i.e. BE induced DNA damage in early stages through a communication process) (Kadhim *et al.*, 2013).

BE and GI have common manifestations of damage e.g. chromosomal rearrangements, micronucleus induction, and delayed lethal mutation/reproductive cell death. For example, Zhao *et al*. (2014) have observed that progeny of bystander AG1522 cells that were co-cultured with irradiated HeLa Cx26 cells showed an enhanced micronucleus formation at 20 population doublings following exposure of the HeLa cells to 0.5 Gy, 3.7 MeV alpha-particles irradiation (Zhao *et al.*, 2014). Additionally, de Toledo *et al.* (2017) have found an increase in micronucleus induction and a rise in oxidative changes in the progeny of bystander cells (normal human fibroblasts) co-cultured with confluent cells (normal or tumor human cells) exposed to either high LET (alpha-particles, 80 cGy, or energetic iron, 200 cGy) or low LET ($^{137}$Cs γ rays, 4 Gy) irradiation. This expression of GI, which is expected to have a role in the generation of second primary cancers in radiotherapy patients, is most likely reliant on the type of junctional communication that occurs between the bystander and irradiated cells in the first few hours following irradiation (de Toledo *et al.*, 2017).

## 1.3 Factors influencing the appearance and manifestation of non-targeted effects

The non-targeted effects following exposure to IR are influenced by several factors such as cell type, genetic predisposition, and dose as well as radiation quality (Kadhim, 2003; Kadhim *et al.*, 2013; Morgan, 2003). Additionally, the rate at which a radiation dose is delivered is one of the main factors of the biological effects of radiation (Zeman, 2017).

### 1.4.1 The effect of dose and dose rate

Despite daily exposure to different kinds of low doses and low dose rates of radiation, little is known about the biological risks of these low dose exposures (Rühm *et al.*, 2015). These risks are the main factors in the establishment of risk assessment and radiation protection (ICRP, 2007). A major risk of exposure to low doses and low dose rates of radiation is cancer and the control of this risk is an essential consideration in developing radiation protection practice (Goodhead, 2009).

One of the main hypotheses used to assess cancer risks associated with radiation exposure is the linear-no-threshold (LNT) model, which assumes that Radiation-induced damage elevates linearly as dose increases (Vaiserman, 2010). With high LET radiation such as alpha-particles, findings show a linear relationship between cancer risk and the increase in radiation dose (Darby *et al.*, 2005). However, the risk associated with low doses and low dose rates of low LET radiation is less than is estimated by linear extrapolation from high doses and high dose rates. This decrease in risk is defined by the Dose and Dose Rate Effectiveness Factor (DDREF) for which the ICRP recommendation is 2 (ICRP, 2007).

The term “high dose rate” (HDR) is commonly applied to acute exposures that endure for a few minutes. In comparison, the term “low dose rate” (LDR) applies to prolonged exposures lasting many hours or days. In general, a given dose of low LET (e.g. x- or gamma-rays) is more effective if it is delivered within a few minutes (HDR) as opposed to a protracted dose given over a period of hours, days or weeks (Hall and Brenner, 1991; Hall and Bedford, 1964).

The various manifestations of GI (micronuclei, apoptosis and chromosomal aberration induction) are induced as a result of exposure to low doses of both high and low LET (Smith *et al.*, 2003). There is considerable evidence that exposure to low doses of high LET irradiation induces GI in both directly irradiated and non-irradiated cells (bystander cells). For example, a single alpha particle traversal was shown to induce a significant increase in chromatid-type aberrations in human T-lymphocytes at 12-13 population doublings following exposure (Kadhim *et al.*, 2001).

Additionally, exposure to 0.2, 0.5 and 1 Gy x-ray irradiation induced GI in the form of delayed aneuploidy of chromosomes in human fibroblasts at 5 passages following irradiation (Cho *et al.*, 2015). Turner *et al*. (2015) have studied the effect of dose and dose rate of x-ray irradiation on the induction of micronuclei as biodosimetry markers in mouse lymphocytes at 24 hours and 7 days following *in vivo* exposure to 0–4.45 Gy x-rays. The findings showed an increase in micronucleus induction over the dose range 0-4.45 Gy x-rays for both HDR and LDR groups with a monotonic rise in formation of binucleate cells with micronuclei (MN/BN) with doses up to 2.2 Gy. However, the HDR group displayed more induction of binucleate cells with micronuclei (MN/BN) compared to the equivalent LDR group (Turner *et al.*, 2015). The effect of dose rate was also observed by Chen, *et al*. (2016) in the induction of damage in rodent testes at 1 day following *in vivo* Synchrotron radiation (SR) x-ray exposure. The results showed that exposure to HDR  4 Gy (1.1 Gy / s) SR x-ray irradiation displayed higher γ-H2AX (DSBs) levels compared to the equivalent LDR exposure (0.11 Gy/s). The dose rate, therefore, has been thought to be an important factor in SR x-ray induced cell damage. This could be used to establish a useful base to control the cell damage in medical applications using SR x-ray (Chen *et al.,* 2016).

Despite the importance of the dose rate in evaluating radiation damage to cells, the molecular mechanisms involved in radiation dose rate effects are still not well known. Nakajima *et al*. (2017) have observed that the alterations in protein expression in the livers of mice following prolonged x-ray exposure (*in vivo*) were different compared to the equivalent acute radiation exposure group. For example, an increase in the expression of proteins related to apoptosis and inflammation (e.g. caspase 12) were displayed at 3 months following a sub-lethal dose of 4 Gy x-ray low dose

rate exposures. However, exposure to 4 Gy x-ray HDR showed an increase in the expression of the protein MyD88 which is related to innate host defence pathways and works as a radioprotector (Nakajima *et al.*, 2017).

Tang and Loke stated that the molecular mechanisms involved in low dose IR induced GI are due to activation of signal transduction pathways such as extracellular signal-related kinase (ERK), mitogen-activated protein kinase (MAPK), tumor necrosis factor receptor alpha (TNF-α), ROS, Ataxia telangiectasia-mutated (ATM) and protein 53 (P53) pathways (Tang and Loke, 2015). With low radiation doses, the indirect reaction is the predominant mechanism leading to induction of ROS where it occurs in the vicinity of DNA (Brigelius-Flohé and Maiorino, 2013).

Moreover, exposure to low dose rate irradiation can lead to distinctive gene expression patterns compared with those observed following acute exposures (Ghandhi *et al.*, 2015). As the DSB repair system is known to work for hours to days following irradiation, the dose rate would range between a Gy per hour and a week, i.e. in the range of 0.001Gy / minute to 0.1 Gy / minute (Niwa *et al.*, 2015). It is also critical to determine whether a person has received a dose at a low dose rate, whether from internal or external sources of radiation, which may cause a mild health risk compared to a corresponding single acute dose exposure (Hall and Brenner, 1991).

Studies into the fraction of cells surviving various rates of IR have demonstrated that the cell survival curves rise and the curves gradually become shallower and straighter as dose rate decreases in studies into early clonogenic cell survival in mammalian cells (Hall and Bedford, 1964; Hall, 1972; Ben-Hur and Elkind, 1974). These results are known to be due to the repair of the critical radiation damage (e.g. DSBs). This repair occurs during irradiation and minimises the chance of severe consequences which could result from the interaction between two or more lesions and which could otherwise result in chromosomal aberrations (Frankenberg-Schwager *et al.*, 1981). While these studies showed dose rate effects at lower dose rates, the findings were complicated by the absence of evidence of a connection between DSB yields and cell survival (Turner *et al.*, 2015).

## 1.4 The mechanism of micronucleus induction as an indicator of cytogenetic damage following irradiation

There are various manifestations of radiation-induced genomic instability which include delayed micronucleus formation, delayed chromosome breaks, delayed dicentrics, delayed apoptosis and delayed reproductive death (Trott *et al.*, 1998)**.** The cytokinesis- block micronucleus (CBMN) assay is an efficient assay capable of directly and indirectly measuring the different dysfunction of cellular and nuclear aspects of the cell such as:

1- Chromosome breaks, DNA mis-repairs, and asymmetrical rearrangement

2- Anaphase checkpoint gene mutations

3- Telomere end-fusions

4- Programmed cell death by necrosis or apoptosis

5- Chromosomal instability phenotype

6- Alteration in mitotic activity and/or cytostasis

7- 7- DNA hypomethylation

(Fenech, 2007)

Micronuclei (MN) are acentric chromatid fragments, acentric chromosome fragments or whole chromosomes, wrapped with nuclear membrane and released outside the main daughter nuclei. Such displaced chromosome and chromatid fragments or whole chromosomes become separated from the spindle during the segregation process in anaphase and eventually fail to be part of the new daughter nuclei at the end oftelophase during mitosis (Fenech *et al.*, 2011).

MN formation can be induced due to chromosomal aberrations, accumulation of DNA damage and defects in the repair system of the cell. MN induction can be induced by different genotoxic agents such as IR and could result in GI, cancer development or cell death. Micronucleus formation, therefore, is considered to be one of the hallmarks of genomic instability (Luzhna *et al.*, 2013).

Regarding the mechanisms of MN formation, those MN containing acentric chromosome or chromatid fragments are a result of unrepaired or misrepaired DNA breaks. This occurs when the repair capacity of the cells is insufficient to repair an excessive level of DSB production. This is due to either inappropriate function of enzymes involved in the non- homologous end-joining pathway (NHEJ) (Hartlerode and Scully, 2009) or mis-repair of DSBs caused by the dysfunctional homologous recombination (HR) (O'Donovan and Livingston, 2010).

Micronucleus formation also results from imperfect segregation of sister chromatids due to absence or inappropriate attachment of chromosome kinetochores and spindle microtubules. When the attachment between microtubule and kinetochore is stable, this attachment produces tension at kinetochores, fixing the chromatid in the correct place. However, if the attachment is an unstable type such as monotelic (one kinetochore is attached and the second sister chromatid unattached), merotelic (both spindle poles are attached to one kinetochore), or syntelic (both sister chromatids are attached to a single spindle pole), this does not lead to a significant tension at kinetochores, thus making the bond easy to dissociate (Cimini and Degrassi, 2005).

However, the main mechanisms of micronucleus formation from whole chromosomes or chromatids derive from (a) hypomethylation of satellite paracentromeric/centromeric repeats, (b) kinetochore defects, (c) microtubule depolymerisation, and (d) defects in checkpoint genes at anaphase (Figure 1.5) (Luzhna *et al.*, 2013). Satellite DNA is usually hypermethylated which causes elongation in satellite repeats, decreasing the kinetochore protein function. This inappropriate kinetochore assembly causes defects in the connection between chromosomes and microtubules of the mitotic spindle at anaphase (Fenech *et al.*, 2011). Due to the effect of genotoxic agents, at times the mitotic spindle may fail to pull apart the chromosomes/chromatids during the segregation process as a result of tubulin depolymerisation. For example, Aypar *et al.* (2011) have found that high (Fe ions, 1 Gy) and low (x-rays, 2 Gy) LET radiation induced hypomethylation of repeat elements LINE-1 and Alu in a human-hamster hybrid cell line and alteration in miRNAs with six following low LET and three following high LET. Those miRNAs were involved in five major pathways: DNA methylation, apoptosis, chromatin remodelling, DNA repair and a cell cycle checkpoint, all of which may eventually

involve the induction of GI. Aypar stated that the misexpression in miRNA could be one of the mechanisms of micronucleus induction (Aypar *et al.*, 2011).

When a DSB is produced in the chromosome and stays unrepaired until replication and the broken ends are misjoined, it results in the formation of dicentric chromosomes and acentric fragments which are subsequently replicated. At anaphase, nucleoplasmic bridges (NPBs) and acentric chromatid fragments (which form MN) are formed when the centromeres are pulled to the opposite poles of the cell. The NPBs may fracture to form micronuclei (Thomas *et al.*, 2003).

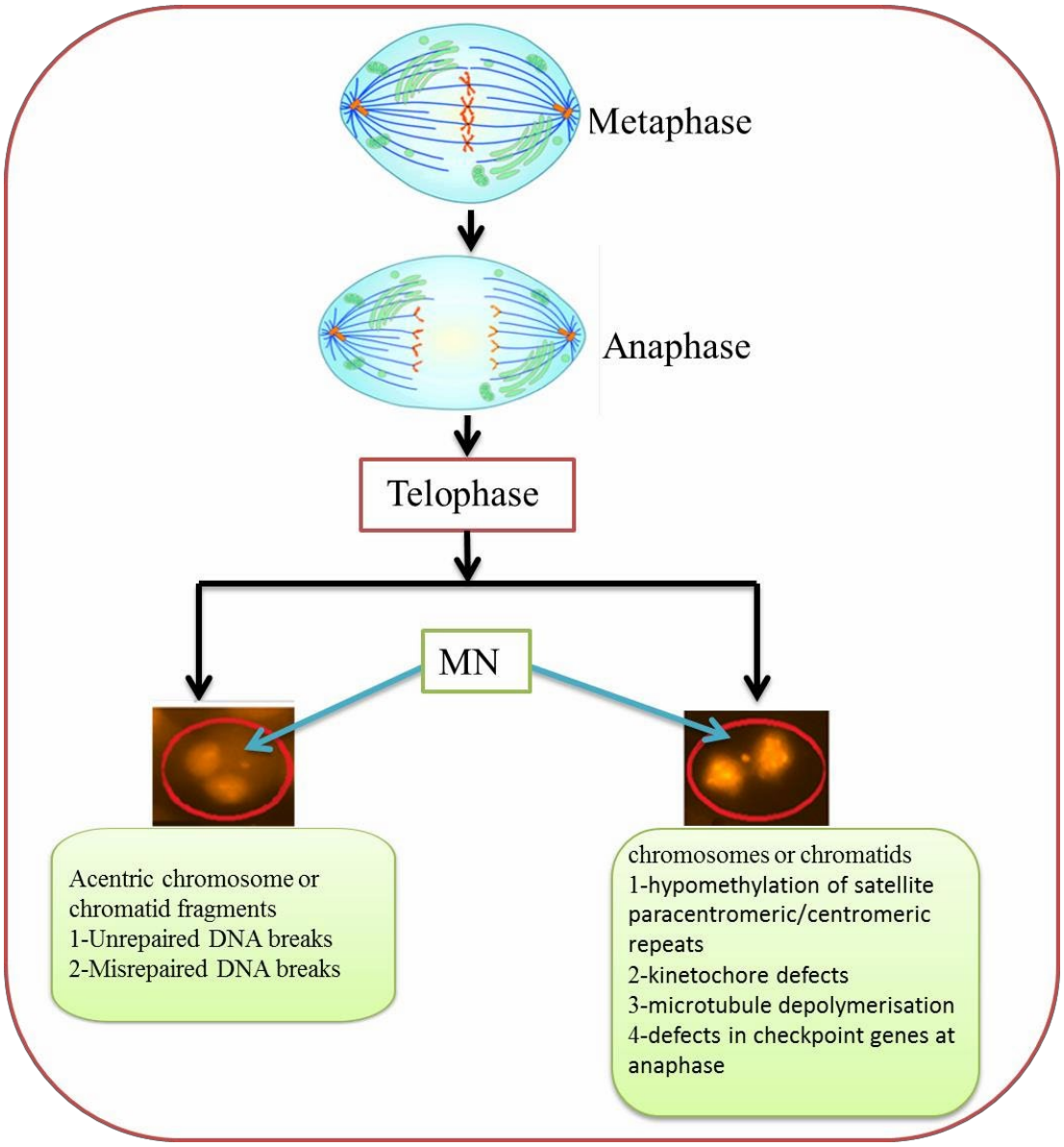


Figure 1.5: Mechanisms of formation of MN. Adapted from Luzhna *et al.* (2013).

The consequences of MN induction on a cellular level are vital as it may cause a loss or gain in genetic material in the daughter cells and generate a major chromosome rearrangement. This may lead to initiation and continuation of malignant cell transformation. Even though the fate of micronuclei has been addressed by many studies utilising different approaches, the mechanisms underlying the potential fate of MN are still not fully described. However, Hintzsche *et al*. (2017) have reviewed six possible principles for potential fate of micronuclei. The four main possibilities are: extrusion of micronuclei from the cell, reincorporation within the main nucleus, degradation and persistence in the cytoplasm. Another two additional fates were expressed as possibilities: the removal of micronuclei by apoptosis and the condensation/chromothripsis of the premature chromosome. (Hintzsche *et al.,* 2017)

## 1.5 Aims of Thesis

This study aims to explore the role of dose, dose rate and radiation quality (x-rays vs alpha-particles) on the induction of genomic instability in HF19, a primary human fibroblast cell line. Cells are analysed at early (1 h following alpha-particles, and immediately and 24 h following x-ray) and late (10th and 20th population doubling) time points, to investigate the induction of genomic instability (GI). Under these radiation conditions, the results were interpreted in light of the biophysical differences between the spatial and temporal distribution of radiation tracks through the cell and across the cell population. An additional aim is to investigate the potential role of ROS, TNF-α and TGF- β1 in the initiation of processes that could lead to DNA damage and genomic instability in HF19 cells after HDR and LDR x-ray irradiation.

As most studies have focused on the differences between low and high LET exposure induced DNA damage, in particular, alpha particles and gamma rays, there has been a lack of focus on the differences between low and high dose rate irradiation induced GI. Therefore, our novel contribution to knowledge is to give a better understanding of how low and high dose rate irradiation affects the induction of GI. Additionally, it adds to our understanding of how radiation dose rate affects the molecular mechanisms involved in the induction of GI, which would contribute to the evaluation of radiation protection, radiation damage, and medical diagnosis and treatment of radiation exposure.

# Chapter 2.
# Materials and Methods

## 2.1 Materials

### 2.1.1 Cell Line, Cell Maintenance and Culturing

HF19, a primary non-transformed human fibroblast, was used for all studies. These cells were derived from non-transformed human fibroblasts from the lung of a 14-week-old female foetus, designated HF19 by Cox and Masson (Cox and Masson, 1975) from MRC, Harwell Campus, Oxfordshire, UK. These cells were cultured in Minimum Essential Medium with Earle's salts without L- Glutamine, and supplemented with 10 % Foetal bovine serum (Sigma: F7524), 2 mM L- Glutamine, (Gibco: 25030), 1 % Non-essential amino acids (Gibco: 11140) and 1 % (w/v) penicillin / streptomycin solution (Sigma: P0781) in a fully humidified 5 % $CO_2$ incubator at 37ºC. Cells were grown initially in 25 $cm^2$ (T25) to 80 % - 90 % confluence. Media was removed from the tissue culture flask; cells were washed twice with 2 ml of sterile DPBS (Dulbecco's phosphate-buffered saline, Gibco, 14190) for 1 minute to remove residual media. The DPBS was discarded and cells were rinsed for 30 seconds with 0.025 % (w/v) trypsin-EDTA solution (0.025 g of 1:250 trypsin (DIFCO, 0152-13-1) and 100 ml of 0.02 % Ethylenediaminetetraacetic acid solution, EDTA (Sigma, E8008)). Cells were then incubated in a humidified 5 % $CO_2$ incubator at 37ºC for 3-5 minutes to allow cells to detach from the flask base. Pre-warmed growth media (15 ml) was added to the flask to inactivate trypsin and to enable collection of detached cells from the flask. Approximately 1.5 x 106 cells were transferred to 75 $cm^2$ (T75) tissue culture flasks. Cells were re-incubated in a humidified 5 % $CO_2$ incubator at 37ºC for several population doublings during cell propagation. Cells were passaged twice weekly.

### 2.1.2 The Muse Cell Analyzer

The Muse cell analyser is a small, fluorescence-based instrument. It is intended for simple and intuitive operation as well as needing a little support. It is provided with an integrated touchscreen that gives an easy-to-utilize software for operating the system.

The Muse system comprises a portable, compact, and simple-to-utilise cell analyser, optimised reagents, and software. It utilises microcapillary technology and miniaturised fluorescent detection to carry out quantitative cell analysis for suspension or adherent cells of 2 to 60 μm diameter. The Muse cell analyser software involves programs for confirming instrument execution and cleaning the instrument's fluidics system as well as a setup module for different assays (Millipore, 2013).

The performance of the Muse system is verified using the system check procedure which assesses counting accuracy and fluorescence detection. The Muse system check kit consists of pre-warmed Muse system check beads and Muse system check diluent (1:20 dilution). The system check procedure was performed before running any of the assays to guarantee that the instrument gives solid, reliable and accurate results (Millipore, 2013).

## 2.2 Methods

### 2.2.1 Routine Cell Culture

#### *2.2.1.1 Recovery of Cells from Liquid Nitrogen*

Cryovials containing 1 ml of cell suspension (90 % media and 10 % DMSO) were removed from liquid nitrogen and thawed quickly in a warm water-bath. Once cells had thawed, they were aseptically transferred to 15 ml Falcon tubes containing 10 ml pre- warmed culture media. The tubes were centrifuged at 259 × *g* for 8 minutes. The supernatant was discarded from each tube to eliminate DMSO. Each cell pellet was then re-suspended in 8 ml pre-warmed culture media and transferred to 25 $cm^2$ tissue culture flasks (T25). The cells were incubated in a humidified 5 % $CO_2$ incubator at 37ºC. Cell attachment (characteristic of live HF19 cells) was checked a few hours after seeding, using an Olympus inverted phase contrast field microscope. When live cells showed successful adherence, the cells were re-incubated and checked again after 24 hours. In the case of no cell adherence, the flask contents were safely disposed and a new cryovial from liquid nitrogen was set up instead.

### *2.2.1.2 Cell Counts Using the Viability Stain, Erythrosin B*

Firstly, an erythrosin B solution was prepared by adding 0.4 g erythrosin B powder (Sigma, E9259), 0.81 g sodium chloride, NaCl (Sigma, S5886) and 0.06 g potassium phosphate monobasic (Sigma) to 100 ml Hank's balanced salt solution, HBSS (Sigma). The solution was placed in a glass beaker with a magnetic stirrer on a hot plate. When the solution started to boil, 100–200 µl of 10 M NaOH (Sigma, 221465) were added until all compounds had dissolved. The concentrated stock solution was then left to cool at room temperature. Finally, the working solution was made by adding 1 ml of stock solution to 4 ml of $dH_2O$. Both concentrated stock and working solutions were stored in a refrigerator at 4ºC.

To perform the cell count, equal volumes of erythrosin B stain and a well-mixed cell suspension were mixed (e.g. 200 µl total volume). Approximately 10 µl of the mixture were then pipetted at the edge of a coverslip sealed on a Neubauer Haemocytometer and allowed to run under the coverslip. The double chamber haemocytometer was used. Each chamber has a grid layout composed of 4 large 1 x 1 mm squares made up of 16 smaller squares. The chamber is designed such that the distance between the bottom of the chamber and the coverslip is 0.1 mm. Therefore, the total volume of each large square is 0.1 $mm^3$ = 0.1 µl. The cells in each of the 4 large squares per chamber were counted as in Figure 2.1 below. Live cells were clear in appearance, while dead cells were observed as red. To calculate the number of live cells per 1 ml of cell suspension the following formula was used:

(Number of cells in the four large squares / 4) x Dilution factor (2) / Volume of 1 square ($10^{-4}$)

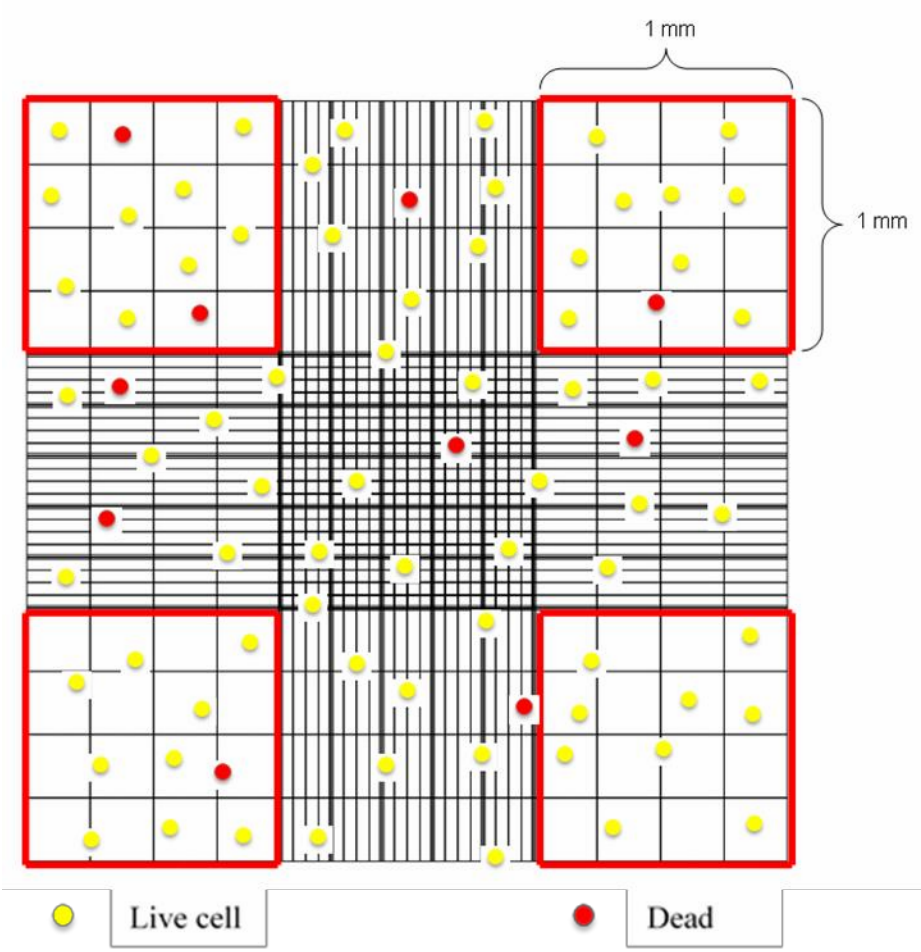


Figure 2.1: A schematic of one counting chamber of the haemocytometer, demonstrating live (yellow) and dead cells (red) in the counting procedure. The red outline shows the 4 large squares used for cell counting.

### *2.2.1.3 Cryopreservation of Cells in Liquid Nitrogen*

Cryopreservation is a process in which cells susceptible to damage caused by unregulated factors are preserved by cooling in liquid nitrogen (-196 °C) to maintain cell longevity. Cells were prepared for liquid nitrogen storage by being grown to 80 % - 90 % confluence in T75 tissue culture flasks. Cell suspensions were prepared as previously described and centrifuged at 262.4 × *g* for 8 minutes. The supernatant was discarded and the pellet was re-suspended to give a single cell suspension in 1 ml freezing media (90 % culture media supplemented with 10 % sterile DMSO) with cell density 1.5–2.5 x $10^6$. The cell suspension was then transferred to a pre-labelled sterile cryovial, which was promptly stored in a freezer at -20ºC for 1-2 hours. The cryovials were then moved to a-80ºC freezer for a period between 4 hours and overnight and eventually placed into liquid nitrogen storage.

## 2.2.2 Irradiation

### *2.2.2.1 Alpha-particle*

Due to the short range of alpha-particle tracks, cells must be irradiated as a monolayer. In brief, the cells were seeded at a density of 2 x $10^5$ in 2 ml of media in Hostaphan dishes. Hostaphan dishes are 30 mm internal diameter glass-walled dishes with bases of 2.5 µm Hostaphan film (Bowler *et al.*, 2006). The cells were then incubated undisrupted for ≈ 44 h at 37°C, 5 % $CO_2$ before irradiation to allow them to form a monolayer of cells. Just prior to irradiation, cell thickness was assessed by confocal microscopy. Cells were shown to have an average thickness < 10 µm.

The cells were irradiated with alpha-particles with an incident energy of 3.26 MeV (LET ≈ 121 keV/µm) which are emitted from a thin uniform 20 mm diameter layer of $^{238}$Pu (Goodhead *et al.*, 1991) (0, 0.0001, 0.001, 0.01, 0.1, 0.5 and 1 Gy alpha-particles). A sham irradiated group (Control) was set up in parallel. All the doses were delivered under 2 minutes. All the irradiations were performed at the CRUK/MRC Oxford Institute for Radiation Oncology, Department of Oncology, University of Oxford.

The cells were incubated (37°C, 5 % $CO_2$) for 1 hour following direct irradiation and then collected from the Hostaphan dishes. A fraction of cells (2x$10^4$) was subjected to the comet assay which was utilised to measure total DNA damage in all experimental groups whilst other fractions (1.5x$10^6$) were seeded into 1xT75 flasks with their irradiated medium for the micronucleus assay. The remainder was then further propagated for assessment of intermediate (10 population doublings or 5 passages) and delayed effects (20 population doublings or 10 passages) as shown in experimental design Figure 2.2.

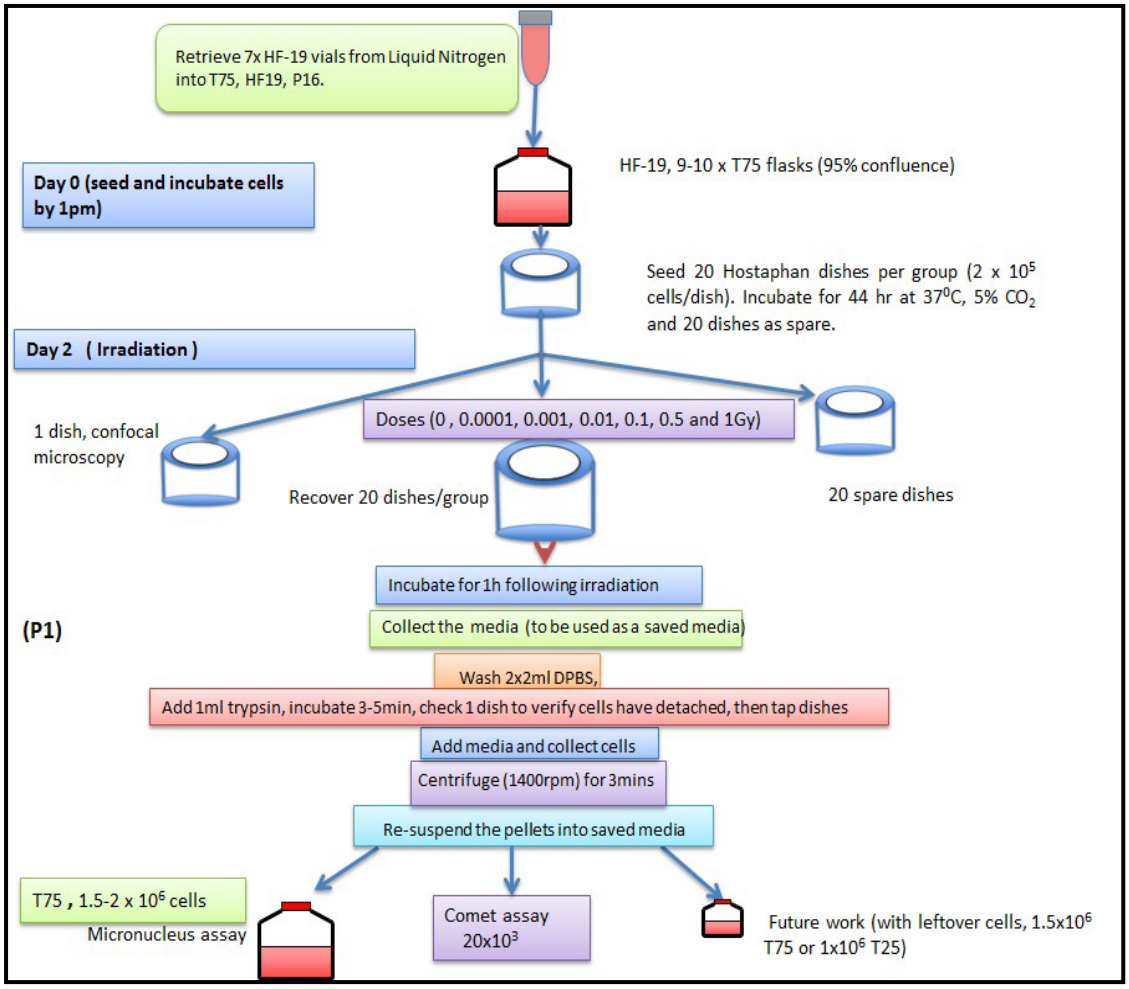


Figure 2.2: Alpha-particle experimental design. Experiments were established to examine the early DNA damage with a comet assay and the induction of micronucleus at 1h following irradiation. The cells were subcultured and maintained for another 10 and 20 population doublings to examine the late cellular responses to alpha -particle exposure.

### *2.2.2.2 X-ray*

Cell irradiations were performed at the Gray Institute for Radiation Oncology & Biology, Department of Oncology, University of Oxford, utilising the MXR321 x-ray machine operating at 250 kV constant potential and 12 mA for irradiation with high dose rate, and 250 kV and 0.3 mA with low dose rate. The x-ray energy deposition is sparse and uniform, ensuring that each cell in the ionisation track path receives some irradiation even at low doses.

Cells were seeded at 1.5 x $10^6$ in T75 tissue culture flasks and incubated for ≈ 24 hours at 37 °C, 5 % $CO_2$ before irradiation. Cells were then exposed to either: 0, 0.1,

0.5, 1, 1.5, 2, 2.5, 3 or 4 Gy X-rays at either a high dose rate (HDR) (0.42 Gy / minute) or at a low dose rate (LDR) (0.0031 Gy / minute) and maintained at 37°C, 5 % $CO_2$ during the irradiation. The $CO_2$ concentration and humidity were maintained by replacing the normal filter caps on the T75 flasks with solid caps prior to irradiation. Additionally, the temperature was monitored directly using a readout monitoring device.

Immediately (less than 3 minutes) following irradiation, fractions of cells were processed for the micronucleus assay. In brief, cells were treated with 6 µg / ml cytochalasin-B for 40 hours in a humidified 5 % $CO_2$ incubator at 37 ºC. The remaining cells were subcultured and incubated for future population doubling studies. Cells were also subjected to the comet assay at first population doubling following irradiation.

### 2.2.3 Measurements of nuclear and cellular area

For low LET (x-ray) radiation, each cell receives approximately the same average dose, as the average number of independent electron tracks hitting each individual cell is large. In contrast, for high LET radiation (alpha-particle radiation), not all cells are necessarily traversed by a radiation track due to the nature of the radiation tracks (Hill *et al.*, 2004). Thus, measurements of the cellular and nuclear area were made to calculate the average number of alpha-particle traversals per cell and per nucleus, by different doses.

Prior to sham/irradiation, two randomly chosen spare Hostaphan dishes of HF19 cells were stained with DIOC6 (3, 3′-dihexyloxacarbocyanine iodide, Sigma), a fluorescent dye which stains the cell mitochondria, endoplasmic reticulum and vesicle membranes. Random ‘saved’ multiple cell images were taken of horizontal sections across these stained monolayer cells. The images were taken by a confocal laser scanning microscope (BioRad-Lasersharp 2000 confocal microscope coupled to a Nikon TE2000 microscope with an ion argon laser operating at 488 nm wavelength). This allowed subsequent measurement of the living cells’ nuclear area and cellular area as shown in figure 2.3. The computer programme ‘Image J’ was initially used to manually draw around the circumference of each nucleus and cell, by which the computer is able to calculate the area of each, as shown in figure 2.3.

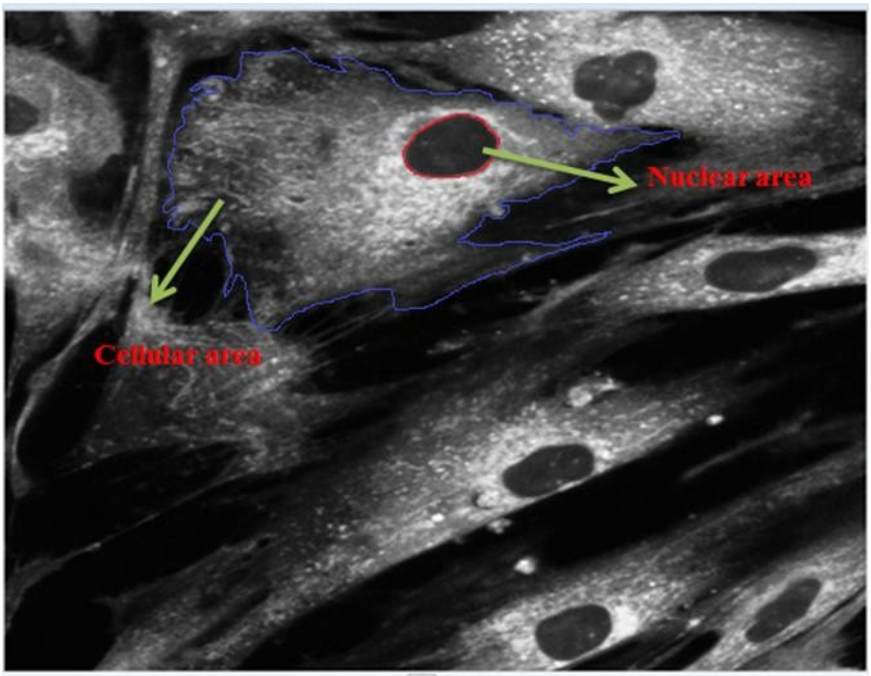


Figure 2.3: Confocal images of living HF19 cells stained with DIOC6

### 2.2.4 Viability Assay

A viability assay measures the ability of cells to preserve or recover viability. Cell survival was measured using the Muse™ Count & Viability Kit. Both dead and viable cells were differentially stained according to their permeability to the DNA-binding dyes in the kit's reagent, enabling discrimination of viable from non-viable cells. The dead cells are able to take up the DNA-binding dye in the reagent stain as their membrane integrity has been lost. The Muse Cell Analyser counts the stained nucleated events and then uses the cellular size properties to differentiate free nuclei and cellular debris from cells to determine a precise total cell count as shown in figure 2.4.

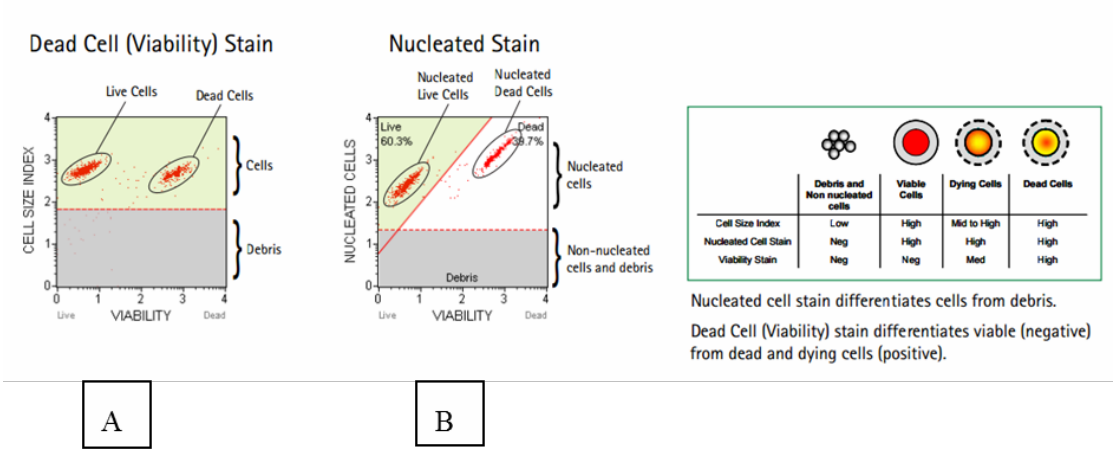


Figure 2.4: Panel A: Muse histogram with a gate marker that allows elimination of debris based on size. Panel B: Muse histogram with a threshold marker that allows elimination of cells that do not have a nucleus. The live cells separate from dead cells using viability discriminator (angled marker) (the figure is taken from Millipore, 2013).

In brief, cells were seeded in T75 flasks at a density of 1.5 x $10^6$ cells/flask and incubated for 24 hours. They were then irradiated with either 0 Gy or 1 Gy at HDR (0.42 Gy / minute) or at LDR (0.00313 Gy / minute). The cell viability assay was then performed 30 minutes and at 8, 24 and 32 hours following irradiation. Trypsin was used to dissociate the cells from the flasks and create single-cell suspensions. Following trypsinization, the cells were collected in their own media (0 Gy or 1.0 Gy respectively) and cell counts were performed on 1 x $10^5$ cells. To this end, 50 µl of the Muse Count & Viability Reagent was added to 450 µl of each cell sample. The samples were subsequently incubated for 5 minutes at room temperature prior to analysis by the Muse Cell Analyser (Millipore, 2013) as shown in figure 2.5.

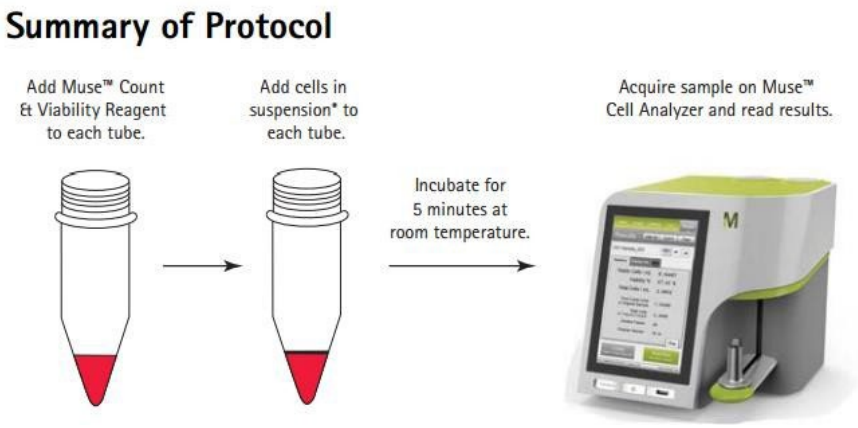


Figure 2.5: Summary of cell viability measurement using the Muse Cell Analyser (the figure is taken from, Millipore, 2013).

### 2.2.5 The cell cycle assay

The cell-division cycle is a vital process that includes a series of events that occur in the cell resulting in cell growth and division into two daughter cells, each in turn producing two further daughter cells. Cell cycle regulation is essential to cell survival as it controls the repair of genetic damage and regulates uncontrolled cell division. Imperfections in cell cycle regulation are a hallmark of tumour cells, and mutations in the genes involved in controlling the cell cycle are common in cancer. The Muse Cell Cycle Kit provides a rapid and reliable measurement of the percentage of cells in the different phases of cell cycle G0/G1, S and G2/M on the Muse Cell Analyser.

The principle of the Muse Cell Cycle assay: the premixed reagent contains the nuclear DNA intercalating stain propidium iodide (PI) and RNAse A. PI differentiates and measures the percentage of cells at various phases of the cell cycle, based on the amount of DNA in each phase in the presence of RNAse to boost the specificity of DNA staining. When cells are in the G0/G1 phase, they contain two copies of each chromosome; however as the cells move into the S phase, DNA synthesis replication of the genetic material occurs so each chromosome now consists of two sister chromatids. Fluorescence intensity from PI is seen to rise until all chromosomal DNA has doubled (G2/M phase), such that in the G2/M phase the fluorescence intensity from PI is twice the intensity of the G0/G1 population. The calculations from this analysis were performed automatically using the Muse Cell Cycle Software Module. Data from the calculations are presented in two plots: firstly a dot plot of DNA content index against cell size index and secondly a histogram of

DNA content index with markers available to investigate the cell populations in each phase of the cell cycle (Figure 2.6).

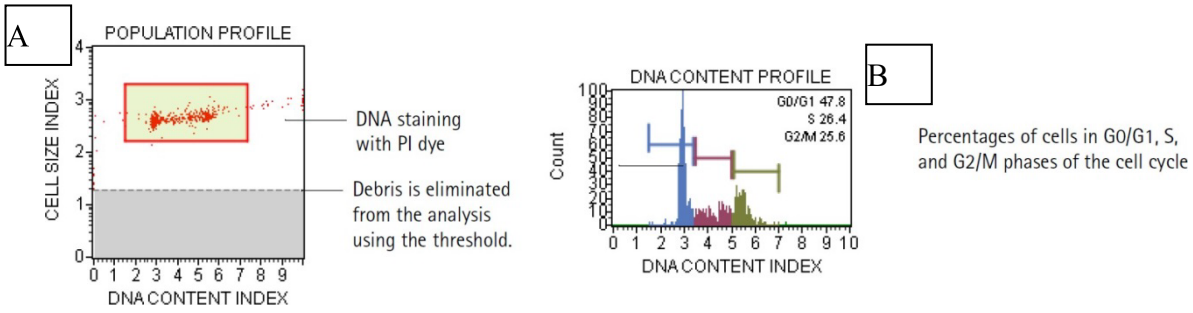


Figure 2.6: Panel A: Dot plot for DNA content and cell size index. Panel B: Histogram for DNA content index with markers available to separate the cell populations in each phase of the cell cycle (the figure is taken from Millipore, 2013).

For analysis on the Muse Cell Analyser following sham/irradiation, trypsin was used to dissociate the cells from the flasks which were then collected in their respective sham/ irradiated media. Aliquots of 1 x $10^6$ cells/ml per group were taken and centrifuged at 300 × *g* for 5 minutes at room temperature (RT). The supernatants were discarded and the pellets were each resuspended in 1 ml of PBS. They were then aspirated up and down several times to mix and further centrifuged at 300 × *g* for 5 minutes at RT. The supernatants were discarded and 1 x $10^6$ cells per group were thoroughly resuspended in 50 µl of PBS. The re-suspended cell solution was transferred in a drop-wise manner to a vortexing (medium speed) tube containing 1 ml of ice-cold 70 % ethanol; they were then put into a -20°C freezer for a minimum of 3 hours. After this, 200 µl of the ethanol-fixed cells were added to a 12 x 75 $mm^2$ polystyrene test tube and centrifuged at 300 × *g* for 5 minutes at RT. The supernatants were removed and 250 µl of PBS were added to each tube. The cell suspension was centrifuged at 300 × *g* for 5 minutes at RT and the supernatant discarded, the cell pellets were thoroughly resuspended and then 200 µl of Muse Cell Cycle Reagent was added. Following this addition, cells were kept at RT in the dark for 30 minutes prior to analysis by the Muse Cell Analyser, as shown in figure 2.7 (Millipore, 2013). The P values of raw data from two experimental groups were calculated using a Student t-test.

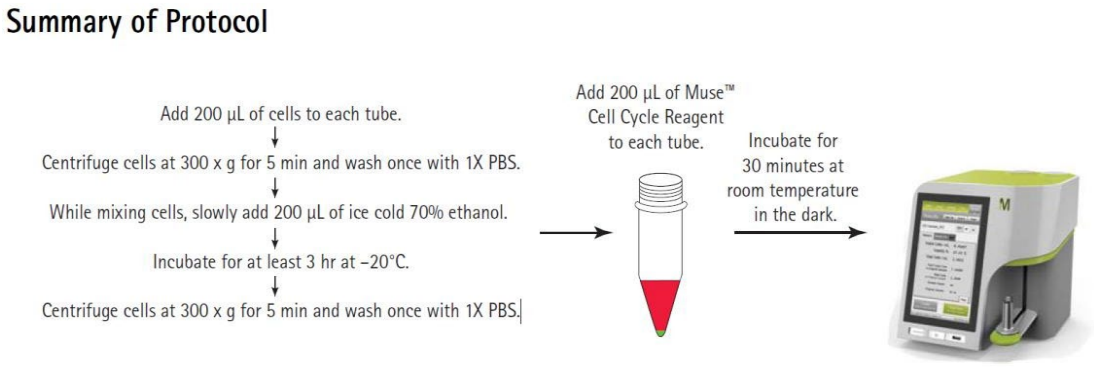


Figure 2.7: Summary of measurement of the percentage of cells at various phases of the cell cycle using the Muse Cell Analyser (figure taken from Millipore, 2013).

### 2.2.6 Oxidative Stress

Reactive Oxygen Species (ROS) are non-radical molecules and chemically reactive radicals derived from molecular oxygen such as peroxide, hydroxyl radical, singlet oxygen, and superoxide. ROS are generated by living organisms as a consequence of normal cellular metabolism and environmental factors, for example, cigarette smoke, radiation or air pollutants (Birben *et al.*, 2012).

ROS can be either harmful to the body (as the free radicals have a special affinity to attack biological molecules such as proteins, DNA, and lipids and alter their functions), or beneficial to the body (they play an important role in the regulation of intracellular signal transduction and in physiological adaptation (Yoshikawa and Naito, 2002). The endogenous antioxidant system neutralises ROS. If a high concentration of ROS is induced such that they cannot be sufficiently scavenged by the cells' antioxidants, a pathological condition can arise termed oxidative stress (Birben *et al.*, 2012). ROS have been involved in the pathophysiology of some diseases such as cardiovascular disease, diabetes, cancer, sepsis, and Alzheimer's disease (Pham-Huy *et al.*, 2008).

The Muse Oxidative Stress Kit was used to determine the percentage and the number of cells undergoing oxidative stress based on the intracellular detection of superoxide radicals. ROS were detected in the cells using the Muse oxidative stress reagent.

The Muse oxidative stress reagent has been widely used to detect ROS in cellular populations and is based on dihydroethidium (DHE) (Bindokas *et al.*, 1996). This

reagent can penetrate the cell where DHE is oxidised by superoxide anions and forms the DNA- binding fluorophore ethidium bromide or a structurally similar product. This product intercalates with DNA giving rise to red fluorescence. The assay distinguishes cells into two populations:

- ROS(-): live cells
- ROS(+): cells exhibiting ROS.

Cells were cultured to 80 % - 90 % confluence. Media was removed from the tissue culture flask; attached cells were washed with sterile 2 x PBS (2 ml for T25 and 5 ml for T75) for 1 minute to remove residual media. PBS was discarded and cells were rinsed with 0.05 % (w/v) trypsin-EDTA solution (0.05 g of 1:250 trypsin (Gibco, 27250-180) and 100 ml of 0.02 % ethylenediaminetetraacetic acid solution, EDTA (Sigma, E8008)) for 30-60 seconds. After trypsinization, cells were incubated in a humidified 5 % $CO_2$ incubator at 37ºC for 5-10 minutes to allow cells to dissociate from the flask base. Cells were re-suspended in 10 ml culture media to inactivate trypsin and to enable collection of detached cells from the flask. Cells were seeded at $1.5x10^6$ cells per T75 for 24 hours prior to irradiation. Following irradiation, media was removed and the attached cells were washed twice with 10 ml sterile DPBS for 1 minute. The DPBS was discarded and the attached cells were rinsed with 0.025 % (W/V) trypsin for 5 minutes. The trypsin was removed and the dissociated cells were collected in 200 µl of DPBS at 1 x $10^6$ to 1 x $10^7$ cells/ml. It is highly recommended that the cell samples be run instantly following the completion of sample preparation. The Muse oxidative stress reagent and 1x assay buffer were warmed to room temperature and protected from light immediately before use. The intermediate solution was prepared by diluting Muse oxidative stress reagent 1:100 with 1x assay buffer and stored in the dark at room temperature. The working solution was then prepared by diluting the Muse oxidative stress reagent intermediate solution 1:80 in 1x assay buffer. The intermediate solution and the working solution must be prepared promptly before utilisation. A 190 µl of the Muse oxidative stress reagent working solution were added to 10µl of cell suspension. The cell suspension was then mixed thoroughly by vortexing at medium speed for 3 to 5 seconds or pipetting up and down. Samples were incubated for 30 minutes at 37°C in the dark. Finally, samples were run on the Muse cell analyser. Collecting the data on the Muse cell analyser

took up to 6 minutes per sample based on the concentration of the sample and desired number of events needed. The results from each run were recorded as a data file and a corresponding spreadsheet file (Figure 2.8), each of which contains the following statistics:

- Sample ID and number.
- ROS(-): negative cells (M1).
- ROS(+): cells with ROS activity (M2).
- Concentration (cells/ml) and percentage of gated cells in each marker.
- Concentration and percent of total cells.
- Dilution factor (input value).
- Fluorescent intensity values for [M1] and [M2] cell populations.

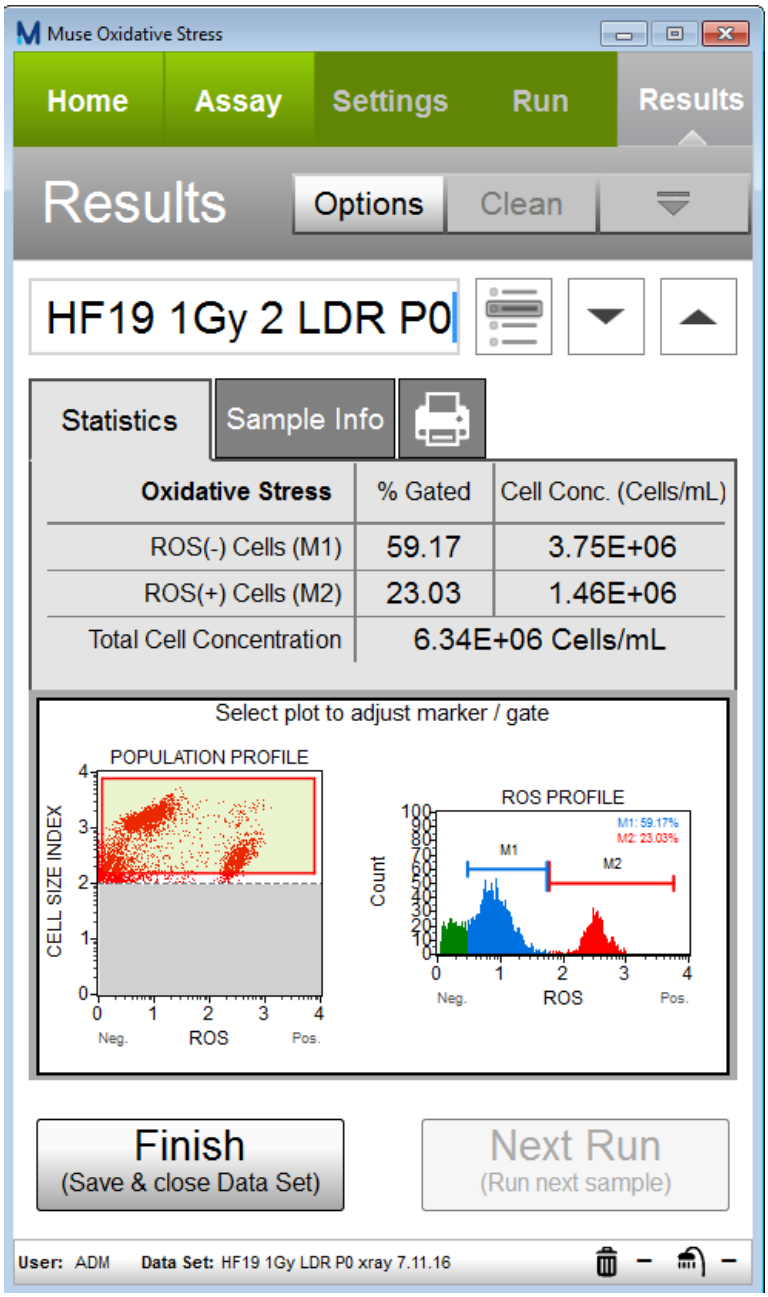


Figure 2.8: Summary data for 1 Gy low dose rate (0.00313 Gy/min) 30 minutes following irradiation, with dot plot and histogram. Cells were irradiated with 1 Gy low dose rate, stained with the Muse oxidative stress kit, and analysed using the Muse cell analyser. The concentration (cells/ml) and the percentages for the gated events in each marker, as well as the total cell concentration, are shown in the table. The first plot displays ROS versus cell size index and the second plot shows ROS staining.

### 2.2.7 Chromosomal Analysis

Metaphase preparation was carried out by harvesting the cells at 60 - 70 % confluence using the Kadhim and Wright method (Kadhim and Wright, 1998). In brief, 10 µg/ml demecolcine (Sigma: D1925) was added to the cells for 1.5 h in a humidified 5 % $CO_2$ incubator at 37ºC to arrest the cells in metaphase. Cells were then collected and centrifuged at 262.4 g for 10 minutes. The supernatant was discarded and the remaining cell pellets were re-suspended in a hypotonic solution (75 mM potassium chloride solution, Sigma: P3911) for 20 minutes at 37ºC. Cells were then centrifuged at 182.2 g for 10 minutes. The supernatants were aspirated and the cell pellets resuspended in 3:1 fixative (75 % methanol: 25 % acetic acid) for 10 minutes. Cells were again centrifuged and pellets re-fixed for 30 minutes. The fixed cells were then dropped onto individually labelled (coded) clean / degreased microscope slides. Slides were aged for 24 hours and then stained with Giemsa stain. They were then mounted and analysed using a bright field light microscope at 100X oil immersion objective. A different number of the metaphases were scored (5-66 metaphases) due to the low frequency of mitotic index in some of the experimental groups. When all slides had been analysed the codes for each slide were revealed.

The statistics were particularly limited for the initial chromosome analysis data due to the limited number of metaphases scored (low mitotic index). Therefore, the micronucleus assay was performed to allow a comparable measurement of chromosome damage as that undertaken by routine cytogenetic analysis. It has been found to be reliable, sensitive, has an easy scoring criterion, statistical power and allows a high number of cells to be analysed quickly (Wolff *et al.*, 2011).

### 2.2.8 Alkaline Comet assay (Single Cell Gel Electrophoresis)

The comet assay is a quick, sensitive and comparatively simple technique for evaluation of total DNA damage (double-strand breaks (DSB)), single-strand breaks (SSB) and base damage) in individual cells (Liao *et al.*, 2009). The comet assay was carried out as explained by (Natarajan *et al.*, 2007, Olive, 2009). Microscope slides were plated with a thin layer of 1 % normal melting point agarose solution (NMPA), (Sigma: A9539) by immersing the clean slides in agar. The excess was wiped from the back and the slides were laid to dry overnight and then kept in a microscope box. On the harvesting day, the cells were detached with 1.5 ml (0.025 %) trypsin and a

cell count was performed. For each group, 2 x $10^4$ cells were mixed with 200 µl of 1 % low melting point agarose (LMPA) (Fisher: BP165). The NMPA pre-coated slides were laid on an ice-chilled metal plate and 200 µl of the LMPA cell suspension mixture was placed immediately onto the chilled slides. The cell-LMPA suspension was spread and flattened by putting a 24 x 50 mm glass coverslip on top. After 5 - 10 minutes the coverslips were taken away to allow complete setting. The slides were then dipped in cold lysis buffer ((2.5 M NaCl, 100 mM $Na_2EDTA$ (pH 8.0), 10 mM Tris-HCl (pH 7.6), 1 % Triton X-100 (pH >10) and 1 % DMSO). The lysis process was performed at 4 °C overnight in the dark. In a cold room (4ºC) slides were then laid horizontally in the alkaline electrophoresis buffer tank (0.3 M NaOH and 1 mM EDTA (pH 13)). The slides were then left for 30 minutes at 19 V and 200 mA. Finally, the slides were neutralised with neutralising buffer (0.5 M Tris-HCl (pH 7.5)) for 3 x 10 minutes then the slides were washed with $dH_2O$ to remove any remaining buffer. The slides were stained immediately with a 1:10,000 dilution of Diamond Nucleic Acid Dye (Promega: H1181) in the dark. The slides were left at 25°C overnight and at least 500 cells per group were analysed using Komet 5.5 Image Analysis Software (Kinetic Imaging Technology / Andor, Germany).

#### *2.2.8.1 Statistical Analyses*

Samples and slides were coded and scored in a 'blind fashion' (i.e. a colleague in the research group kindly coded them). The P values of raw data from all experimental groups were calculated to compare the treatment groups with its control. The Y error bars for all experimental groups were generated by calculating the standard error of the mean (±SEM) for all groups. The comet assay data were examined for normality and they were not normally distributed. Therefore, data were subjected to a Mann-Whitney test (SPSS statistics 21) to measure the P-value. As the results have extreme scores, the median was used instead of the mean. This is due to the high sensitively of the mean to extreme scores whereas the median is insensitive to them (Salkind, 2010).

### 2.2.9 Micronucleus Assay

The Micronucleus assay (MN assay) is an easy, sensitive and quick analysis to measure chromosome damage; indicative of chromosome fragments and whole chromosomes left in the cytoplasm during cell division. Thus, the MN assay can be used as an alternative method for dose estimation in case of radiation accident (Shirsath *et al.*, 2014). Micronuclei are fragments of damaged chromosomes, or whole chromosomes, wrapped with nuclear membrane and released outside the main daughter nuclei. They are the result of non- or mis-repaired DNA breaks that emerge due to the exposure to various clastogenic agents (Strauss *et al.*, 2012).

At particular time-points following irradiation, cells were cultured in T75 culture flasks to 70 – 75 % confluence. They were then treated with 6 µg / ml cytochalasin-B for 40 hours in a humidified 5 % $CO_2$ incubator at 37ºC. Cytochalasin-B (Sigma: C6762, a stock solution dissolved in pure ethanol) is an inhibitor of mitotic spindle fibre formation and thus stops cytokinesis, therefore cells are identified by their binucleated appearance after one nuclear division. For each experimental group, post-incubation with cytochalasin-B, the media was collected and saved in a labelled sterile universal tube. The flasks were washed twice with 10 ml PBS, the first PBS was added to the universal tube but the second wash of 10 ml PBS was discarded. The cells were detached from each flask by adding 1.5 ml (0.025 %) trypsin-EDTA solution for 30 - 60 seconds and incubated at 37ºC for 3-5 minutes to allow cells to dissociate from the flask base. The trypsin-EDTA solution was also collected and added to the universal contents. Dissociated cells were collected with the universal tube contents (saved media, PBS and trypsin) and added back to the universal tube. All cells were centrifuged at 200 × *g* in a Jouan B4 centrifuge at RT for 10 minutes. The supernatants were discarded and the remaining pellets were re-suspended by flicking the end of the tubes. Once re- suspended, 1 ml of hypotonic solution (warmed KCl; 0.55 g potassium chloride (Sigma, P3911) and 100 ml ultrapure water kept in a 37 °C water bath) was subsequently added to each tube in a drop-wise manner and then a further 10 ml KCl was added. The tubes were then incubated in a 37 °C water bath for 5 minutes. Following this, the cells were treated with 3 drops of 25 % glacial acetic acid in methanol (3:1 fixative); all tubes were inverted once and centrifuged at 200 × *g* for 10 minutes at RT. The supernatants were discarded and the pellets thoroughly resuspended prior to addition of 10 ml of 3:1 fixative (added drop-

wise), and left at RT for 10 minutes. Cells were further centrifuged at 200 × *g* for 10 minutes at RT; supernatants were discarded and pellets re-suspended in 0.5 - 1 ml of 3:1 fixative depending on the pellet size. The fixed cell suspension was dropped onto individually labelled, clean / degreased microscope slides and these were left to dry at RT before analysis.

### *2.2.9.1 Staining of slides*

Acridine Orange (AO) is a nucleic acid selective metachromatic red fluorescent stain, which is commonly used in cell cycle determination and enables visualisation of nuclear changes. A phosphate buffer was prepared using 1 tablet (pH 6.8) in one litre of distilled water ($dH_2O$). In brief, two Coplin jars were each filled with 50 ml prepared buffer (pH 6.8), to the first jar 0.0031 g acridine orange (Sigma: A6014) was added. Slides were stained for 25 seconds in the acridine orange/buffer solution and then quickly dipped for a few seconds in the buffer-only jar. Finally, they were left to dry at RT before analysis on a fluorescent microscope (figure 2.9).

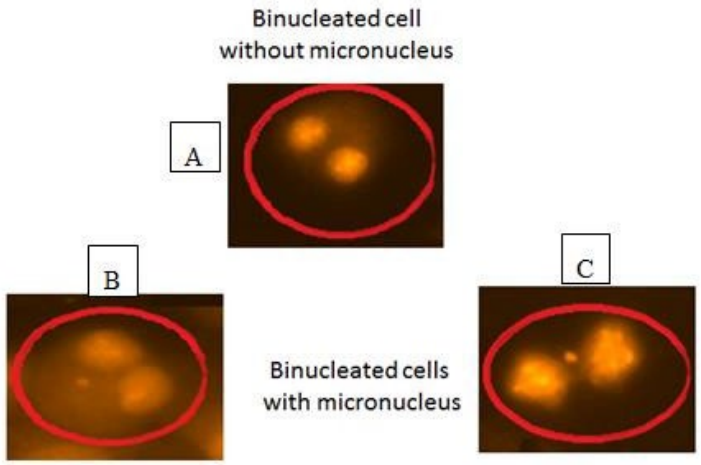


Figure 2.9: Scoring of binucleated cells: (A) a binucleated cell without micronucleus, (B & C) binucleated cells with micronucleus of different size.

### *2.2.9.2 Scoring micronuclei (MN)*

Slides were coded and analysed in a blind and random fashion to avoid observer bias (i.e. slides were coded by a colleague in the research group). Micronuclei were scored only in binucleate cells (BN) and at least 500 binucleate cells were scored per group. The data was presented as the percentage of BN cells with micronuclei (% BN +MN).

#### *2.2.9.3 Statistical analysis*

The P values of raw data from all experimental groups were compared and calculated. Data were examined for normality. The MN data was shown not to have normal distribution thus it was further subjected to Fisher's exact test to calculate the P values. P values ≤0.05 were considered statistically significant. The standard error of the mean (±SEM) was calculated to generate error bars for all experimental groups.

### 2.2.10 Western Blot Assay

Western blotting is a well-established and broadly utilised method for detecting and analysing proteins in a given sample. The technique relies on the specific binding of antibodies to proteins which are immobilised on a membrane to form an antibody-protein complex. The bound antibody is then detected using one of several detection methods (Yang and Ma, 2009).The protocol was modified from Liu *et al*. (2016). In order to release the protein of interest, the membrane of the cells should be disrupted and cell lysis ensured. The sham and irradiated HF19 cells were trypsinized and collected with 10 ml PBS. Cells ($10^7$ cells / 1 mL) were then centrifuged at 300× *g* for 7 minutes at 4°C. The PBS was aspirated and the pellet was re-suspended in a 100 µl cold lysis RIPA buffer (Sigma, 089k6003) in a 1.5 ml Eppendorf immersed in ice. A 25-gauge needle with a 1 ml syringe was used to shred the cells by pipetting them up and down a few times. A Bradford assay was used to measure the protein concentration, using a standard curve constructed from bovine serum albumin BSA (Acas, 268131000) at a series of concentrations (1000, 500, 250, 125, 62.5, and 31,25 µg/ml). The samples were treated with DNase (Thermo Fisher Scientific, 2238G2) (1:10) in a water bath at 37°C to digest the genomic DNA. From each sample, 50 µg of protein in less than 30µl of the sample solution was added to 1/3 (v/v) loading buffer and 5 % (v/v) β-mercaptoethanol. Equal amounts of protein lysate (50 µg per sample) were loaded to gel electrophoresis for protein separation using 0.1 % sodium dodecyl sulphate-polyacrylamide running buffer (1g SDS (Fisher scientific, S/P530/53), 190mM Glycine (Sigma, 56-40-6), 25mM Trizma base (Sigma – Aldrich, BC2205) in one litre distilled water) at 150 V for 1.5 hours. Generally, proteins travel different distances down the gel according to their molecular weight. The proteins were then transferred to a membrane (Immobilon-P, IPVH00010, pore size 0.4) which was soaked in methanol and then in transfer buffer. The membrane

was set under the gel and two layers of western blotting filter paper (Thermo scientific, 84783) soaked in transfer buffer (Thermo scientific, 84731) were placed above and below the gel and membrane. The whole set of gel, membrane and filter paper was subjected to an electric field by putting them between two plates forming an anode (+) and a cathode (-) in the fast blotter pierce G2 machine (Thermo Scientific) at 25 V and 1.3 A for 7 minutes. The membrane was blocked using 5 % milk TBST (TBST: 8g NaCl (Sigma, 57653-1KG), 2.4 g Trizma HCl (Sigma, T5941-1KG) and 800 ml distilled water, then pH adjusted to 7.6 using HCl, 1ml Tween 20 (Sigma, P5927) was then added, and the solution made up to one litre). The membrane with the blocker was left on the tube rollers for one hour. The membrane was then washed three times for five minutes with TBST buffer. Next, the membrane was treated with two primary antibodies for one and a half hours in a cold room on the tube rollers. The first antibody was an anti-TNF-alpha antibody (Abcam, ab9635) at 0.2 µg/µl of milk/TBST and the second was anti-TGF beta 1 antibody at 0.5 µg/µl of milk/TBST (Abcam, ab92486). The membranes were washed three times with TBST for five minutes. Subsequently, the membrane was treated with the secondary antibody Goat Anti-Rabbit IgG H&L (HRP) (Abcam, ab6721) at 1:1000 of TSBT buffer for 1 hour at room temperature. The membrane was again washed three times with TBST for 5 min before adding ECL western blotting detection reagent (GE Healthcare, RPN2235) (1:1 Luminol (RPN2235VI): peroxide (RPN2235V2)). Finally, the membrane was imaged using a Bio-rad imaging scanner and the band intensity was measured using Image Lab software (Liu *et al.*, 2016).

# Chapter 3.
# Early and late effects of high LET alpha-particles on HF19 primary human fibroblast cells

## 3.1 Introduction

Exposure to the naturally occurring radioactive gas radon and its resulting alpha-particle emitting progeny dominates human exposure to radiation and is now known to be the second largest cause of lung cancer after smoking (Milner *et al.*, 2014). As exposure is primarily via inhalation, the largest dose of alpha particles is received by lung cells, although other organs may also receive a significant dose (Dionian *et al.*, 1986). Exposure to alpha-particles may also result from their use in targeted radiotherapy (Sartor *et al.*, 2012) as well as occupational exposures (e.g. in the nuclear industry) (Sumption *et al.*, 2015).

The goal of this study was to evaluate the variation in response of HF19 cells (primary non-transformed human fibroblast cells) exposed to 121 keV $\mu m^{-1}$ alpha-particles as a function of dose (0.0001 - 1 Gy). The biological response was assessed by determining the formation of micronuclei (MN) in binucleate cells along with using the alkaline comet assay to assess DNA damage in HF19 cells. In particular, these assays were used to investigate the induction of Radiation-induced genome instability (RIGI), assessed at early (1 hour) and late (10th and 20th population doublings) time points.

## 3.2 Results

### 3.2.1 Calculating the average number of alpha-particle track traversals per nucleus and per cell

The nuclear and cellular areas were measured to calculate the average number of alpha- particle traversals for a given dose as described previously (see chapter 2, section 2.2.3). While at high doses all cells are traversed, at lower doses there is an increasing fraction of cells that are not traversed. At very low doses, only a small fraction of cells are traversed by a single alpha-particle track. Due to the high LET on those few cells traversed, however, the energy absorbed by the cell, and therefore the

dose to the traversed cell may be large (Hill *et al.*, 2004). The average number of tracks (randomly distributed) per cell, N, traversing a mean nuclear area or cellular area, A (in $\mu m^2$) for a given dose D (in Gy) is given by equation 1.

Equation 1: $N = AD / 0.16 L$,

where L is the LET in $keV\mu m^{-1}$, which is taken as 121 keV $\mu m^{-1}$ (Hill *et al.*, 2004).

The nuclear and cellular area distributions measured for the HF19 cell line using the computer programme 'Image J' are displayed in figure 3.1 and figure 3.2 respectively, giving an average nuclear and cellular area of 189 $\mu m^2$ and 1557 $\mu m^2$. These averaged values were used to calculate the average number of alpha-particle track traversals per nuclear area and cellular area of the HF19 cells, which results are given in table 3.1.

The spatial distribution of α-particles across the Hostaphan dishes and through cells follows the Poisson distribution. Therefore not all cells will be traversed by an equal number of alpha-particle tracks and at a given dose not all cells will be traversed. The fraction of cells traversed, F, by λ tracks (λ = 0, 1, 2, …) is given by equation 2.

Equation 2: $F = \frac{\lambda^n e^{-\lambda}}{n!}$

Where n is the mean number of alpha -particles traversals per cell (equation 1).

Therefore the fractions of cells traversed by one or more tracks, $F_{1+}$, is given by the equation 3.

Equation 3: $F_{1+} = 1-\exp(-n)$

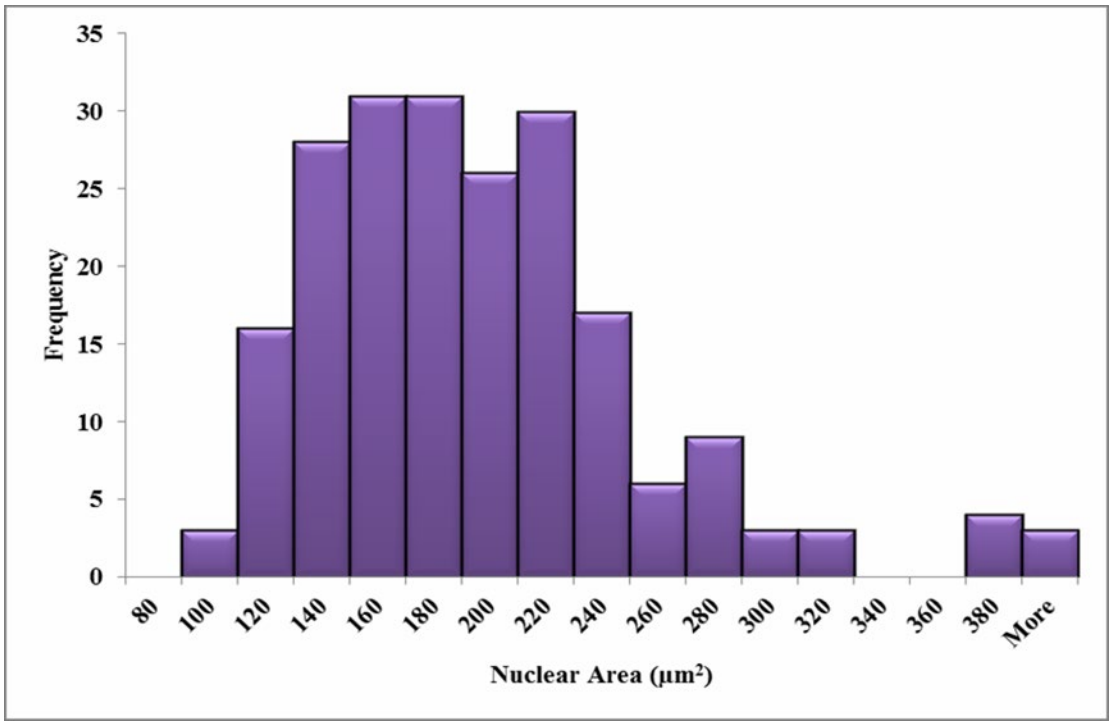


Figure 3.1: Measured nuclear area distributions for the HF19 cell line. The mean area is 189 µm$^2$ for 211 cells over three experiments.

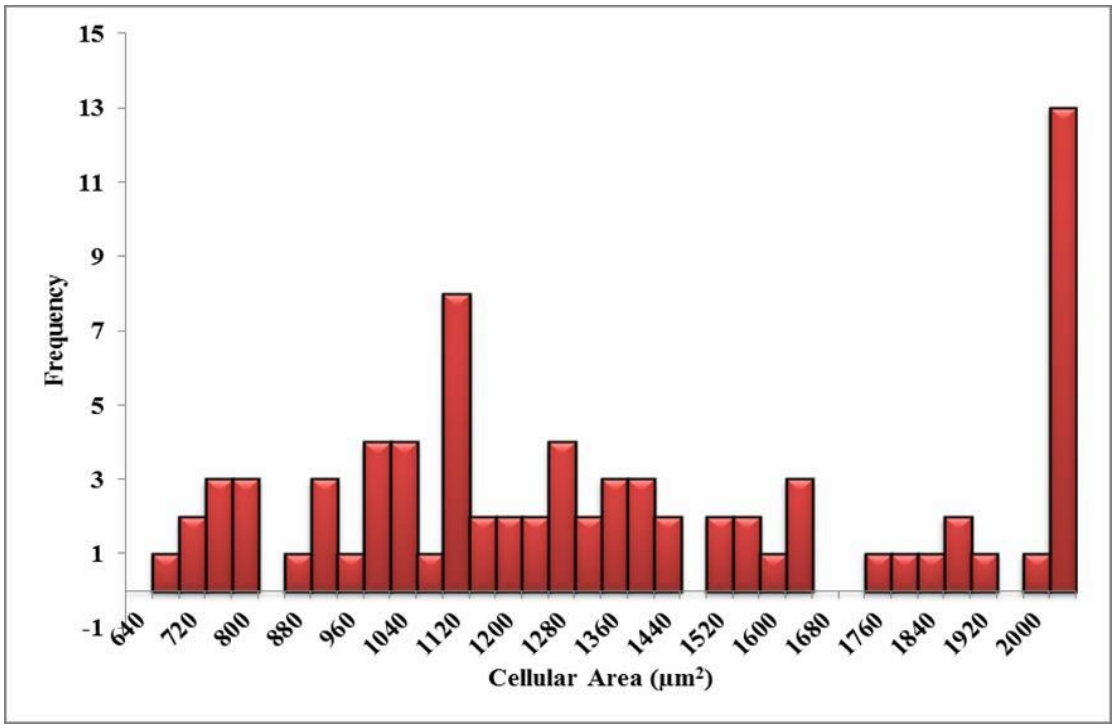


Figure 3.2: Measured cellular area distributions for the HF19 cell line. The mean cellular area is 1557 µm$^2$ for 80 cells over three experiments.

Table 3.1: The variation in the average number of alpha-particle track traversals per cell and per nucleus for the HF19 cell line and corresponding calculated percentages of nuclei and cells traversed as a function of alpha-particle dose. The calculations were based on average cellular and nuclear areas of 1557 $\mu m^2$ and 189 $\mu m^2$ respectively

| Dose (Gy) | Calculated average α-particle track traversals per cell (% of cells traversed by 1 or more tracks) | Calculated average α-particle track traversals per nucleus (% of nuclei traversed by 1 or more tracks) |
|---|---|---|
| 0.0001 | 0.008(0.8%) | 0.0009 (0.097%) |
| 0.001 | 0.080(7.72%) | 0.009 (0.97%) |
| 0.01 | 0.804(55.25% | 0.0976 (9.3%) |
| 0.1 | 8.042(99.96%) | 0.976 (62.32%) |
| 0.5 | 40.211(100%) | 4.881 (99.24%) |
| 1 | 80.423(100%) | 9.762 (99.99%) |

### 3.2.2 Early and late total DNA damage in HF19 cells post low and high doses of alpha-particle irradiation: Comet assay

In order to examine the susceptibility of HF19 to different doses of alpha-particle radiation, the total DNA damage and formation of micronuclei were measured as described previously (see chapter 2, section 2.2.8 and section 2.2.9). The cells were exposed to alpha-particle radiation over a wide range of doses (0.0001-1 Gy). The DNA damage was measured by an alkaline comet assay and the induction of micronuclei in binucleate cells was scored at early (1 h following irradiation), intermediate and delayed time points.

The alkaline comet assay was used to assess the total DNA damage in the HF19 cells caused by the various doses (0.0001-1 Gy) of alpha-particle irradiation at differing time- points as described in chapter 2, section 2.2.8. At very low levels of DNA, the damage is measured using the shape of the comet tail. The percentage of DNA in the tail which represents the DNA damage was scored in each group of approximately 1000 cells for two separate but parallel experiments (the whole slides were scanned).

The results were analysed statistically using the Mann-Whitney U test. Firstly, to highlight the average increase in the magnitude of damage, the median of the percentage of DNA in the tail was presented (Figure 3.3, panels A and B). Secondly, to highlight the varying distributions of damage, data were presented in box plots, which show the entire population of cells (Figure 3.3, panel C).

All control samples showed low levels of background DNA damage with median values of 0.85 ±0.48 %, 0.47 ±0.23 % and 1.67 ±0.27 % for 1 hour, 10 population doublings and 20 population doublings (delayed response) following irradiation respectively.

In general, at 1 hour following the alpha-particle radiation hit, an early large induction of DNA damage was observed across all irradiated groups compared to the corresponding control, as shown in figure 3.3 panels A, B, and C. The individual data sets from two independent experiments showed a variation in the median of the percentage of DNA in the tail but with a similar trend in DNA damage induction between different radiation-level groups except for irradiation at 1 Gy (figure 3.3, panel A). Due to the nature of the alpha-particle tracks, it is important to look at the distribution of the damage using box plots, which is done in figure 3.3 panel C. All doses demonstrated a number of cells with tail DNA up to 50 % and some cells irradiated with 0.0001, 0.001 and 1 Gy showed tail DNA up to 100 %. The highest level of DNA damage was observed with 0.0001 and 0.5 Gy irradiated cells. They were approximately 22 and 15 fold higher respectively compared to the control.

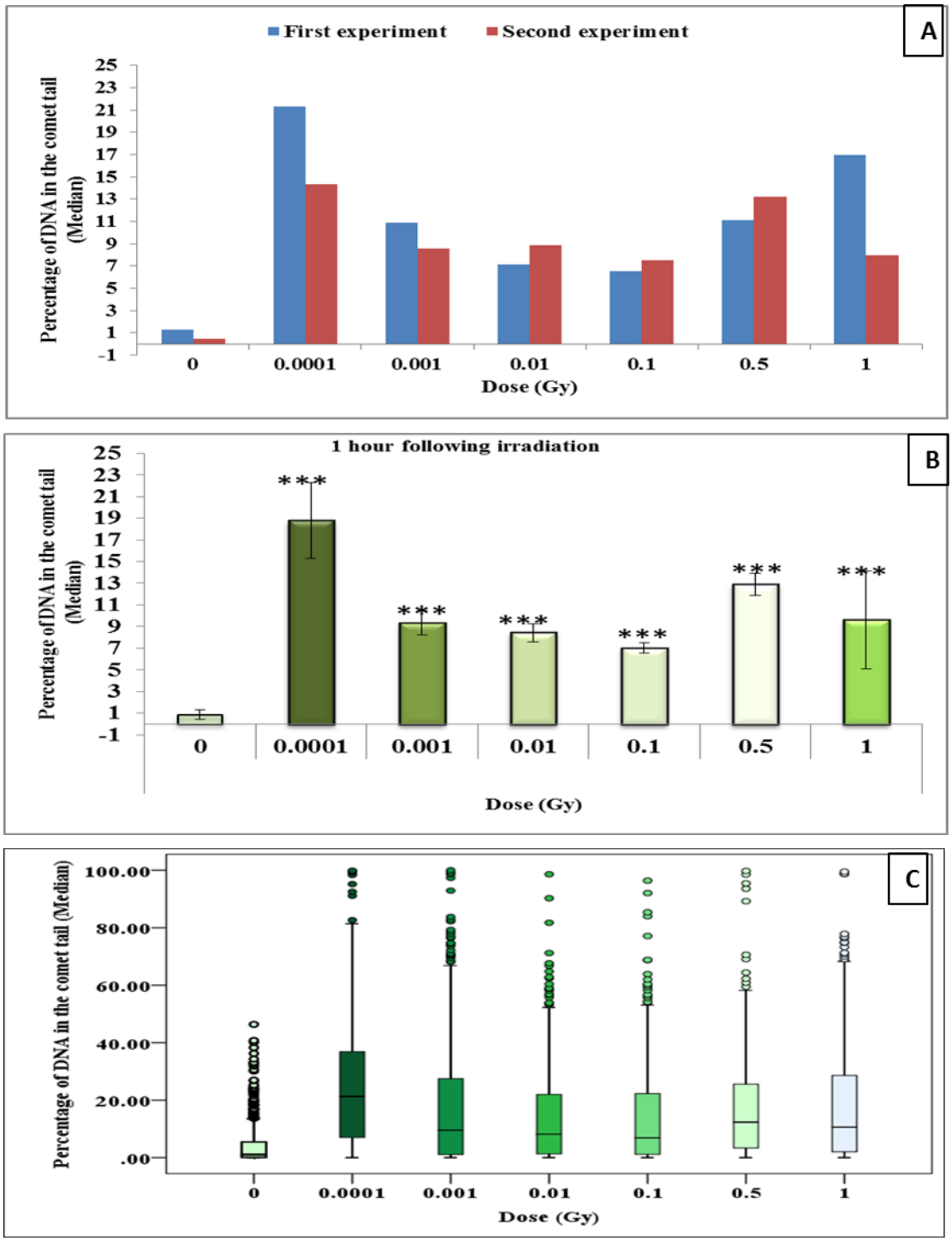


Figure 3.3: Percentage of DNA (damage) in the comet tail in HF19 cells 1 hour following alpha-particle irradiation. HF19 cells were exposed to different doses of alpha irradiation and incubated for 1 hour prior to performing the comet assay. Panel A displays the variation in results between two independent experiments. Panel B illustrates the DNA damage measured by the comet assay (% tail DNA) as combined data for 1000 cells which were scored from two separate, independent experiments. All doses showed highly significant DNA damage (***p≤0.01). Panel C (the box-plot) shows the distribution of damage. The error bars represent the standard error of the median of replicate experiments (±SEM). (*=P≤0.05, **=P≤0.01 ***=P≤0.001).

After 10 population doublings, levels of DNA damage had dramatically reduced; however, they remained above control in the results of both of two separate, parallel experiments (Figure 3.4 panel A). The progeny of HF19 cells irradiated with 0.0001, 0.01and 1 Gy alpha-particle radiation revealed a large induction of total DNA damage 1.74 ± 0.40 %, 1.83 ± 0.34 % and 1.62 ± 0.37 % respectively, which was significantly higher ($p \leq 0.001$) than the control 0.47 ± 0.23 %, as shown in figure 3.4 panel B. There was a smaller, but still nearly twofold increase in DNA damage with the progeny of 0.001, 0.1 and 0.5 Gy cells, 0.99 ± 0.40 %, 0.73 ± 0.37 % and 0.70 ± 0.35 % respectively, compared to the corresponding control.

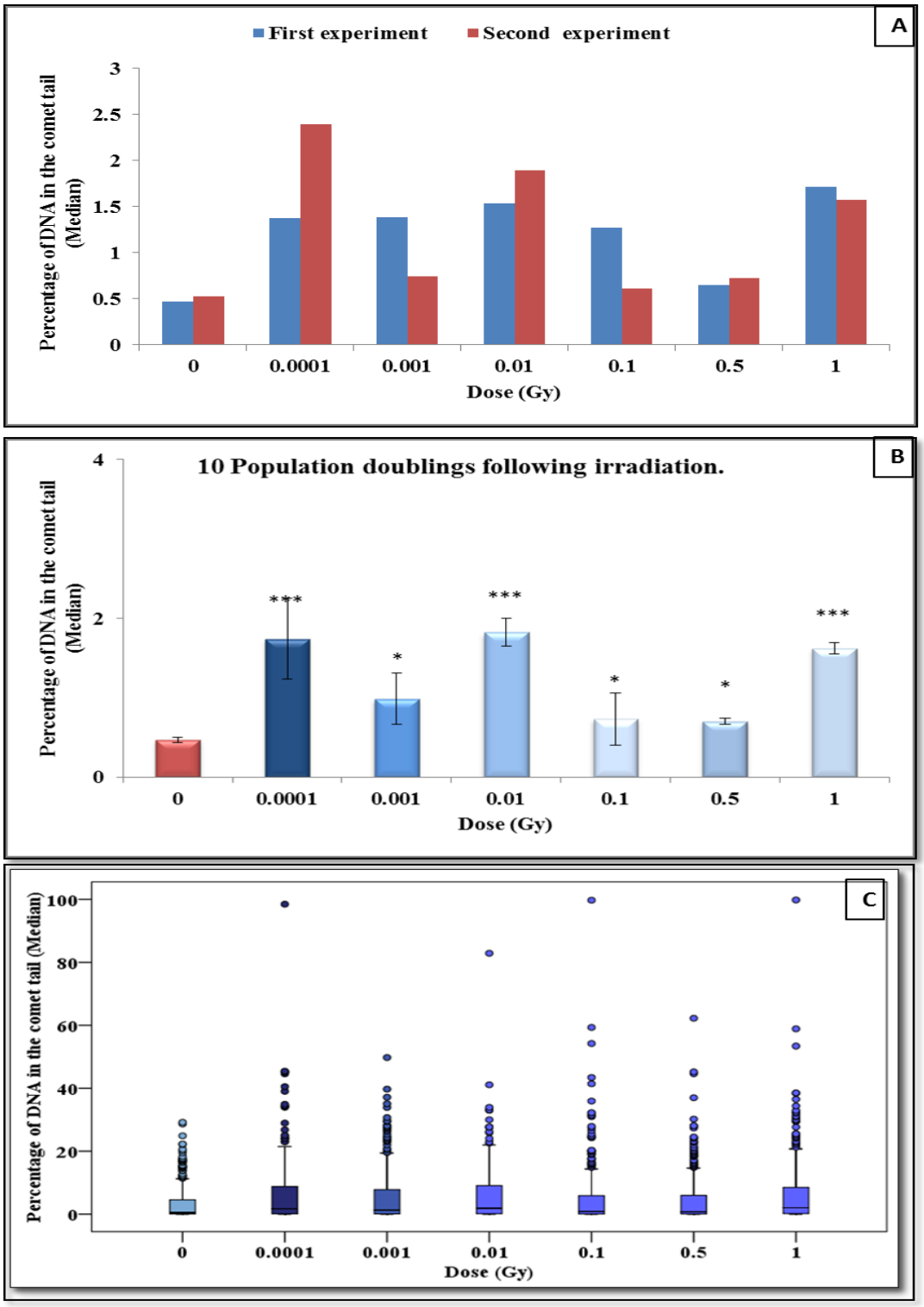


Figure 3.4: Intermediate responses within the progeny of alpha-particle irradiated cell populations after 10 population doublings following irradiation. Panel A presents the individual median values as a function of dose for two independent but parallel experiments. Panel B shows the variation in median values as a function of dose for 1000 cells from both the two parallel but separate experiments. Panel C exhibits the DNA damage distribution of combined data from two parallel but separate experiments. The error bars represent the standard error of the median of replicate experiments (±SEM). (*=P≤0.05, **=P≤0.01 ***=P≤0.001)

At 20 population doublings post irradiation, the level of total DNA damage within the two separate experiments was still high within the progeny of 0.0001and 0.01 Gy compared to the corresponding control (figure 3.5 panel A). The progeny of 0.001 and 1 Gy showed a slight increase in the level of DNA damage (1.89 ±0.32 % and 1.61 ± 0.46 %) compared to control for the first experiment, but not for the second one, which may potentially be because of the high level of damage observed in the control.

At 20 population doublings following irradiation, the median tail DNA of 0.1 and 0.5 Gy irradiated cells (1.61 ± 0.46 % and 1.26 ± 0.34 %) was much more in line with the control value (1.67 ± 0.27 %) as shown in figure 3.5 panel B, whereas the 0.0001 and 0.01 Gy groups showed significantly higher induction of DNA damage. The data for the combined experiments showed an increase in DNA damage for the 0.001 and 1 Gy irradiated groups but this was not a statistically significant result.

However, the distribution of damage was greater than that of control groups for all irradiated groups, suggesting an enhanced level of DNA damage induced post radiation in the progeny of the original cell, even when the median level of damage was not above the control (see figure 3.5 panel C).

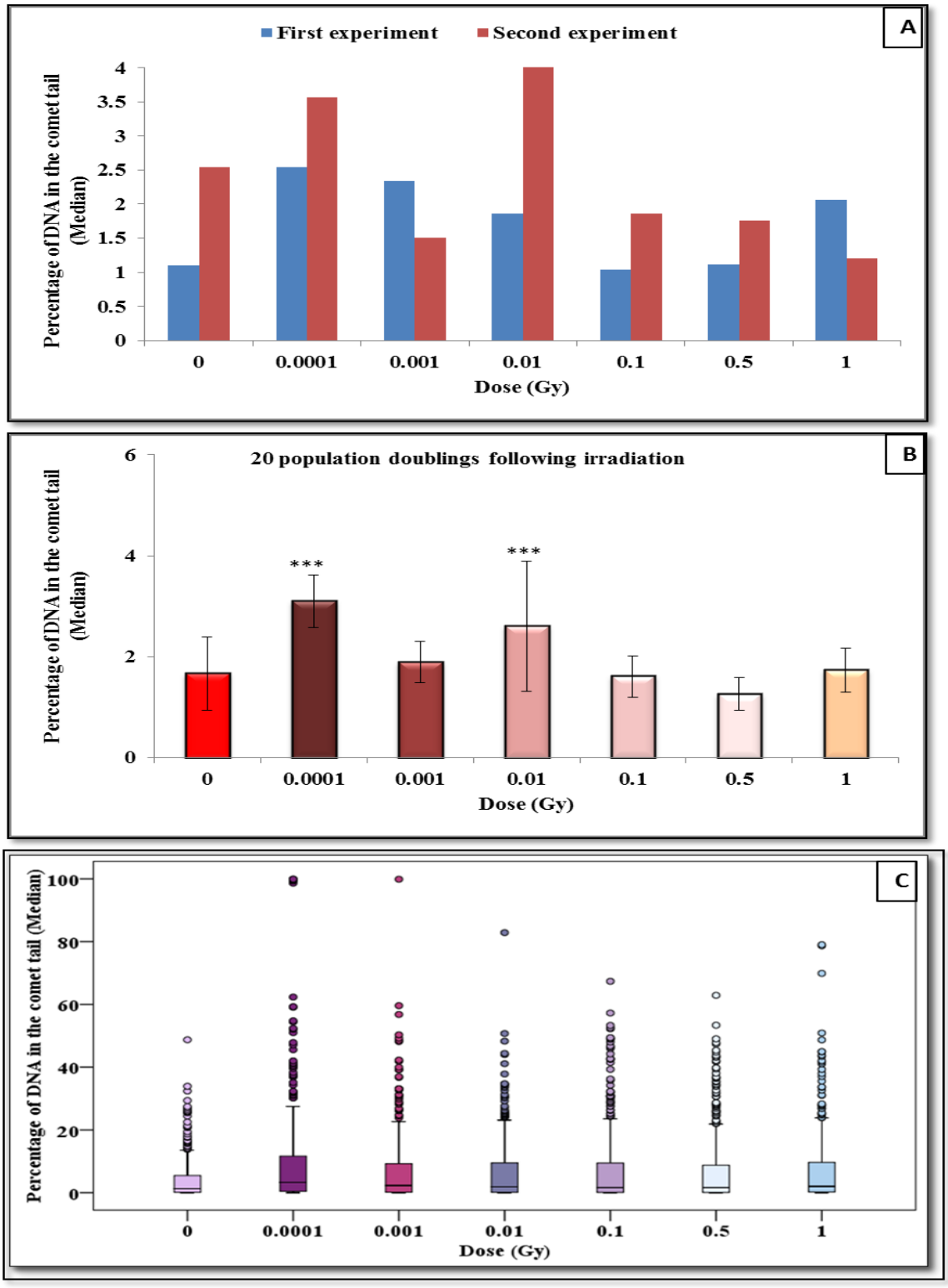


Figure 3.5: The delayed DNA damage in the progeny of alpha-particle irradiated cells following 20 population doublings determined using the comet assay. Panel A presents the individual median values as a function of dose for two independent but parallel experiments. Panel B shows the variation in median values as a function of dose for 1000 cells from two parallel but separate experiments. Panel C exhibits the delayed DNA damage distribution in alpha -particle irradiated cells. The error bars represent the standard error of the median of replicate experiments (±SEM). (*=P≤0.05, **=P≤0.01 ***=P≤0.001).

### 3.2.3 Early and late induction of micronuclei in binucleate HF 19 cells post low and high doses of alpha-particle irradiation: Micronucleus assay

Micronucleus formation was assessed using a cytokinesis-blocked micronucleus assay as described in chapter 2 section 2.2.9. Cells were treated with 6 μg / ml cytochalasin-B for 40 hours at 5 hours following irradiation in a humidified 5 % $CO_2$ incubator at 37ºC. The data are displayed as a percentage of binucleate cells containing micronuclei over total binucleate cells in sham and irradiated HF19 cells. The data of two biological replicates for each dose point at the three-time points (early (5 hours following irradiation), intermediate and late responses) were combined. At least 1000 binucleate cells were analysed in each group (the whole slides were scanned). The error bars represent the SEM (calculated from the median of two separate experiments). Figure 3.6 panel A and B shows the frequency of micronucleus formation in the control (unexposed/un-irradiated cells) and irradiated cells at 5 hours following irradiation (early time-point). Generally, a large induction of micronuclei across all irradiated doses was observed with only very small differences between the two separate experiments as shown in figure 3.6 panel A.

The combined data of both experiments demonstrate a 1.5-fold increase ($P \leq 0.05$) in the induction of micronuclei after exposure to 0.0001 Gy, compared to the control (see figure 3.8 panel B). The formation of micronuclei almost doubled to 8.54 ± 0.28 %, 8.26 ± 0.28 %, 8.20 ± 0.27 % and 8.09 ±0.27 % as the doses increased to 0.001, 0.01, 0.1 and 0.5 Gy respectively, compared to the control (3.79± 0.19 %, $P \leq 0.001$). There was an approximately 2.5-fold increase after exposure to 1 Gy ($P \leq 0.001$).

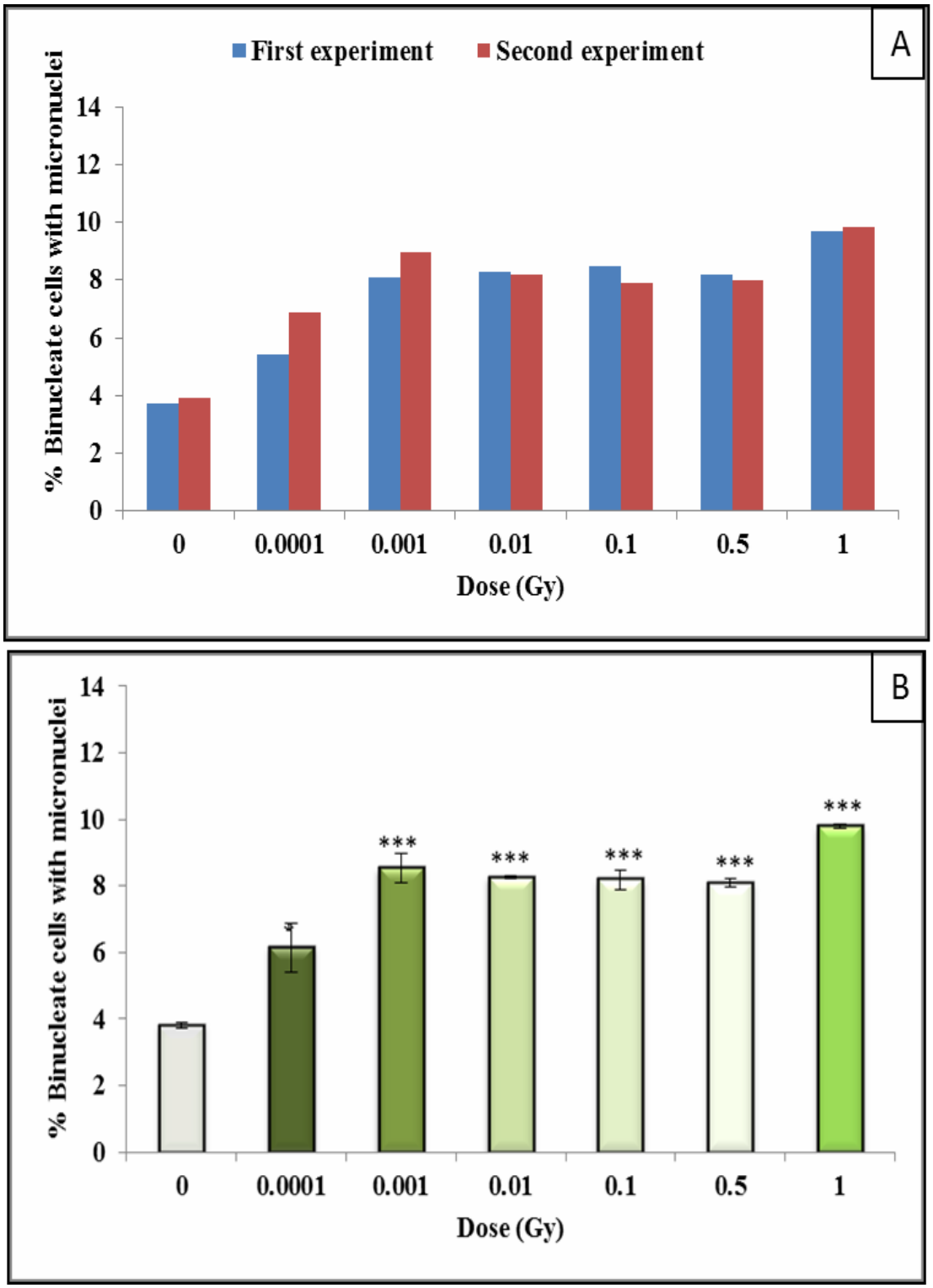


Figure 3.6: Percentage of binucleate cells containing micronuclei over total binucleate cells in control and irradiated HF19 cells at 5 hours following irradiation. Panel A shows the data from the individual experiments from two separate experiments run in parallel. Panel B represents the combined data for 1000 cells from two independent but parallel experiments as a function of dose. Error bars represent the standard error of the mean of replicate experiments (±SEM) from the two independent experiments. P-values were calculated using Fisher's exact test for comparison of data with associated un-irradiated control. * $p \leq 0.05$, ** $p \leq 0.01$, *** $p \leq 0.001$.

In general, the results show a similar trend in the binucleate cells with micronuclei at 10 population doublings following irradiation as for the early time-point with a variation in the trend between the individual data sets for only the 0.001 and 0.1 Gy irradiated groups as shown in figure 3.7 panel A.

For the combined data for both experiments, in the 0.001, 0.01and 0.1 Gy dose groups the formation of MN in binucleate cells rose by more than a factor of 2 (9.64±0.25 %, 8.73±0.28 %, 9.31±0.28 %, respectively) compared to the control (3.81±0.19 %) as shown in figure 3.7 panel B. A high level of binucleate cells with micronuclei was also observed after exposure to 0.0001, 0.5 and 1 Gy, compared to control, which was significant (figure 3.7 panel B).

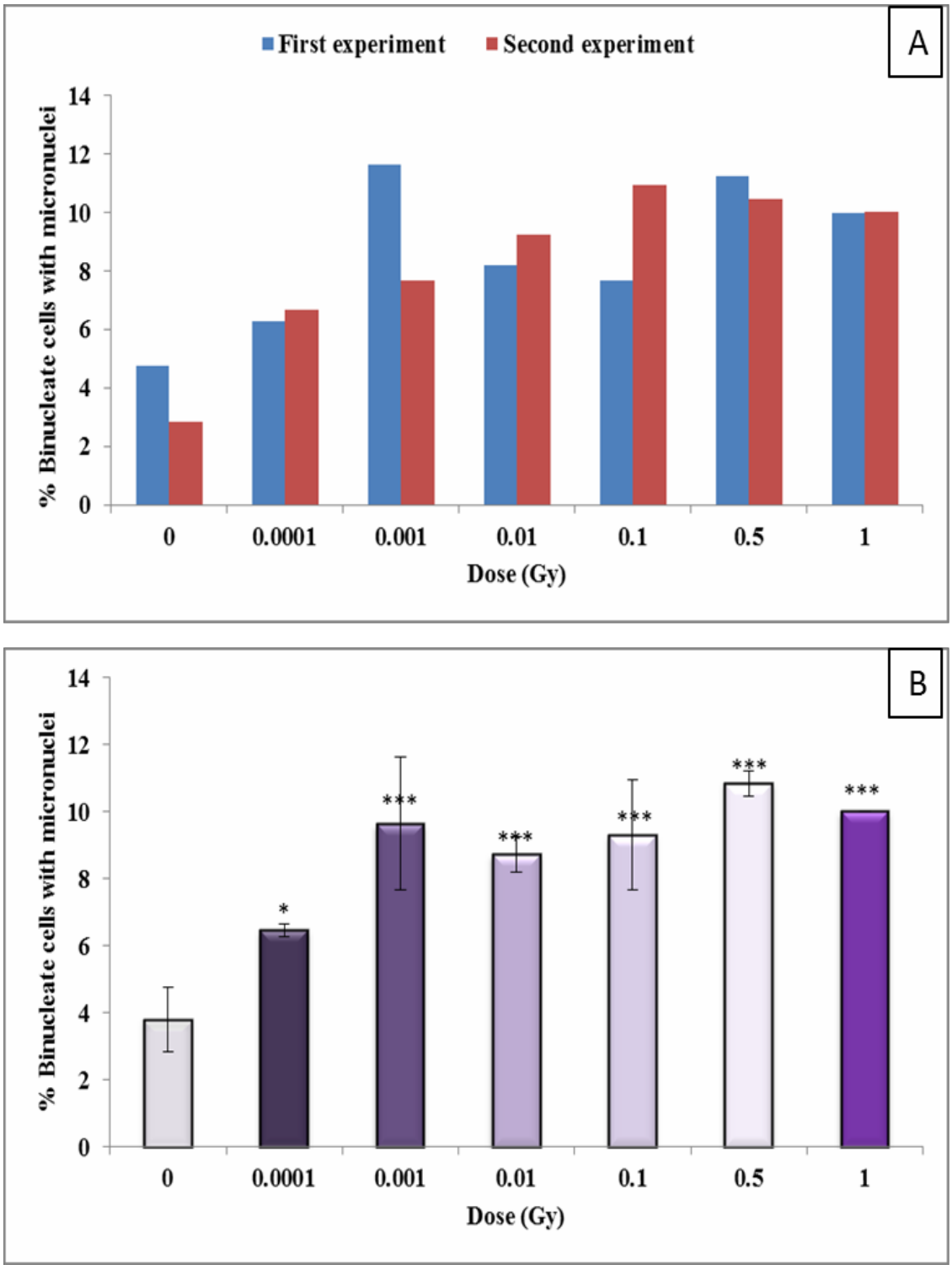


Figure 3.7: Percentage of binucleate cells containing micronuclei over total binucleate cells in control and irradiated HF19 cells at 10 population doublings. Panel A shows the individual data values as a function of dose from two independent but parallel experiment s. Panel B shows Intermediate analysis of the variation in the percentage of binucleate cells containing micronuclei values as a function of dose for 1000 cells from two parallel but separate experiments. Error bars represent the standard error of the mean of replicate experiments (±SEM). P-values were calculated using Fisher's exact test. * $p \leq 0.05$, ** $p \leq 0.01$, *** $p \leq 0.001$.

The results of the delayed cellular response at 20 population doublings following irradiation showed a greater increase in micronuclei induction across all irradiated groups with the same trend between the separate two experiments (see figure 3.8 panel A).

For the combined data for the two independent experiments, HF19 cells demonstrated a significant rise in the binucleate cells with MN, 9.78±0.30 %, 11.46±0.32 %, 12.42±0.33 % and 10.17±0.30 % respectively in the 0.001,0.01,0.5 and 1 Gy irradiated cell groups compared to the control, 5.09±0.22 % ($P \leq 0.001$), as shown in figure 3.8 panel B. The largest induction of binucleate cells with micronuclei was observed in the progeny of 0.5 Gy irradiated cells, which was more than double compared to the corresponding control, figure 3.8 panel B.

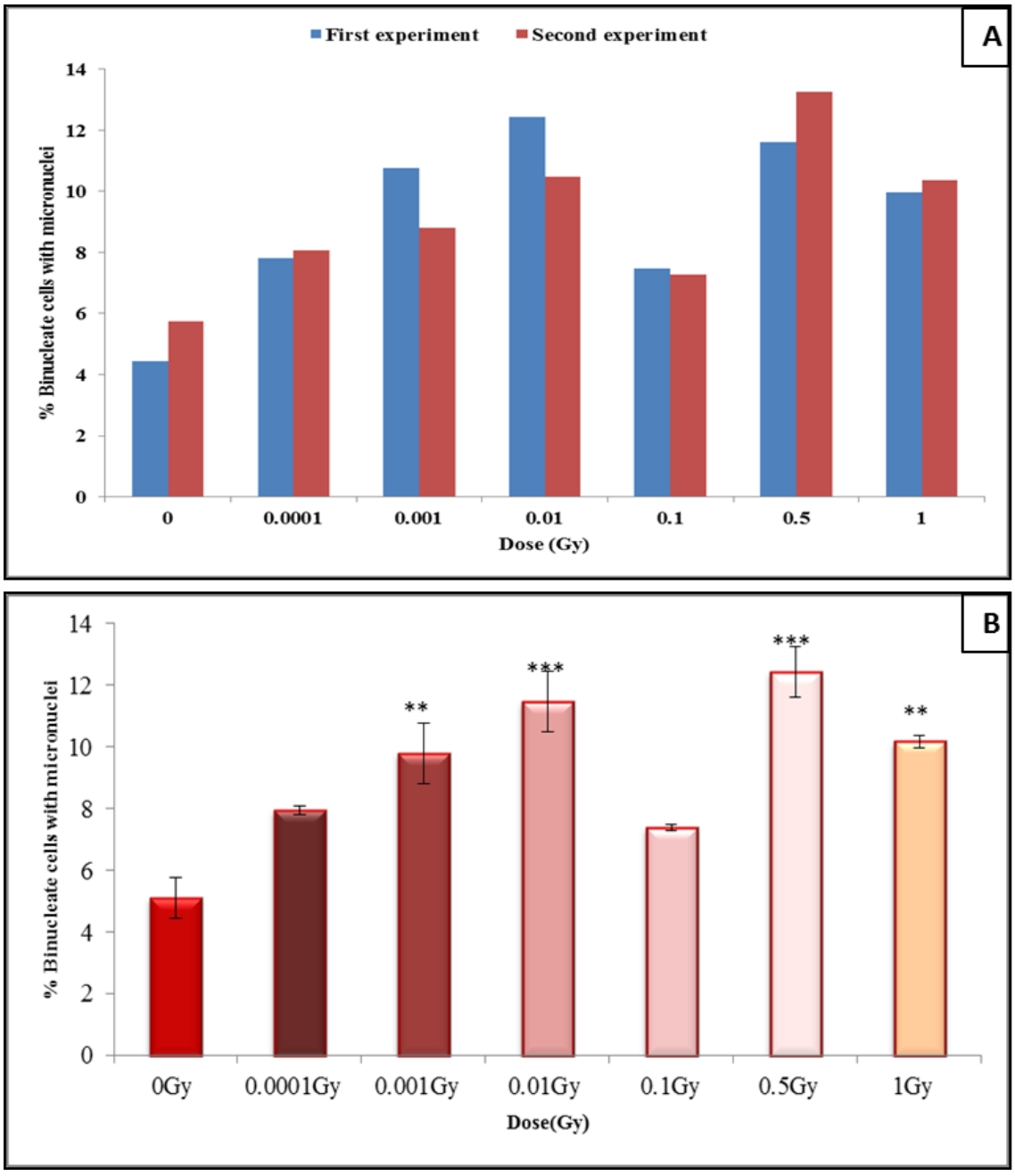


Figure 3.8: Percentage of binucleate cells containing micronuclei over total binucleate cells in control and irradiated HF19 cells at 20 population doublings following irradiation. Panel A reveals the individual data of the variation in the percentage of binucleate cells containing micronuclei values as a function of dose from two independent but parallel experiments. Panel B shows delayed analysis of the variation in the percentage of binucleate cells containing micronuclei as a function of dose for 1000 cells from two parallel but separate experiments. Error bars represent the standard error of the mean of replicate experiments (±SEM). P -values were calculated using Fisher's exact test. * $p \leq 0.05$, ** $p \leq 0.01$, *** $p \leq 0.001$.

## 3.3 Discussion

Previous studies have shown that 0.4 Gy alpha-particle irradiation is able to induce early (at 3 population doublings following irradiation) and delayed (at 20 and 35 population doubling) unstable aberrations, particularly chromatid-type aberrations, in HF19 normal human fibroblast cells compared to control cultures (Kadhim *et al.*, 1998). Ghandhi *et al*. (2008) found that both direct and bystander exposure of human fibroblast IMR-90 lung cells at 0.5 Gy alpha irradiation elevated micronucleus induction and modulated the gene expression at 24 hours following irradiation (Ghandhi *et al.*, 2008). Genomic instability was also observed in immobilised human T-lymphocytes at 12-13 population doublings following high LET irradiation using microbeam technology where each cell centre in a given population of cells was traversed by a single $^{3}He^{2+}$ particle (used as a surrogate alpha-particle). The results showed that approximately 25 % of the cells in the surviving progeny displayed a significant increase in nonclonal chromosomal aberrations ($p<0.001$) with a high frequency of chromatid-type aberrations at 12-13 population doublings following irradiation (Kadhim *et al.*, 2001). Moreover, it is known that bystander effects can also mediate the induction of genomic instability in biological systems. Bowler *et al.* (2006) stated that genomic instability was significantly induced in a bystander cell population of murine primary haemopoietic stem cells following alpha-particle exposure at 10–13 population doublings post-irradiation (Bowler *et al.*, 2006).

It is very well documented that the MN/cytokinesis-block micronucleus (CBMN) assay is one of the most common cytogenetic biodosimetry techniques (Wilkins *et al.*, 2017). For example, a dose-response curve of micronucleus frequencies can be generated using micronucleus assay as a rapid radiation dose assessment technique in human peripheral blood lymphocyte cells following 2–10 Gy irradiation using a Gamma cell 40 $^{137}Cs$ irradiator (Lyulko *et al.*, 2014). Additionally, Wuttke *et al.* (1998) emphasise that a micronucleus assay is a useful tool in biological dosimetry, in cases where either high LET irradiation or mixed beam experiments are involved as the source of radiation exposure. For *in vitro* exposure, the MN method gave a linear response in lymphocyte cells following both neutron irradiation as well as mixed exposure (neutron beam that was followed by 240-kV X-rays) (Wuttke *et al.*, 1998).

The MN assay has also been used as an indicator of genomic instability in lymphocytes of patients with early colorectal adenocarcinoma and neoplastic polyps (Karaman *et al.*, 2008). Kennedy *et al*. (1996) used MN assay as a marker of genomic instability in normal human bronchial epithelial (NHBE) cells exposed to six equal fractionated doses of alpha-particles (0.857 Gy / min) over a 17 day period to achieve a total dose of 2 or 4 Gy. The elevated level of binucleate cells containing micronuclei in the extended progeny of bronchial epithelial cells, in either passage 4, 5 or 6, was evidence that genomic instability is induced following exposure to alpha-particles (Kennedy *et al.*, 1996).

MN assay is used as a biodosimeter in practical situations since the yield of MN increases linearly with dose following exposure to high LET radiation (Vral *et al.*, 2011) as shown by the findings of significant studies. For example, the findings of Seth *et al*. (2014) showed that the number of micronuclei and nucleoplasmic bridges increased linearly with dose following direct exposure to 0.5, 1, 1.5, and 2 Gy neutrons in normal human lymphoblastoid cell lines (GM15036 and GM15510). However, they found that exposure to high LET neutrons did not induce a bystander effect in these cells. Cells treated with neutron irradiated-cell conditioned media (ICCM) did not display significant increases in micronucleus formation compared to controls for either cell line (Seth *et al.*, 2014). Additionally, Curwen *et al*. (2012) have observed an initial linear response in peripheral blood cells with one simple aberration and with multiple aberrations (acentrics, multicentrics and rings) following exposure to low doses of 3.26 MeV alpha-particles (21 mGy, 56 mGy, 92 mGy, 193 mGy, 365 mGy, 469 mGy) although this response flattened at higher doses (Curwen *et al.*, 2012). Turning to our results, they reveal high and statistically significant early induction of micronuclei in HF19 cells following exposure to 0.0001, 0.001, 0.01, 0.1, 0.5 and 1 Gy at 5 hours following irradiation. However, the increase in micronucleus induction reached a plateau at 0.001 mGy where only 8 % of the cells and ≈1 % of nuclei were traversed by alpha-particles. This is in agreement with the previous findings of Azzam *et al*. (2001) who found a higher frequency of micronucleus induction in AG1522 normal human-diploid skin fibroblasts following exposure to very low fluences of alpha-particles at 1–10 cGy. Azzam's study

illustrated that radiation-traversed cells are not solely responsible for the biological response or genetic damage, but that cells in a population in the vicinity of directly hit cells (bystander cells) can also play a role. This can be seen from the fact that the micronucleus induction increased by 3-fold following exposure to 1–3 cGy and 4-fold after exposure to 10 cGy with more cells traversed by alpha-particles at 10 cGy compared to 1–3 cGy. Therefore, the amount of the response at low doses indicates that non-hit bystander cells also experienced DNA damage (Azzam *et al.*, 2001).

In this study, an early elevation (5 h following irradiation) of MN/BN above the control level was observed at 0.0001 Gy ($P \leq 0.05$), where only 0.8 % of the cells and ≈0.1 % of nuclei were traversed by alpha-particles. This effect was increased by up to 2.5-fold with 0.001, 0.01, 0.1, 0.5 and 1 Gy ($P \leq 0.001$), at which the level of MN/BN reached a plateau. One possible explanation is this response is due to alpha-particles depositing most of their energy in the form of relatively small numbers of densely ionising tracks compared to the large number of sparsely scattered ionising electron tracks generated by low LET exposure through the hit cells (Hill *et al.*, 2004). Additionally, ROS induction could be another explanation for the significant MN induction level as an early effect following irradiation of 0.0001, 0.001, 0.01, 0.1, 0.5 and 1 Gy. In support of this idea, it has been documented that a single alpha-particle could instantaneously induce the production of tens of thousands of ROS per track when it traverses a mammalian cell (Feinendegen, 2002). Such bursts of ROS cause a temporary change in cellular signalling, cellular homeostasis, and damage in the direct irradiated and bystander cells. The site and size of these bursts of ROS determine whether there is a prevalence of change in physiological signalling or damage (Feinendegen *et al.*, 1983; Pollycove and Feinendegen, 2001). Werner *et al.* (2014) have found that an increase in ROS levels following exposure to high LET (Fe ion) and low LET (x-ray photons) in HBEC-3KT cells has an independent threshold-like response regardless of radiation quality and dose. This response persisted for 14 days, at which time genomic instability was manifested by increased micronucleus induction, a 3-fold and a 2-fold increase compared to the control following exposure to Fe ions and x-rays respectively (Werner *et al.*, 2014). The existing cell signalling such as ROS leads to an increase in the background level of ROS within the cell and cell population, and this can last over a long period of time,

which may help explain the observation of these effects many population doublings later.

A similar trend was observed after 10 population doublings following 0.0001 Gy irradiation. Additionally, 0.001, 0.01, 0.1, 0.5 and 1 Gy progeny at the delayed time-point illustrated approximately the same trend as the data at 1 hour post exposure, although a slightly higher induction of MN/BN was observed. These results agree with Kadhim *et al.* (1992) who found that a high frequency of non-clonal aberration was produced in the clonal descendants of haemopoietic cells following exposure to α- particles at 0.2-0.8 Gy $min^{-1}$ which transmitted to their progeny (Kadhim *et al.*, 1992).

At a dose of 1 Gy (100 % of the cells being hit), 13-fold more cells in the cell population experience a nuclear insult by alpha-particles than those at a dose of 0.001 Gy (7.72% of the cells being hit). Therefore, the extent of the response at low doses indicates that non- traversed bystander cells also experienced DNA damage. These results are in agreement with the findings of Lorimore *et al.* (1998) who observed that alpha-particles induced chromosomal instability in primary haemopoietic stem cells; however, this instability was also displayed in the progeny of nonirradiated cells which was explained as a result of unexpected interactions between irradiated (1 Gy alpha-particle irradiation) and nonirradiated (bystander) cells. This was demonstrated by irradiating the mouse bone marrow cells with alpha-particles either with or without an interposed grid between the alpha-particle source and the dishes in which the cells were irradiated, which resulted in a reduction in the proportion of traversed clonogenic cells. The cells irradiated with alpha- particles without the grid interposed between source and dishes absorbed a dose of 1 Gy (Lorimore *et al.*, 1998).

Work presented here also agrees with that of Kennedy *et al.* (1996), who suggested that the high increase in MN/BN cells that presented in the progeny of normal human bronchial epithelial cells irradiated with fractionated doses of alpha-particles (total doses 2-4 Gy) indicated that the genetic alterations detected in these cells were not a direct consequence of radiation exposure. Instead, he theorises that these are a result of genomic instability, which could present as an early change following exposure to alpha-particles (Kennedy *et al.*, 1996).

The fact that there was a persistence of induction of micronuclei at 10 population doublings (GI) even with low doses 0.0001, 0.001 where only 0.8 % and 7.72% of cells were traversed by alpha-particles also agrees to some extent with Portess *et al.* (2007) who observed that alpha-particle induced apoptosis at 65 hours following irradiation in non- irradiated transformed 208Fsrc3 cells following co-culture with irradiated non- transformed 208F cells at a dose as low as 0.29 mGy where only 1.1% of the cells were traversed. The apoptosis levels reached a plateau at 25 mGy where 96 % of cells were traversed by alpha-particles. These findings were thought to be due to the modulation of ROS/NOS and TGF-β signalling produced in irradiated cells following irradiation, which resulted in an elevation in extracellular levels of active TGF-β (Portess *et al.*, 2007).

This is also in agreement with previous findings by Azzam and colleagues, who found that the gene expression data obtained from AG1522 normal human-diploid skin cells exposed to very low fluences of alpha-particles indicated that the effects of these doses are not restricted to cells with DNA traversed directly by these particles. In the same study, the level of DNA damage in bystander cells measured several hours following irradiation with alpha-particles exceeded that shown in normal metabolism. This is because of the involvement of gap junction-mediated intercellular communication (GJIC) in mediating the bystander response (Azzam *et al.*, 2001). Azzam *et al.* (2002) have suggested that at low doses of alpha-particles, superoxide and hydrogen peroxide were both involved in causing the radiation effect. As Cu-Zn superoxide dismutase (SOD) converts superoxide to hydrogen peroxide, the fact that SOD acts as a protective agent against micronucleus formation suggests that the superoxide-mediated reactions causing induction of micronuclei in bystander cells are not identical to those of hydrogen peroxide (Azzam *et al.*, 2002).

Because of the weakness of superoxide oxidation and its excellent reductive properties, one suggestion could be that the reduction of metal ions from their less reactive forms (i.e., $Fe^{3+}$and $Cu^{2+}$) to their very reactive lower oxidation state forms (i.e., $Fe^{2+}$and $Cu^{+}$) could provide the pathway for a super-oxide mediated reaction generating micronuclei. Some membrane components could be directly oxidised by these reduced species. This may lead to the formation of by-products of lipid peroxidation (i.e., hydroperoxides and aldehydes) which may cause cell toxicity or

have mutative effects. Alternatively, these metals may participate in the decomposition of hydroperoxides to form hydroxyl or alkoxyl radicals, which are highly reactive species (Azzam *et al.*, 2002)

Additional observations have been made to investigate the role of the bystander effect in the induction of genomic instability. Zhou has observed that two genes, COX-2 and IGFBP-3, were involved in the radiation-induced bystander effect in normal human lung fibroblasts (NHLF) post 0.5 Gy alpha-particle irradiation. This was determined using a microarray specific for cell signalling genes (Zhou *et al.*, 2005). Furthermore, TGF-β and ROS have been reported as mediators in the induction of bystander effects in normal human diploid lung fibroblasts (HFL1) following alpha-particle irradiation at 1.0-19 cGy (Iyer and Lehnert, 2000).

When the irradiated cells propagated to 20 population doublings, the progeny of 0.0001 and 0.1 Gy showed an increase in MN/BN but this was statistically insignificant. The 0.001, 0.01, 0.5 and 1 Gy progeny showed a highly significant induction of MN/BN compared to the corresponding control. This delayed appearance of unrepaired DNA damage in HF19 cells is notably similar to the late chromatid-type aberrations found in 0.4 Gy progeny in which 100 % of HF19 cells are traversed by alpha-particles (Kadhim *et al.*, 1998). Although the 0.1 Gy progeny did not show the same pattern as the other irradiated groups, it is possible that this group would also have followed the same plateau line as cells irradiated with 0.01, 0.5 and 1 Gy if sufficient repeats had been performed. The delayed response of the 0.1 Gy progeny showed one of the main characteristics of RIGI, namely that RIGI does not increase with an increase of radiation dose.

The time at which the comet assay, a method to quantify total DNA damage, is performed is vital. As the assay was performed 1 hour following irradiation, the residual DNA damage is more likely to be measuring either unrepaired DNA lesions affected mostly by the slower DNA repair kinetics (Trzeciak *et al.*, 2008) or an enhancement in the background level of SSB production as a result of an enhancement of oxidative stress. The damage measured can, therefore, be considered to be early damage, rather than initial damage.

The comet assay showed high induction of residual DNA damage (1 hour following irradiation) in irradiated populations of HF19 cells across all doses. This damage is seen clearly through the cell distribution in the boxplot in Figure 3.3. Although only 0.8 % and 8 % of the cells were hit following irradiation with 0.0001 and 0.001 Gy, the induction of total DNA damage was high compared to the corresponding control. From these results, we can speculate that a bystander signal is generated within the first hour following irradiation and that the signal has a harmful effect on HF19 cells. These findings agree to some extent with Lin *et al.* (2014) who found that the induction of sister chromatid exchanges (SCE) (DNA damage) was observed in CHO and L-1 cells where only 0.8 % of the nuclei were traversed by 1.4 mGy alpha-particle irradiation. Therefore, the vast majority of the surviving cells expressing sister chromatid exchanges happened in unirradiated bystander cells (Lin *et al.*, 2014).

These results are also partially in agreement with the findings of Portess *et al.* (2007) who observed an increase in transformed cell apoptosis (in non-irradiated transformed 208Fsrc3 cells following co-culture with irradiated non-transformed 208F cells) post irradiation with low as 2 mGy γ-rays and 0.29 mGy alpha-particles. This effect is linked to the role of the cytokine in radiation-induced signalling which was confirmed utilising a TGF-β neutralising antibody. TGF-β worked as a stimulator to the irradiated cells to make peroxidase (PO) and •NO which in turn results in a huge increase in ROS/RNS signalling in transformed cell apoptosis (Portess *et al.*, 2007).

The number of DNA lesions detected per cell immediately following 1 Gy of low LET x-rays or gamma-rays is approximately: double strand breaks = 40, base damage ≥ 1000, single strand break = 1000 (Hall and Giaccia, 2006). Most of these lesions are repaired successfully by the cells (Hall and Giaccia, 2006). The majority of DSBs are re-joined following irradiation within 1-2 hours (Shuryak, 2016). Some types of DNA damage can be repaired quickly, causing difficulties in detection in living organisms. For example, the halftime of repair for some types of base damage caused by ROS is on the scale of 30 minutes and as short as 3 min (Olive and Banath, 2006). However, as mentioned in chapter 1 section 1.2, the high LET (alpha-particles) has a heterogeneous energy deposition pattern with a highly densely

ionising track. 1 Gy high LET produces approximately 3-4 ionising tracks per cell nucleus (dependent on cell morphology) leading to approximately 30-40 DSBs and 70 % complex DSBs (Kadhim *et al.*, 2006). The proportion of DSB complexity elevates with increasing LET (Goodhead, 1999). For example, 70 % of DSBs produced by high LET contain three or even more breaks (Goodhead and Nikjoo, 1997). This induction of complex DNA damage shows the relationship between the relative biological effects and the LET. The more complex the components of the initial damage, the more severe biological damage appears as a final effect due to the less rapid working of the cell's repair system. This leads to a greater unrepaired residual number of DSBs as a result of the deposition of high LET radiation in the cells (Delara *et al.*, 1995). The complex DNA damage induced by high LET consists of multiple DNA lesions (damaged bases, SSDs, and DSBs closer to each other), which are associated with an increase in chromosomal aberrations, carcinogenesis and cell killing compared to simple DNA lesions produced by low LET radiation (Asaithamby *et al.*, 2011).

The predominant cause of single-strand breaks is ROS which induce DNA base or sugar damage resulting in SSB formation. Additionally, DNA double strand breaks which occur at a lower frequency than SSBs, can also result following replication after ROS-induced lesions (Lindahl, 1993). Most single strand breaks were repaired quickly in PBMCs (peripheral blood mononuclear cells) and most of other cells following irradiation with $^{137}$Cs γ irradiation at doses 0–10 Gy, where the cells were being kept on ice. The vast majority of DNA lesions were removed in the first 5-10 min by fast DNA repair components. The amount of residual DNA damage following 30 min irradiation was dependent on two main parameters; the fast and slower DNA repair components (Trzeciak *et al.*, 2008).

At 10 population doublings following irradiation, the 0.0001, 0.01 and 1 Gy groups still revealed a highly significant level of DNA damage ($P \leq 0.001$) (figure 3.4). The 0.001, 0.1 and 0.5 Gy progeny displayed a significant induction of DNA damage (P-value $\leq 0.05$). In spite of this difference in significance, the distribution in the irradiated groups after 10 population doublings in Figure 3.4 panel B look quite similar to each other.

At 20 population doublings post irradiation, the 0.0001 and 0.01 Gy groups showed a significant induction of DNA damage ($P \leq 0.001$), with initial traversal of 0.8 % and 55.25 % of cells respectively. That indicates that HF19 cells are susceptible to the induction of GI in the progeny at 0.0001 and 0.01 Gy at the delayed endpoint. Nagasawa and Little indicated that the mutation frequency per alpha-particle track at low doses rose unexpectedly, as directly irradiated as well as bystander cells are prone to the formation of mutations. The induction of HPRT delayed mutations was observed in Chinese hamster ovary (CHO) cells 8-10 days following alpha-particle irradiation over the range of 0.05 - 1.2 Gy (Nagasawa and Little, 1999).

However, the median of 0.001, 0.1, 0.5 and 1 Gy progeny did not show a significant increase in DNA damage even though 100 % of cells were traversed, although there are a number of cells that showed extensive DNA damage as seen in the boxplot in Figure 3.5 panel B in which the damage exceeded 30 % tail DNA within the progeny at these doses following 20 population doublings. This could be due to the removal of damaged cells from the cell culture through cell death pathways, as at 20 population doublings following irradiation cells traversed by alpha-particles are poorly repairable. One suggestion is that in order to see if alpha-particles can induce GI with HF19 cells more time-points may be required. In addition, GI can be manifested by using different biological endpoints and techniques at these delayed time-points.

At least 1000 cells were examined for MN and comet assay. This has done using two separate experiments (two biological replicates). The number of binucleate cells examined in MN assay per each group was more than sufficient to give a powerful statistical analysis. On the other hand, Azzam *et al.* (2001, 2002) and Wong *et al.* (2010) analysed 500 binucleate cells to measure the MN induction by alpha-particle irradiation (Azzam *et al.,* 2001; Azzam *et al.,* 2002; Wong *et al.,* 2010). Furthermore, the number of cells analysed using comet assay was also more than sufficient compared to 100-200 cells on duplicated slides analysed by Di Giorgio *et al.* (2004) and Rössler *et al.* (2006) to detect DNA damage induced by alpha particles (Di Giorgio *et al.,* 2004; Rössler *et al.,* 2006).

Additionally, the G*Power results for measuring sample size indicate that the number of binucleate cells analysed in each group was more than sufficient, except

with the 0.0001 Gy group. The comet assay data showed the same trend of sample size. However, 0.1 and 0.01 Gy groups, which showed less induction of DNA damage compared to the equivalent irradiated groups, needed to be repeated at least one more time.

## 3.4 Conclusion

In conclusion, alpha-particle irradiation at 0.0001 - 1 Gy is able to produce a significant induction of micronuclei (at 5 hours following irradiation) and DNA damage (at 1 hour following irradiation) as an early effect. This damage was still evident in all irradiated groups until 10 population doublings. At 20 population doublings, the induction of micronuclei in binucleate cells was still present across all irradiated groups; however, although the progeny of 0.0001 and 0.1 Gy showed an increase in micronucleus formation, this increase was not statistically significant. Genomic instability, therefore, is manifested in HF19 cells by increased micronucleus induction following 0.0001 - 1 Gy alpha-particle irradiation. However, the delayed response seen in the comet assay data showed that the progeny of 0.0001 and 0.01 Gy irradiated cells experienced the induction of GI, which was manifested by a highly significant induction in DNA damage. Conversely, the progeny of 0.001, 0.1, 0.5 and 1 Gy irradiated cells showed no significant increase in DNA damage. It is possible that the persistent elevation of ROS caused repeated insults to the genome which resulted in the formation of micronuclei.

Although progress has occurred in radiobiological research tools, much remains to be learned about how low and high doses of high LET irradiation affects the induction of GI. This study gives a better understanding of biological effects induced in vitro in cell populations exposed to low doses of alpha-particles that are directly relevant to the assessment of health risks to the public from exposure to radon.

# Chapter 4.
# Investigating the susceptibility of HF19 cells to the induction of genomic instability following high (0.42 Gy / min) and low (0.0031 Gy / min) dose rate x-ray irradiation

## 4.1 Introduction

Ionising radiation (IR) deposits its energy in the form of highly structured tracks of ionisation and excitation events. These can not only produced single sites of DNA damage such as single strand breaks (SSBs) or base damage, but the correlated events along these tracks can result in a clustering of damage sites producing both simple double-strand breaks (DSBs) and also complex DSBs (simple DSBs with additional strand breaks and/or base damage within a few base pairs) (Goodhead, 1994, Nikjoo *et al.*, 1994). Correlation of damage to DNA and the surrounding molecular environment can also result in DNA-DNA and DNA-protein cross-links. It is well known that DSBs are one of the most serious types of DNA damage induced by IR as they are more difficult to repair than many other lesions and inaccurate repair of DSBs (e.g. mis-rejoining of broken DNA strands from different chromosomes) can lead to cytotoxic or carcinogenic genomic alterations (Savage, 2002). This damage is generated by direct interaction with DNA or indirectly as a result of radicals (most notably the hydroxyl radical) which are produced as a result of IR interactions in the surrounding water (Hall and Giaccia, 2006).

The conventional dogma in the radiobiology field states that the biological effects of radiation are due to the deposition of energy in the cell nucleus (Morgan, 2012) that has enough energy to ionise DNA and much of the research has focused on relatively high dose rates due to its applications in medicine particularly radiotherapy. The radiation risks at low doses are less studied but are equally important from the standpoint of radiation protection and typical exposures. Low dose and low dose rate effects are primarily stochastic in nature; however, the risks at high doses are deterministic effects (Little *et al.*, 2009). At low dose rates, killing by sub-lethal damage would be less crucial as the prolonged exposure allows time for these lesions to repair during the exposure period (Dillehay, 1990). When cells

experience sub-lethal radiation injury, in many cases the cells are able to correctly repair the damage during the 24 hours following exposure (Miller *et al.*, 2003). However, in the last 2 decades, much evidence has illustrated that radiation also has non-targeted effects which include genomic instability and bystander effects (Morgan, 2012). Transmissible genomic instability in the progeny of cells exposed to ionising radiation can be manifested in different ways such as gene mutations, chromosomal instability, micronucleus formation and an enhanced death rate (Miller *et al.*, 2003; Kadhim *et al.*, 2013). There is clear evidence that in addition to direct exposure, GI can be induced in bystander (non-hit) cells which receive mediated factors from irradiated cells via gap- junctions or secreted factors. Therefore, the perturbation in inter- and intra-cellular signalling within the cell population of hit and non-hit cells may result in a long term change in the oxidative stress in these cells which may ultimately lead to an increase in GI (Lorimore *et al.*, 2003).

This genomic instability can be mediated by many factors such as epigenetics, microRNAs and cytokines following radiation exposure (Fenech, 2006; Filkowski *et al.*, 2010). Radiation-induced genomic instability within irradiated and bystander cells can be influenced by the genotype of the cell being studied, the cell type and the radiation dose and quality (Kadhim *et al.*, 2006; Kadhim *et al.*, 1994). More investigations are required to explain the induction of genetic and epigenetic changes as long-term health effects caused by Ionising irradiation (Tang *et al.*, 2017).

The term “high (acute) dose rate” (HDR) is commonly applied to acute exposures that endure for a few minutes. In comparison, the term “low dose rate” (LDR) applies to prolonged exposures lasting many hours or days. The low dose rate was defined as below 6 mGy / h according to United Nations Scientific Committee on the Effects of Atomic Radiation (UNSCEAR) (Graupner *et al.*, 2016). In general, a given dose of low LET (e.g. x- or gamma-rays) is more effective at inducing an effect if it is delivered within a few minutes (HDR) as opposed to a protracted dose given over a period of hours, days or weeks (Hall and Brenner, 1991; Hall and Bedford, 1964). The biological effects (the induction of micronuclei, increased induced cell death and cell cycle arrest) associated with low-dose rate (LDR) radiation exposures are not yet well characterised (Turner *et al.*, 2015). Despite the relevance of low dose rate (LDR) radiation exposure to radiation protection, to occupational scenarios and to

accidents like those at Fukushima and Chernobyl, there is still a lack of knowledge about its biological effects (Graupner *et al.*, 2016). Therefore, knowledge of the biological effects of LDR exposures experienced in the natural environment is a necessity to construct a good framework for protection in all exposure situations (ICRP, 2007).

In this study, therefore, we looked at the effect of acute dose (high dose rate) and low dose rate x-ray irradiation on the induction of GI in normal human diploid lung fibroblasts, designated HF19, over a time frame which is more relevant to environmental and occupational exposures. Data are presented for a range of assays including cell viability assay, cell cycle measurement, oxidative stress assay, micronucleus assay and comet assay at early and late (10th and 20th population doublings) time points.

## 4.2 Results

### 4.2.1 Cell viability

The percentages of both dead and viable cells following irradiation were measured for 1 Gy HDR and LDR irradiated groups using the Cell Analyser (Muse) according to the DNA-binding dyes' permeability to the reagent, i.e. dead cells lose their membrane integrity, allowing the dye to stain their nuclei, thus allowing differentiation from the non-stained live cells. The viability assay was performed at different times: 30 minutes, 8, 24 and 32 hours following irradiation for two separate but parallel experiments. The results showed the same trend with very small variation between the separate two experiments across all time endpoints (figure 4.1 panel A).

The combined data of both experiments demonstrate for the HDR group, that the cell viability data showed the percentage of viability was lower in the irradiated cells compared to the corresponding controls at all time points following 1 Gy x-ray irradiation. A significant reduction in cell viability was observed in 1 Gy irradiated cells 30 minutes and at 8 hours post-irradiation (79.1 % and 87.5 % ($p \leq 0.05$) respectively) compared to their corresponding controls (89.3 % and 89.5 %). After 24 hours, the percentage of viable cells in the 1 Gy group decreased significantly to 87.4 % compared to the control 93.1 %. However, at 32 hours, viability in the 1 Gy

irradiated cells was lower than the corresponding control cells but this was not statistically significant (figure 4.1 panel B).

The LDR group experimental results, as shown in figure 4.1 panel B, showed a reduction across all groups: at 30 minutes and 8, 24 and 32 hours following 1 Gy low dose rate (0.0031 Gy / minute) x-ray irradiation compared to the corresponding control (see table 4.1). A significant decrease in the viable cells ($p \leq 0.05$) was observed only after 24 and 32 hours following irradiation, although the cells showed a non-significant reduction in the percentage of viability at all early time points compared to control, as shown in figure 4.1 panel B.

Both 1 Gy HDR and LDR x-ray irradiation led to decrease in the cell viability of HF19 cells. The control group had the highest cell viability rate, followed by LDR and HDR at 30 minutes and 8 hours following irradiation. This decrease in cell viability post LDR was statistically insignificant but there was a significant decrease following the HDR exposure compared to the control. When cells were analysed after 24 and 32 hours, the trend had changed. The control group maintained the highest levels of cell viability at 24 and 32 hours, but a significant reduction in cell viability rate was shown with both HDR and LDR at 24 hours post irradiation compared to the control. In contrast to the percentage of viable cells found at 30 minutes and 8 hours following irradiation, the decrease of cell viability rate was greater in LDR compared to the equivalent HDR. Eventually, at 32 hours, the cell viability rate at 1 Gy HDR had almost returned to the control level but the LDR group still showed a significant reduction.

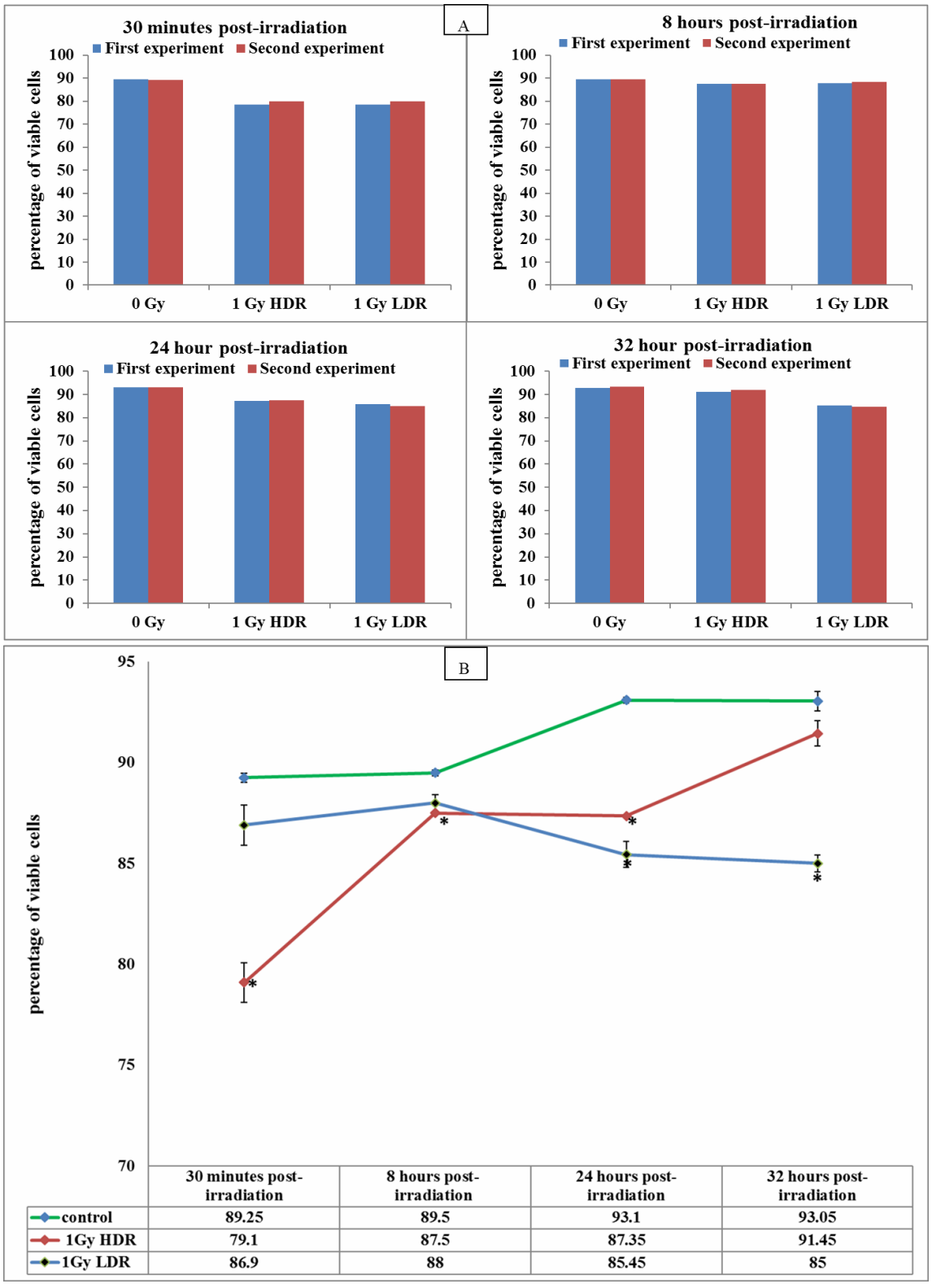


| | 30 minutes post-irradiation | 8 hours post-irradiation | 24 hours post-irradiation | 32 hours post-irradiation |
|---|---|---|---|---|
| control | 89.25 | 89.5 | 93.1 | 93.05 |
| 1Gy HDR | 79.1 | 87.5 | 87.35 | 91.45 |
| 1Gy LDR | 86.9 | 88 | 85.45 | 85 |

Figure 4.1: Percentage of viable HF19 cells at different time points: 30 minutes, 8, 24 & 32 hours following HDR and LDR 1.0 Gy x-ray irradiation. Panel A shows the data from the individual experiments from two parallel but separate experiments. Panel B represents the combined data of two independent parallel experiments. Error bars represent the standard deviation from two independent experiments. * $P < 0.05$, ** $P<0.01$, *** $P<0.001$

### 4.2.2 Cell cycle analysis

The percentage of cells in the G0/G1, S and G2/M phases of the cell cycle in irradiated/sham cells was measured by utilising the cell analyser (Muse) as shown in figure 4.2. The cell cycle assay was performed at different time points: 30 minutes, 8, 24 and 32 hours following irradiation. The data were collected from two biological replicate experiments. The cell analyser presented the percentage of cells in G0/G1, S and G2/M phases; thus a high percentage of cells in the G0/G1 phase meant a low percentage of cells in G2/M phases and vice versa. The percentage of cells in the G0/G1 phase at 30 minutes following irradiation with 1 Gy HDR (0.42 Gy / minute) was significantly high (70.3 %) compared to the corresponding control (67.1 %) using a Student t-test. This percentage decreased to 69.15 % after 8 hours following irradiation. However, the percentage of cells in the G0/G1 phase significantly rose to 88.35 % and 89.15 % respectively after 24 and 32 hours following irradiation compared to their corresponding controls (71.05 % and 69.55 % respectively) as shown in figure 4.2 panel A.

For LDR irradiated cells, a significant increase in the percentage of cells in the G0/G1 phase of the cell cycle occurred at 30 minutes following 1 Gy x-ray irradiation compared to control. However, this increase was not significant at 8 hours following irradiation. The highest percentage of cells in the G0/G1 phase (87.0 %) was observed after 24 hours following irradiation compared to the corresponding control (71.1 %.) This percentage decreased to 68.4 % after 32 hours following irradiation (see figure 4.2 panel A).

Irradiation with HDR and LDR of HF19 cells resulted in delayed progression through the G1, S, and G2 phases of the cell cycle as shown in figure 4.2 panel A, B and C. In both HDR and LDR irradiated cells, the proportion of cells in the G0/G1 phase at 30 minutes following irradiation was significantly higher compared to the control. Interestingly, at 8 hours following irradiation, both HDR and LDR irradiated cells exhibited the same percentage of cells in the G0/G1 phase as the control. However, at 24 hours post-irradiation, both the HDR and LDR irradiated group had the same behaviour, with a significant increase in the proportion of cells arrested in the G0/G1 phase. Eventually, at 32 hours following irradiation, the LDR group showed the same

percentage of cells as the control in the G0/G1 phase but the HDR group showed a highly significant increase compared to the control.

Conversely, S-phase data at HDR demonstrated the opposite pattern to the G0/G1 phase. The percentage of cells in S-phase in the irradiated cells was significantly ($p \leq 0.05$) lower than the control at 30 minutes post irradiation. Data suggested that the reduction in the percentage of cells was due to the high number of cells in G0/G1 which were arrested by irradiation. Data showed a significant decrease in cell percentage in S phase from 12.85 % to 8.85 % following HDR x-ray irradiation. However, cells returned to the normal level (9.3 %) compared to the control (8.65 %) at 8 hours post irradiation. Interestingly, cells showed a significant reduction in cell percentage ($p \leq 0.05$, 3.6 %) at 24 hours post irradiation in S-phase compared to the control (10.95 %). Cells continued showing a high reduction in the cell percentage in S-phase at 32 hours following HDR x-ray irradiation, the irradiated cells percentage being at 3.9 % while the control was 11.8 %. The data at the latter time-point (32 hours) was not statistically significant, although a high difference in the percentage level of cells was observed. This could have been due to the large standard deviation error bar of the control cells, which affected the p-value of the Student t-test as shown in figure 4.2 panel B.

The irradiated cells showed a reduction in the percentage of cells in the S-phase of the cell cycle compared to the control following 1 Gy x-ray irradiation at LDR. A significant decrease was shown at 30 minutes (11 %) and after 24 hours (5.15 %) following irradiation compared to their corresponding controls (12.85 % and 10.95 % respectively), as shown in figure 4.2, panel B. The percentage of cells in S-phase at 8 and 32 hours was similar to the control group.

Irradiation with HDR and LDR of HF19 cells led to a significant delay in progression through S-phase of the cell cycle at 30 minutes and 24 hours following radiation exposure. This delay is due to the slowing of DNA synthesis. However, at 8 hours following irradiation, HDR and LDR group showed the same the percentage of cells in S-phase as the corresponding control. Later, at 32 hours following irradiation, the LDR group revealed the same proportion of cells in S-phase as the control but the HDR group displayed a reduction. This reduction with HDR was not statistically significant compared to the control.

A small increase in cell percentage was observed in the HDR irradiated cells in G2/M phase at 30 minutes following irradiation compared to the control as shown in figure 4.2 panel C. Cells in G2/M showed a similar pattern to the cells in S-phase after 8, 24 and 32 hours. Cells returned to the normal level after 8 hours following irradiation compared to the control. The cell percentage in G2/M phases significantly ($p \leq 0.05$) decreased in the irradiated cells (7.85 %) compared to the corresponding control (16.05 %) at 24 hours following irradiation. Similarly, in the cells 32 hours following irradiation, a reduction in the percentage of cells in the G2/M phase was observed in the irradiated cells (6.75 %); however, it was not statistically significant compared to the control (16.6 %) as shown in figure 4.2, panel C.

At LDR cell irradiation, cells in G2/M showed a similar pattern to the cells at S-phase after 8, 24 and 32 hours. A small reduction in the percentage of cells in G2/M phase was shown after 30 minute time point (16.8 %), at 8 hours (18.35 %) and at 32 hours (19 %) following irradiation compared to their controls (17.55 %, 19.45 % and 16.60 % respectively), although these values were not statistically significant compared to the controls. However, at 24 hours there was a significant reduction ($p \leq 0.05$) in the percentage of cells in G2/M (7.65 %) compared to the control (16.05 %), as shown in figure 4.2 panel C.

In the G2/M phase, HDR and LDR irradiated cells exhibited the same the percentage of cells in G2/M phase as the control, 30 minutes and at 8 hours following irradiation. However, at the 24 hour time-point the HDR and LDR irradiated cells had the same trend as in S-phase with a significant decrease in the percentage of cells in G2/M phase compared to the control. The HDR and LDR groups continued with the same trend as in S-phase with a small decrease in the HDR group and no change within the LDR group as shown in figure 4.2 panel C.

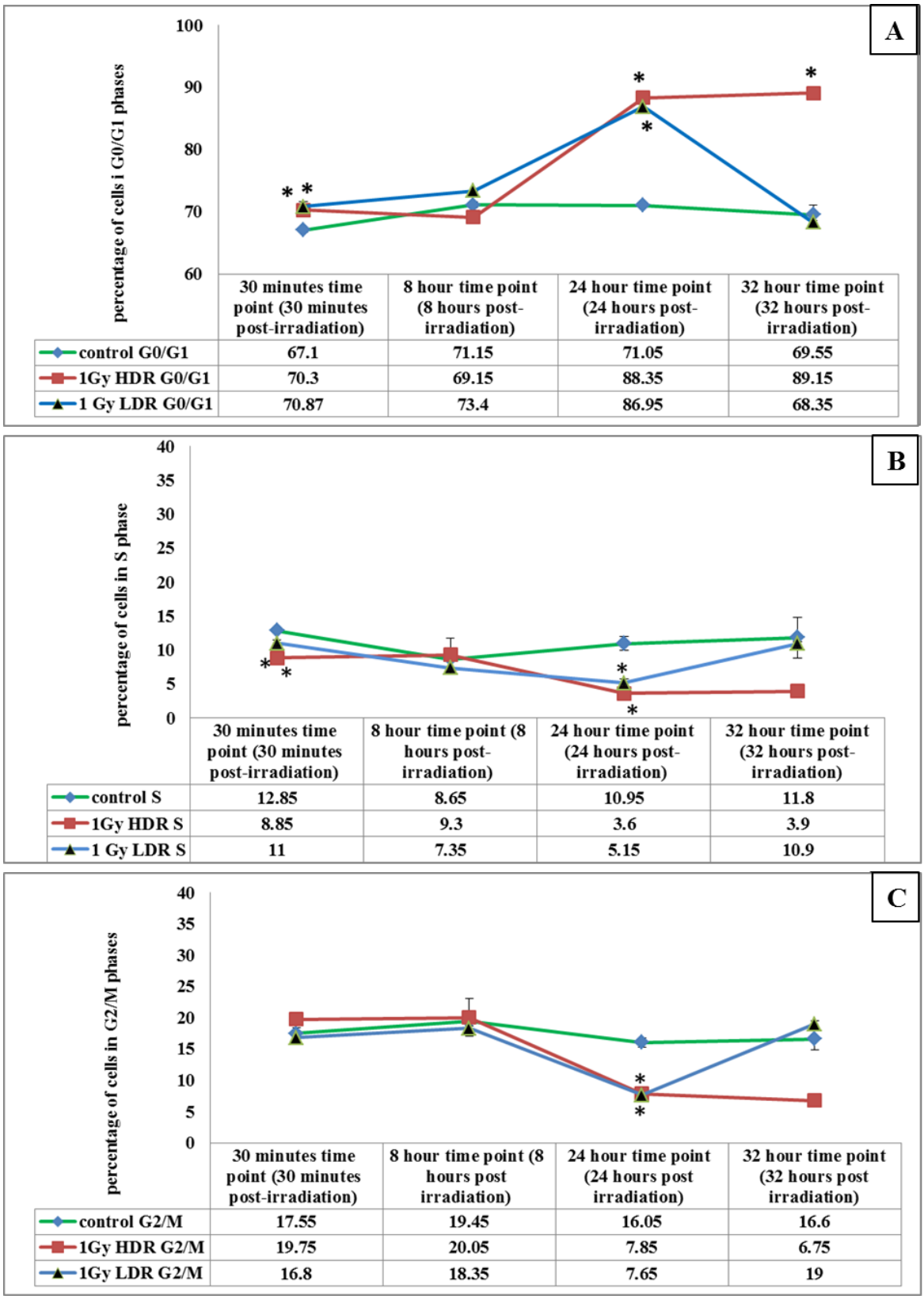


| | 30 minutes time point (30 minutes post-irradiation) | 8 hour time point (8 hours post-irradiation) | 24 hour time point (24 hours post-irradiation) | 32 hour time point (32 hours post-irradiation) |
|---|---|---|---|---|
| control G0/G1 | 67.1 | 71.15 | 71.05 | 69.55 |
| 1Gy HDR G0/G1 | 70.3 | 69.15 | 88.35 | 89.15 |
| 1 Gy LDR G0/G1 | 70.87 | 73.4 | 86.95 | 68.35 |

| | 30 minutes time point (30 minutes post-irradiation) | 8 hour time point (8 hours post-irradiation) | 24 hour time point (24 hours post-irradiation) | 32 hour time point (32 hours post-irradiation) |
|---|---|---|---|---|
| control S | 12.85 | 8.65 | 10.95 | 11.8 |
| 1Gy HDR S | 8.85 | 9.3 | 3.6 | 3.9 |
| 1 Gy LDR S | 11 | 7.35 | 5.15 | 10.9 |

| | 30 minutes time point (30 minutes post-irradiation) | 8 hour time point (8 hours post irradiation) | 24 hour time point (24 hours post irradiation) | 32 hour time point (32 hours post irradiation) |
|---|---|---|---|---|
| control G2/M | 17.55 | 19.45 | 16.05 | 16.6 |
| 1Gy HDR G2/M | 19.75 | 20.05 | 7.85 | 6.75 |
| 1Gy LDR G2/M | 16.8 | 18.35 | 7.65 | 19 |

Figure 4.2: panel A, B and C: The percentage of HF19 cells in G0/G1 phase (panel A), S -phase (panel B) and G2/M phase (panel C) as a function of time (30 minutes, 8, 24 and 32 hours) after irradiation with 1 Gy x-rays at HDR (0.42 Gy / minute) and LDR (0.00313 Gy / minute). Error bars represent the standard deviation from two independent experiments. * $P < 0.05$, ** $P<0.01$, *** $P<0.001$.

### 4.2.3 A cell response curve following exposure to acute/high dose rate x-ray irradiation.

#### *4.2.3.1 Micronucleus assay (MN assay)*

A micronucleus assay was utilised to evaluate chromosomal damage following x-ray irradiation. Five hundred binucleate cells were analysed from each experiment. The experiment was repeated three times on different days. In general, a large, initial induction of micronuclei was observed across all irradiated groups immediately following x-ray irradiation, as shown in figure 4.3. The individual data from three independent experiments showed a variation in the percentage of binucleate cells with micronuclei but with the same trend except for the 4 Gy group (figure 4.3).

The cells showed a significant increase in micronucleus formation ($p \leq 0.001$) immediately following irradiation for all doses studied (0.5 - 4 Gy delivered at 0.42 Gy / min), compared to the control (figure 4.4, combined data). The 1.5 Gy showed lower response compared to 1 and 2 Gy but the micronucleus induction level was statistically significant compared to the control cells.

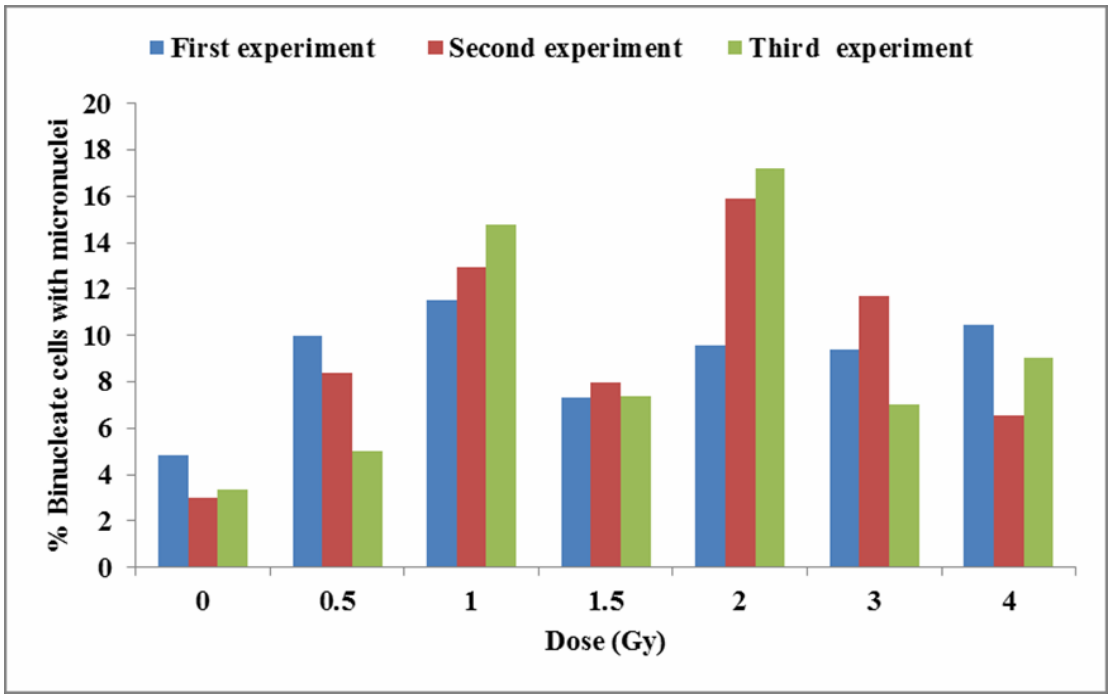


Figure 4.3: Variation in the percentage of binucleate cells (BN) with micronuclei (MN) (%MN/BN) in HF19 cells among the experiments (first, second and third experiments) as a function of x-ray dose (HDR, the dose rate of 0.42 Gy/min). Cytochalasin B was immediately added following irradiation (< 5 minutes).

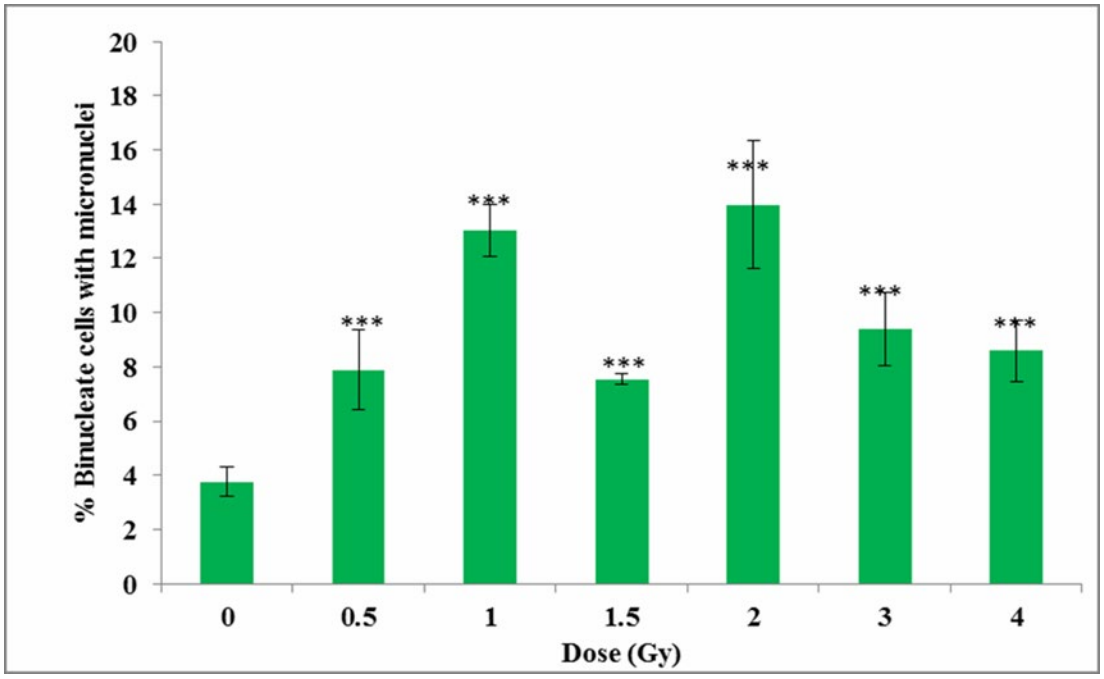


Figure 4.4: A bar chart representing the relationship between x -ray dose (HDR, dose rate of 0.42 Gy / min) and the percentage of binucleate cells (BN) with micronu cleus (MN) (%MN/BN) induction in HF 19 cells following x -ray irradiation, with cytochalasin B immediately following irradiation. Combined data from three independent experiments. Error bars represent the standard error of the mean of replicate experiments (SEM).* $P < 0.05$, ** $P<0.01$, *** $P<0.001$.

## 4.2.4 Early, intermediate and delayed response of HF19 to dose ranges at high (0.42 Gy /minute) and low dose rates (0.0031 Gy / minute) of x-ray irradiation.

### *4.2.4.1 DNA damage: Comet assay*

The alkaline comet assay was used to assess the variation of SSB and alkali-labile sites in the HF19 cells following irradiation as a function of dose delivered at either a high dose rate (0.42 Gy / min) or a low dose rate (0.0031 Gy / min) at differing time-points following irradiation. This method allows very low levels of DNA damage in individual cells to be analysed by measurement/assessment of the comet tail shape, which ultimately represents the percentage of DNA damage. Each experimental group had 500 comet tails analysed from one single experiment. The results were analysed statistically using the Mann-Whitney U test. Initially, the data were exhibited as the median of DNA in the comet tail, as shown in Figure 4.5, to highlight the average increase in the magnitude of damage. To highlight the varying distributions of damage in the entire population of cells, the data were additionally represented in box plots (Figure 4.6 and 4.7). Figure 4.5, 4.6 and 4.7, show the early (24 hours following irradiation) DNA damage induction in HF19 cells following irradiation at HDR and LDR. At HDR, a significant increase ($p \leq 0.001$) in DNA damage was observed in the 0.1 Gy (7.15 ±0.86 %) and 0.5 Gy cells (4.02 ±1.14 %) compared to the control (1.26 ±0.23 %). In contrast, no significant induction of DNA damage was observed following 1 Gy. DNA damage was significantly increased following 1.5 Gy (4.98 ±0.76 %) and 2 Gy (10.22 ±1.11 %) compared to the control, but levels were lower for the 2.5, 3 and 4 Gy doses though these were still significantly higher than the control (3.50 ±0.87 %, 2.4±0.99 % and 7.37±1.10 %, respectively).

At LDR, the exposure of HF19 to different doses demonstrated an early induction of DNA damage following irradiation which was significant with 0.1 Gy ($P \leq 0.001$), 0.5 Gy ($P \leq 0.05$), 1 Gy ($P \leq 0.001$), 2 Gy ($P \leq 0.001$), 2.5 Gy ($P \leq 0.001$) and 4 Gy ($P \leq 0.001$) x-ray irradiation compared to control as shown in Figure 4.5. The 0.1 and 2 Gy groups presented the greatest induction of DNA damage with 24.3 ±1.0 % and 24.8 ±1.28 % respectively compared to the control (1.262 %). However, there was no induction of DNA damage at 1.5 and 3 Gy (1.73 ±1.07 % and 1.00 ±1.10 % respectively) compared to control (1.26 ±0.23 %), as shown in Figure 4.5.

There is no consistent difference observed between the HDR and LDR experiments across the dose range, although there appears to be a large difference in radiation response between HDR and LDR groups evident at 0.1 and 2 Gy; however this is likely to be a result of the data being obtained from a single experiment. Looking at the distribution of the damage in Figure 4.6 and 4.7, a few cells in both the HDR and the LDR group showed tail DNA of up to 60 %.

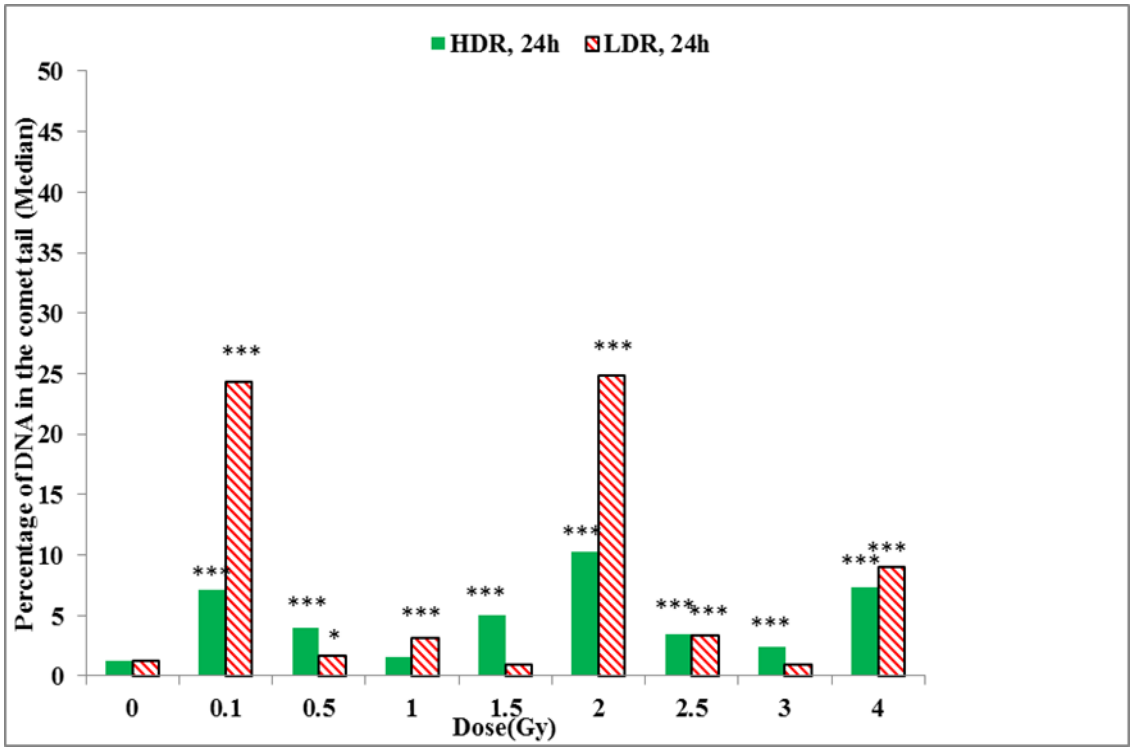


Figure 4.5: Variation in the percentage of DNA in the comet tail after 24 h following completion of the irradiation as a function of dose, delivered at a high dose rate (0.42 Gy / min) or low dose rate (0.0031 Gy / min). The data points represent one single experiment. * P < 0.05, ** P<0.01, *** P<0.001.

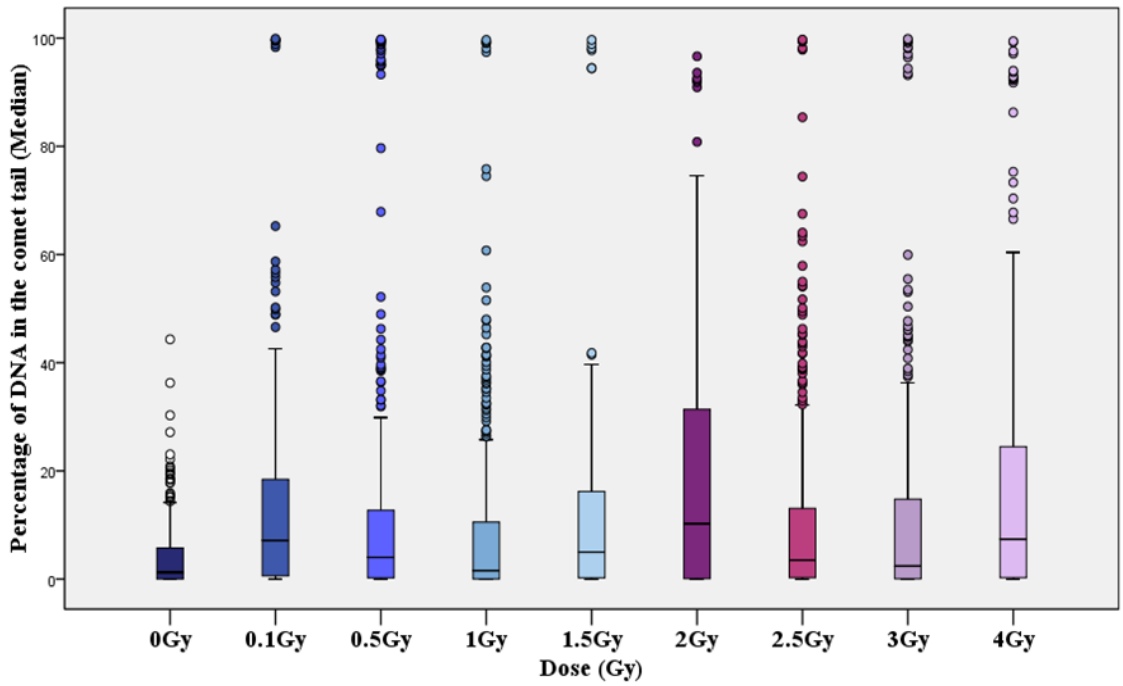


Figure 4.6: The box-plot shows the distribution of damage in HF19 tail after 24 h following completion of the irradiation as a function of dose, delivered at a high dose rate (0.42 Gy / min). The data points represent one single experiment. * P < 0.05, ** P<0.01, *** P<0.001.

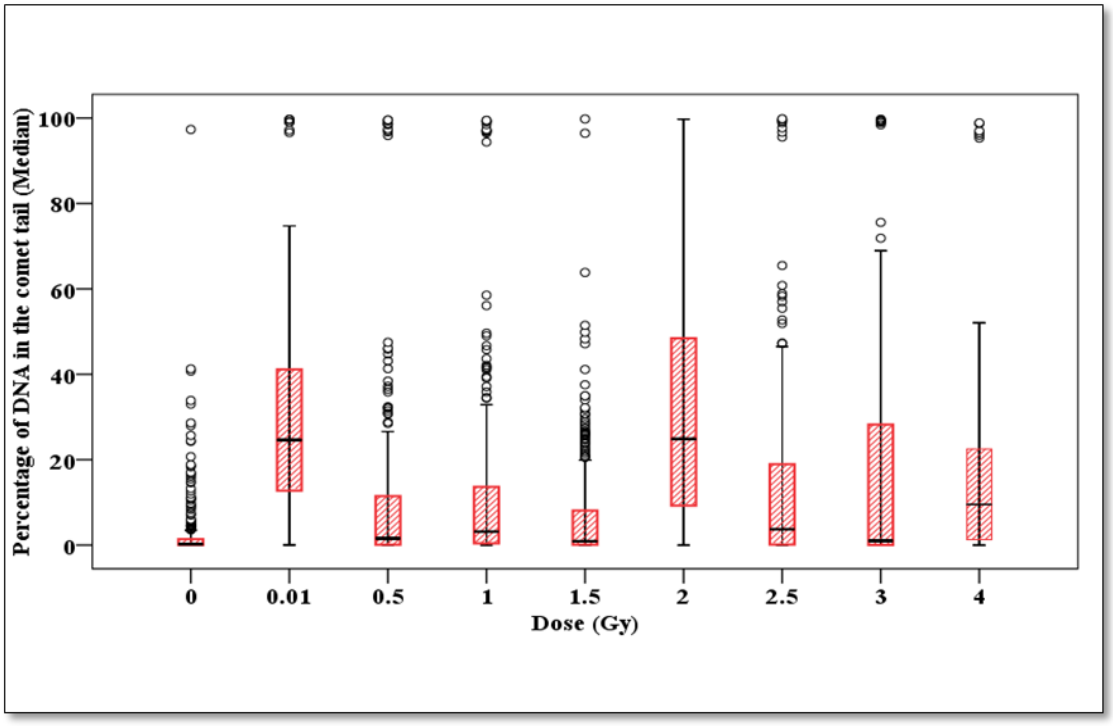


Figure 4.7: The box-plot shows the distribution of damage in HF19 tail after 24 h following completion of the irradiation as a function of dose, delivered at a low dose rate (0.00313Gy / min). The data points represent one singl e experiment. * P < 0.05, ** P<0.01, *** P<0.001.

At 10 population doublings (intermediate time-point) in the progeny of the HDR group, the HF19 irradiated cells for all doses with the exception of 3 Gy demonstrated a significant increase in the level of DNA damage ($p \leq 0.001$) compared to the control, as shown in Figure 4.8. In contrast, the 3 Gy group demonstrated a reduction in DNA damage (2.255 ±0.854 %). The highest levels of DNA damage were observed in the 0.1, 1 and 2.5 Gy groups (35.69 ±1.330 %, 23.85 ±1.158 % and 44.375 ±1.1628 % respectively) and modest levels of damage were observed in the 1.5 Gy and 4 Gy groups (11.46 ±1.001 % and 0.04 ±0.935 % respectively).

With the LDR group, a large, highly significant induction of DNA damage ($p \leq 0.001$) was observed in the progeny of 1.5 and 2.5 Gy irradiated cells (13.276 ±0.973 % and 12.066 ±0.868 %) compared to control (0.680 ±0.312 %). Moreover, there was also a significant induction of DNA damage ($p \leq 0.001$) observed within the progeny of 1, 2 and 4 Gy irradiated cells (1.826 ±0.482 %, 2.572 ±0.670 % and 2.966 ±0.826 % respectively) compared to control. In contrast, the progeny of 0.1 and 3 Gy demonstrated a reduction in DNA damage compared to the control, as shown in Figure 4.8.

It is clearly seen that more DNA damage was induced in the progeny of all the HDR groups at 10 population doublings compared to their corresponding LDR groups across most of the dose range. For the LDR data, there is a suggestion that an enhanced response may be possible at higher rather than lower dose. Data were also displayed in box plots demonstrating the entire population of cells to highlight the varying distributions of damage (Figure 4.9 and 4.10).

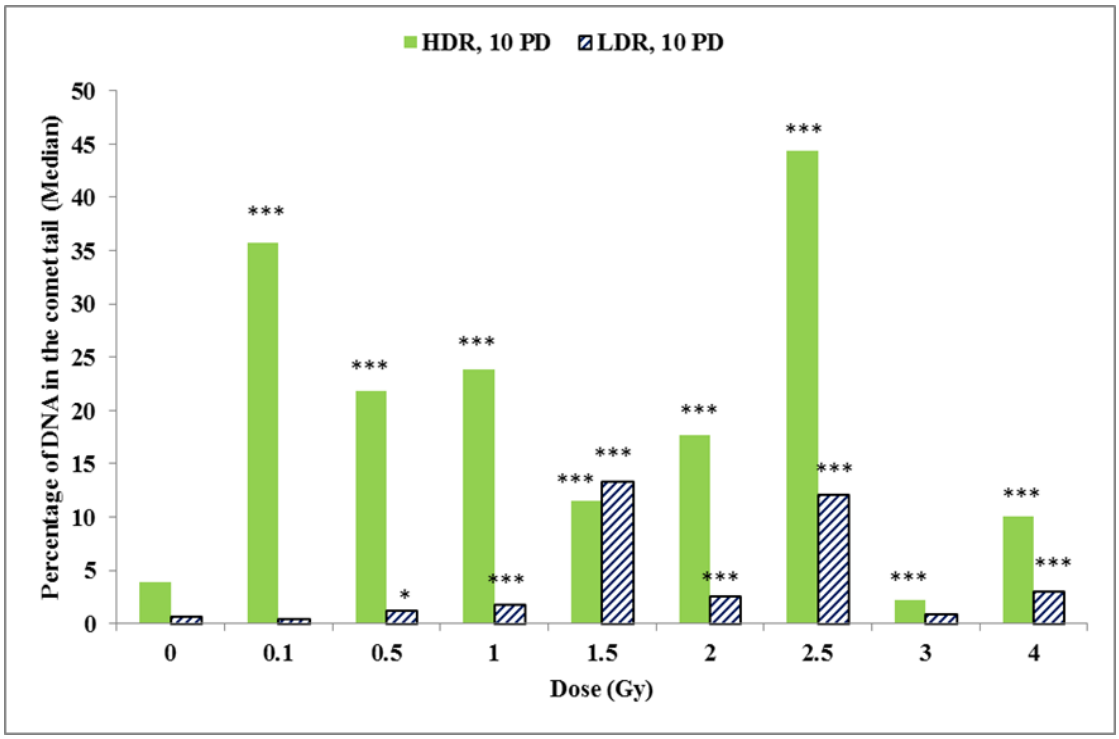


Figure 4.8: Intermediate responses within the progeny of directly irradiated HF19 cells after 10 population doublings following irradiation as a function of dose, delivered at a high dose rate (0.42 Gy / min) or low dose rate (0.0031 Gy / min). The data points represent one single experiment. * P < 0.05, ** P<0.01, *** P<0.001.

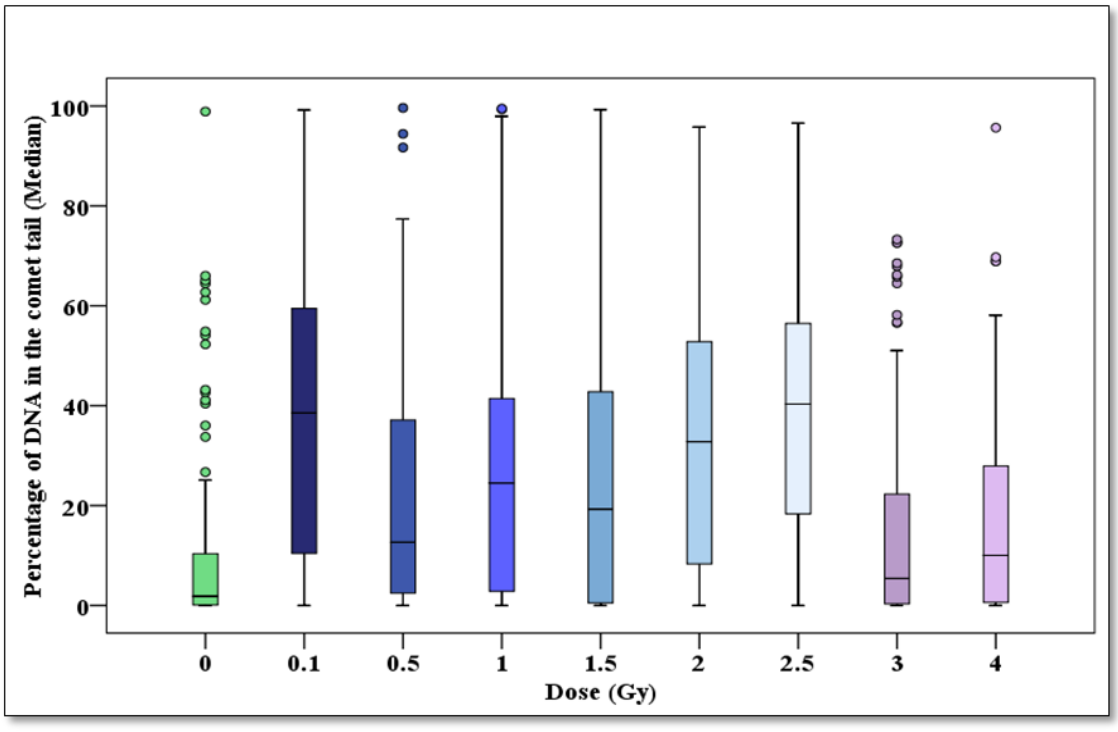


Figure 4.9: The box-plot shows the distribution of da mage in HF19 after 10 population doublings following irradiation as a function of dose, delivered at a high dose rate (0.42 Gy / min). The data points represent one single experiment. * P < 0.05, ** P<0.01, *** P<0.001.

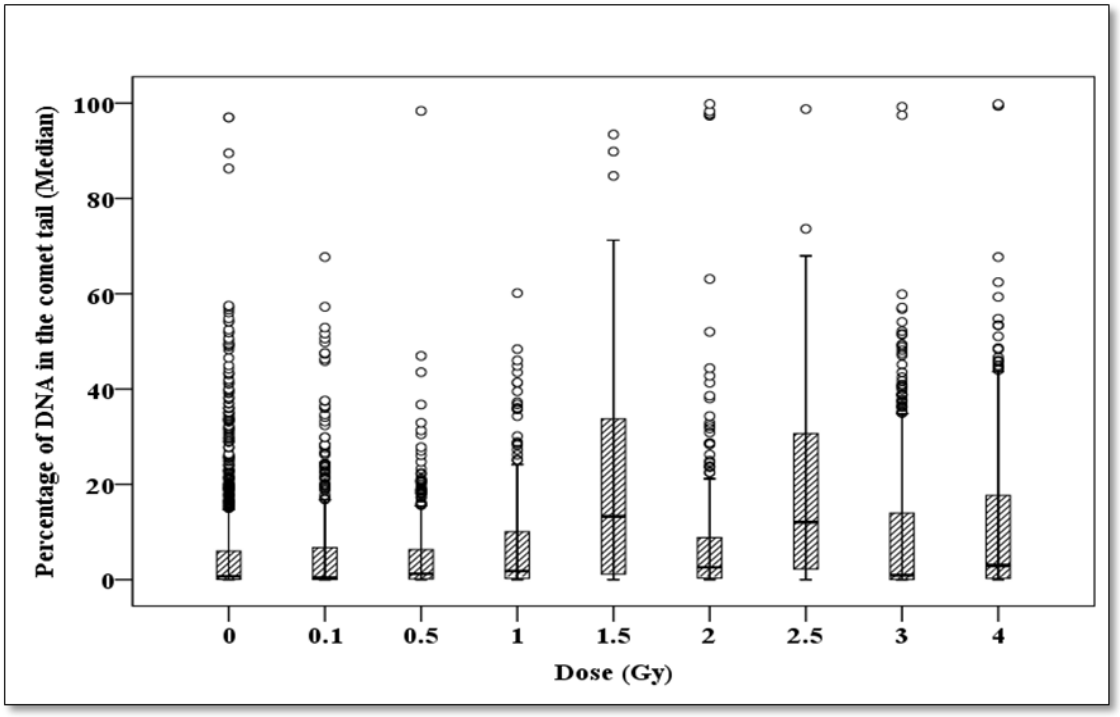


Figure 4.10: Box-plot illustrating the distribution of damage in HF19 after 10 population doubling following irradiation as a function of the dose delivered at a low dose rate (0.00313Gy / min). The data points represent one single experiment. * P < 0.05, ** P<0.01, *** P<0.001.

At the delayed time-point (20 population doublings) the data indicate that in general both HDR and LDR irradiation are capable of producing an enhanced level of DNA damage with no consistent difference between the two dose rates. For HDR the percentage of DNA damage for the 0.5, 1, 1.5, 2 and 2.5 Gy irradiated progeny was significantly higher ($p \leq 0.001$) than the control, while the damage in the 3 and 4 Gy was not statistically significant (Figure 4.11). For the LDR irradiated cells, a large induction of DNA damage was observed in the 0.5, 1.5 and 2 Gy groups ($p \leq 0.001$), whereas a significant response was observed in just the 2.5 and 3 Gy groups ($p \leq 0.05$), and no significant difference was observed in the 0.1, 1 and 4 Gy groups compared to the control. The distribution of DNA damage throughout the entire population of cells for both HDR and LDR groups is displayed in Figure 4.12 and 4.13.

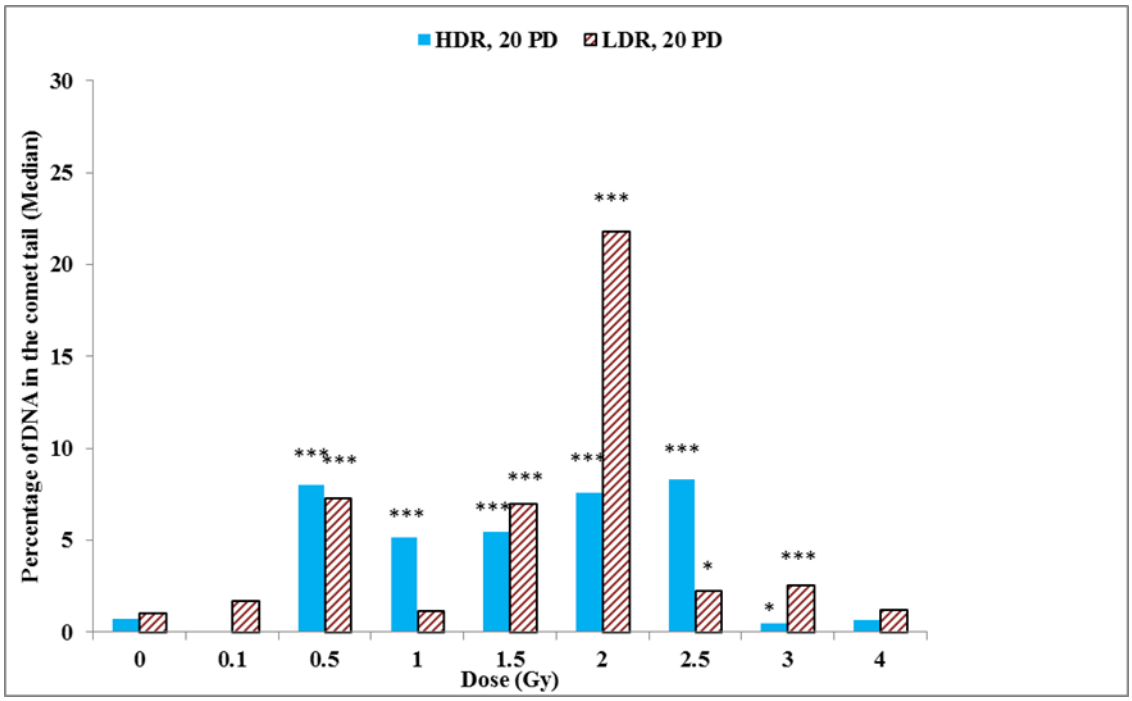


Figure 4.11: Delayed responses within the progeny of directly irradiated HF19 cell populations after 20 population doublings following irradiation as a function of dose, delivered at a high dose rate (0.42 Gy / min) or low dose rate (0.0031 Gy / min). The data points represent one single experiment. * P < 0.05, ** P<0.01, *** P<0.001.

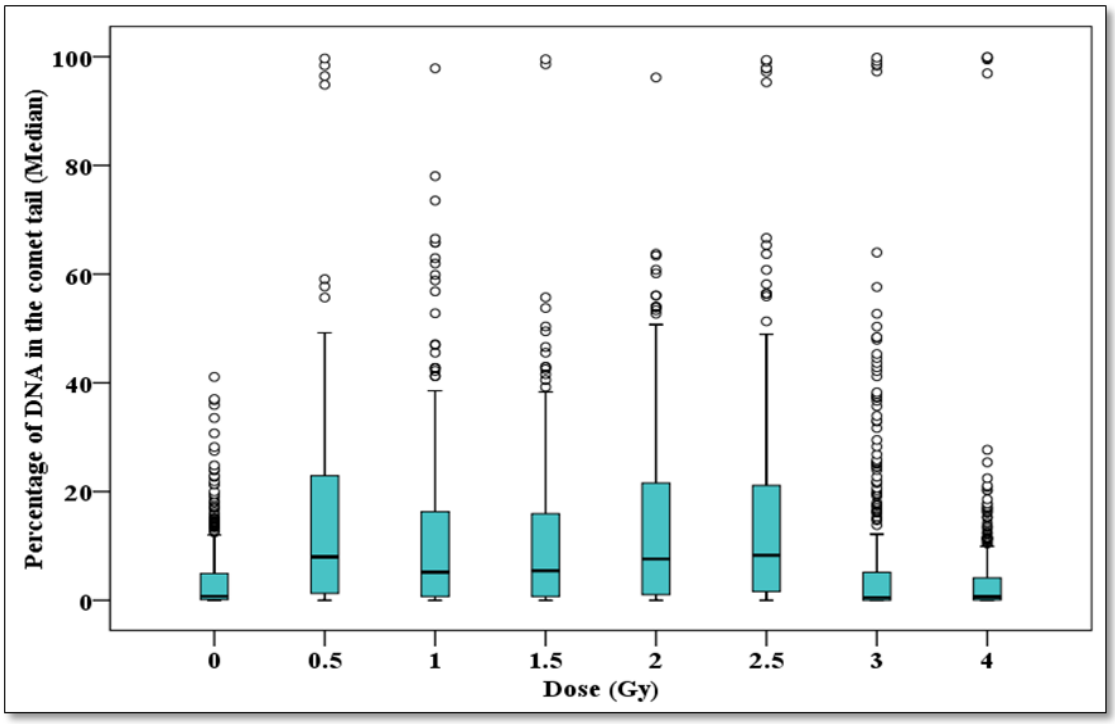


Figure 4.12: Box-plot illustrating the distribution of damage in the progeny of directly irradiated HF19 cell populations after 20 population doublings following irradiation as a function of dose, delivered at a high dose rate (0.42 Gy / min). The data points represent one single experiment. * P < 0.05, ** P<0.01, *** P<0.001.

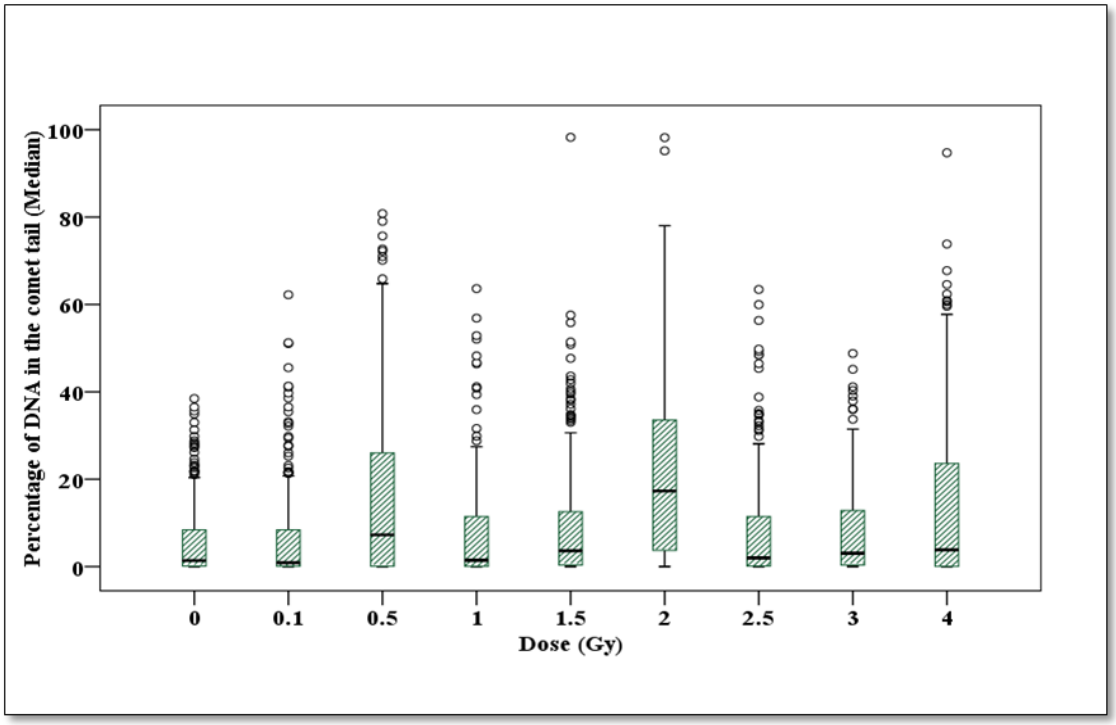


Figure 4.13: Box-plot illustrating the distribution of damage in HF19 after 20 population doublings following irradiation as a function of the dose delivered at a low dose rate (0.00313Gy / min). The data points represent one single experiment. * P < 0.05, ** P<0.01, *** P<0.001.

### *4.2.4.2 Micronucleus assay*

In order to estimate chromosomal damage in cells, cytokinesis-blocked micronucleus assay (CBMN) was utilised in the current study. Data were presented as a percentage of binucleate cells containing micronuclei (%MN/BN); in other words, cells were analysed for the induction of MN in only the BN cells from one single experiment. In general, the percentage of binucleate cells with micronuclei (%MN/BN) in HF19 at 24 h following irradiation (1 PD) was greater than in the un-irradiated controls following high dose rate (HDR; 0.42 Gy / min) x-ray irradiation, as shown in Figure 4.14. Additionally, for low dose rate exposure (LDR: 0.0031 Gy / min), there was a significant induction of micronuclei for all doses except 2.5 Gy and 3 Gy. Apart from lattermost two doses, the findings suggested that micronucleus induction levels were higher for cells exposed to LDR x-rays compared to the equivalent HDR x-ray exposure. Interestingly an extremely large increase in %MN/BN was demonstrated at 4 Gy following LDR exposure compared to the equivalent HDR exposure. The reason for this is however unclear.

HF19 cells were further analysed at 10 population doublings (10 PD) following exposure to HDR and LDR x-ray irradiation. In general, the yield of %MN/BN was observed to be elevated compared to controls following HDR exposures; these differences were significant in all doses except 1 and 4 Gy, as shown in Figure 4.15. Likewise, following LDR exposure, the yield of %MN/BN was again typically higher than the control but was not statistically significant for 1 Gy and 2.5 Gy compared to the control ($P>0.05$). There was no obvious trend between the results obtained for LDR compared to HDR as a function of dose.

At 20 population doublings post HDR irradiation, all experimental groups with the exception of the progeny of 0.1, 0.5 and 1.5 Gy irradiated cells displayed significant induction of micronuclei compared to the control, as shown in Figure 4.16. The highest percentage of MN ($12.054 \pm 0.012$ %) was observed within the progeny of 1 Gy irradiated cells ($p \leq 0.001$). For LDR exposures significant increases were observed for 0.1, 1.5, 2 and 2.5 Gy compared to the control. A small increase in micronucleus induction was also shown in the 0.5 and 1 Gy progeny; however, these levels were statistically insignificant compared to the control cells. Again there was no obvious trend between the results for LDR compared to HDR as a function of dose.

In general, the dose-to-dose variability probably reflects experimental variability, but appears to be a consistently elevated response following irradiation over wide ranges of doses delivered at either high or low dose rates. Additionally, the level of effect observed (if averaging across all the doses used) is reasonably consistent at 1, 10 and 20 population doublings; that is to say, it is typical of the same order of magnitude.

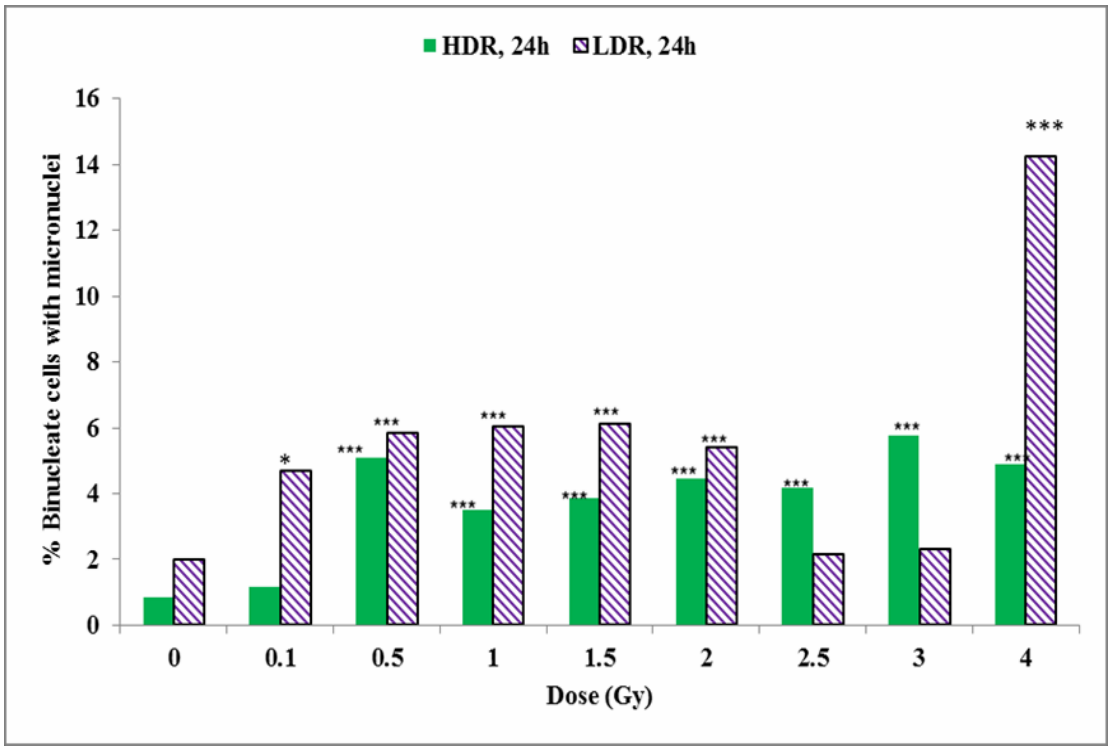


Figure 4.14: The percentage of binucleated cells (BN) with micronuclei ( MN) (%MN/BN) induced in HF 19 cells observed after 24 h following completion of the irradiation (cytochalasin B added 24 h post irradiation) following x -ray irradiation utilising high dose rate (0.4 2 Gy / min) versus low dose rate (0.003 1 Gy / min). The data points represent one single experiment. * P < 0.05, ** P<0.01, *** P<0.001.

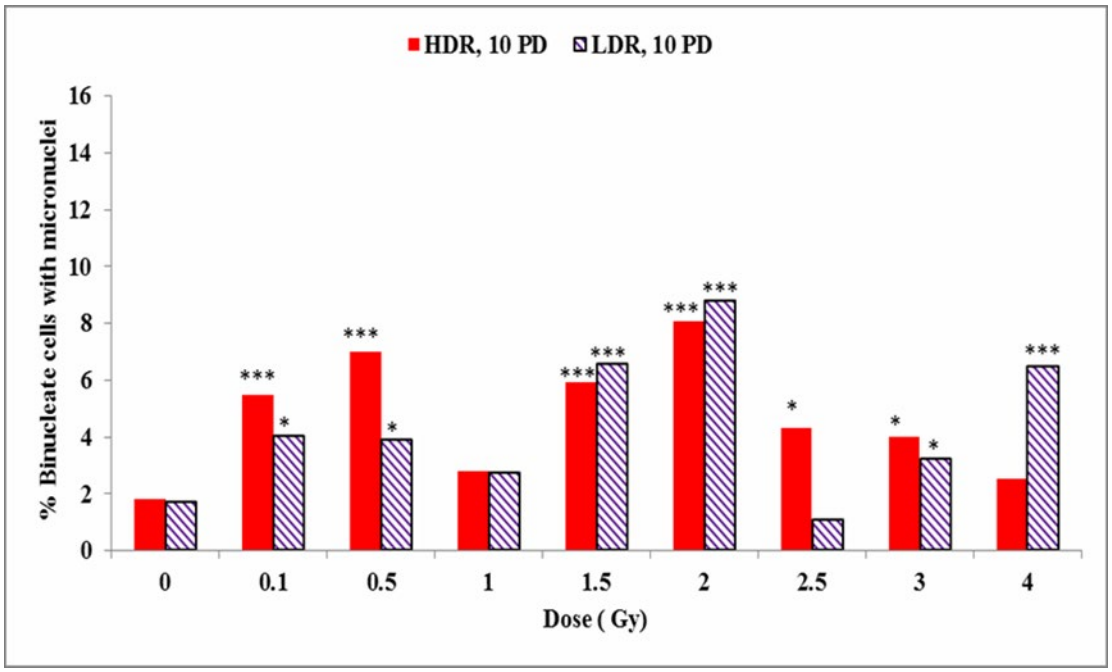


Figure 4.15: The percentage of binucleate cells (BN) with micronuclei ( MN) (%MN/BN) induced at 10 population doublings as a function of dose following high dose rate (0.42 Gy / min) versus low dose rate (0.0031 Gy / min) irradiations. The data points represent one single experiment. * P < 0.05, ** P<0.01, *** P<0.001.

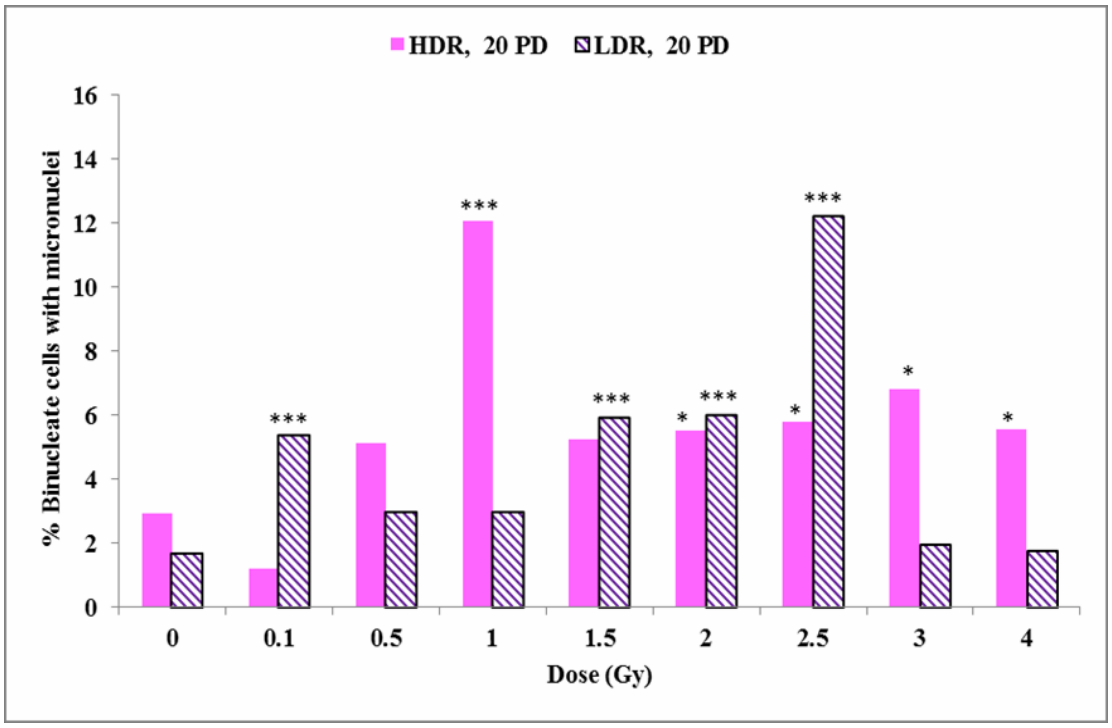


Figure 4.16: The percentage of binucleate cells (BN) with micronuclei (MN) (%MN/BN) at 20 population doublings as a function of dose following high dose rate (0.42 Gy / min) versus low dose rate (0.0031 Gy / min) irradiations. The data points represent one single experiment. * $P < 0.05$, ** $P<0.01$, *** $P<0.001$.

4.2.5 HF19 response to 0, 0.1 and 1 Gy high (0.42 Gy / minute) and low (0.00313 Gy / minute) dose rate x-ray irradiation (Micronucleus assay). Initially, we examined the susceptibility of HF19 cells to the induction of GI following HDR and LDR x-ray irradiation over a wide range of doses. In the coming section, the study focuses more on the susceptibility of HF19 cells to the induction of GI at 0.1 and 1 Gy and assesses the variability of the observed response across multiple independent experiments. These are two doses that can be considered relevant to diagnostic and therapeutic procedures respectively. As 0.1 Gy x-ray irradiation is considered to be a diagnostically relevant dose, for instance for a full body CT scan (BER, 2010) and is the upper limit of what is generally considered to be a low dose exposure (BEIR VII, 2005) (UNSCEAR, 1986). The 1 Gy x-ray dose is a comparatively high dose commonly used for radiobiology experiments and is also closer to the 1.8 or 2 Gy fractions typically used in radiation therapy.

### *4.2.5.1 Micronucleus assay*

Micronuclei induction was measured using the cytokinesis-blocked micronucleus assay (CBMN) and the data were displayed as the percentages of binucleate cells (BN) within micronuclei (%MN/BN).The cells were treated with 6 µg / ml cytochalasin-B at <5 minutes following irradiation for 40 hours in a humidified 5 % $CO_2$ incubator at 37 ºC. This has been done for all groups (control, HDR pre LDR (where HDR irradiation was performed before the LDR irradiation), LDR, and HDR post LDR (where HDR irradiation was performed after the LDR irradiation) as shown in the experimental design for x-ray irradiation (Figure 4.17). Due to the difference between HDR and LDR in the timing of adding Cytochalasin-B and subsequent time of collection, different collection efficiencies are more likely to be obtained as like is not being compared with like. For this reason, a post-acute (HDR) group was irradiated following LDR group exposure. Figure 4.18 shows initial induction of %MN/BN in HF19. The data for each dose has been pooled from four biological replicates (except the 10 population doublings data which comprises only 2 biological replicates) and the error bars show the standard error of the mean (SEM).

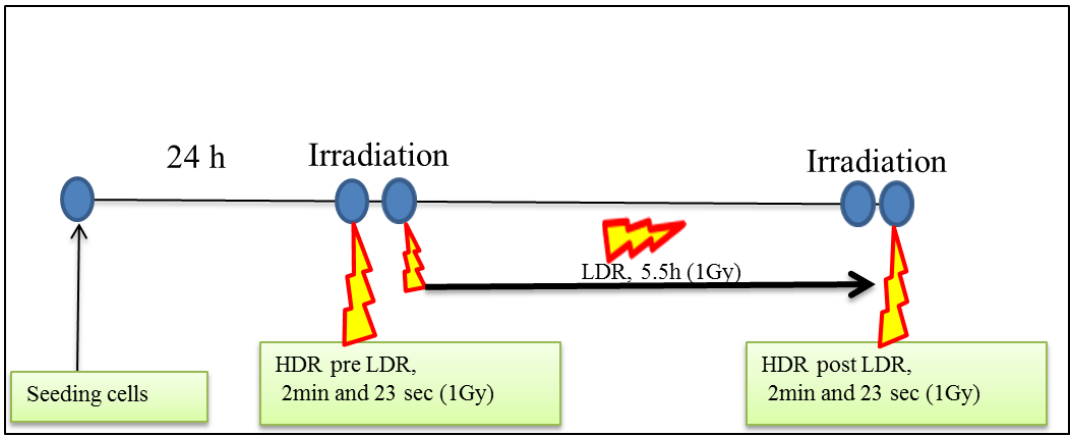


Figure 4.17. Experimental design for x-ray irradiation. Cells were seeded at 1.5 x $10^6$ in T75 flasks and incubated for ≈ 24 hours. Irradiation was performed as follows:
1- The first group, HDR pre LDR, where HDR irradiation was performed before the LDR irradiation
2- The second group, low dose rate, LDR
3-The third group of cells, HDR post LDR, where HDR irradiation was performed after the LDR irradiation

In general, immediately following an x-ray radiation insult, an initial large induction of micronuclei was observed across all irradiated groups compared to the corresponding control, as shown in figure 3.18 panel A. The individual data sets from four independent experiments showed a variation in the percentage of

binucleate cells with micronuclei. The combined data of four experiments demonstrate a significant induction of binucleate cells (BN) with micronuclei immediately following 0.1 and 1 Gy LDR x-ray irradiation (6.43 ±0.25 % ($p \leq 0.05$) and 9.39 ± 0.29 % ($p \leq 0.001$)) respectively compared to the control (3.63 ±0.22 %), as shown in Figure 4.18 panel B. A similar response was observed following 0.1 and 1 Gy x-ray irradiation when doses were given at a high dose rate (HDR); the percentage of micronucleus induction of these cells was 5.188 ±0.221% ($p \leq 0.001$) and 6.431 ±0.245 % ($p \leq 0.001$) respectively compared to the control (3.634 ±0.224 %). However, the findings indicated that 0.1 and 1 Gy low dose rate irradiation showed a higher level of micronucleus formation immediately following irradiation compared to the corresponding high dose rate groups. Interestingly, 1Gy post-acute (HDR) cells (where HDR irradiation was performed after the LDR irradiation) revealed greater micronucleus formation compared to the equivalent LDR cells.

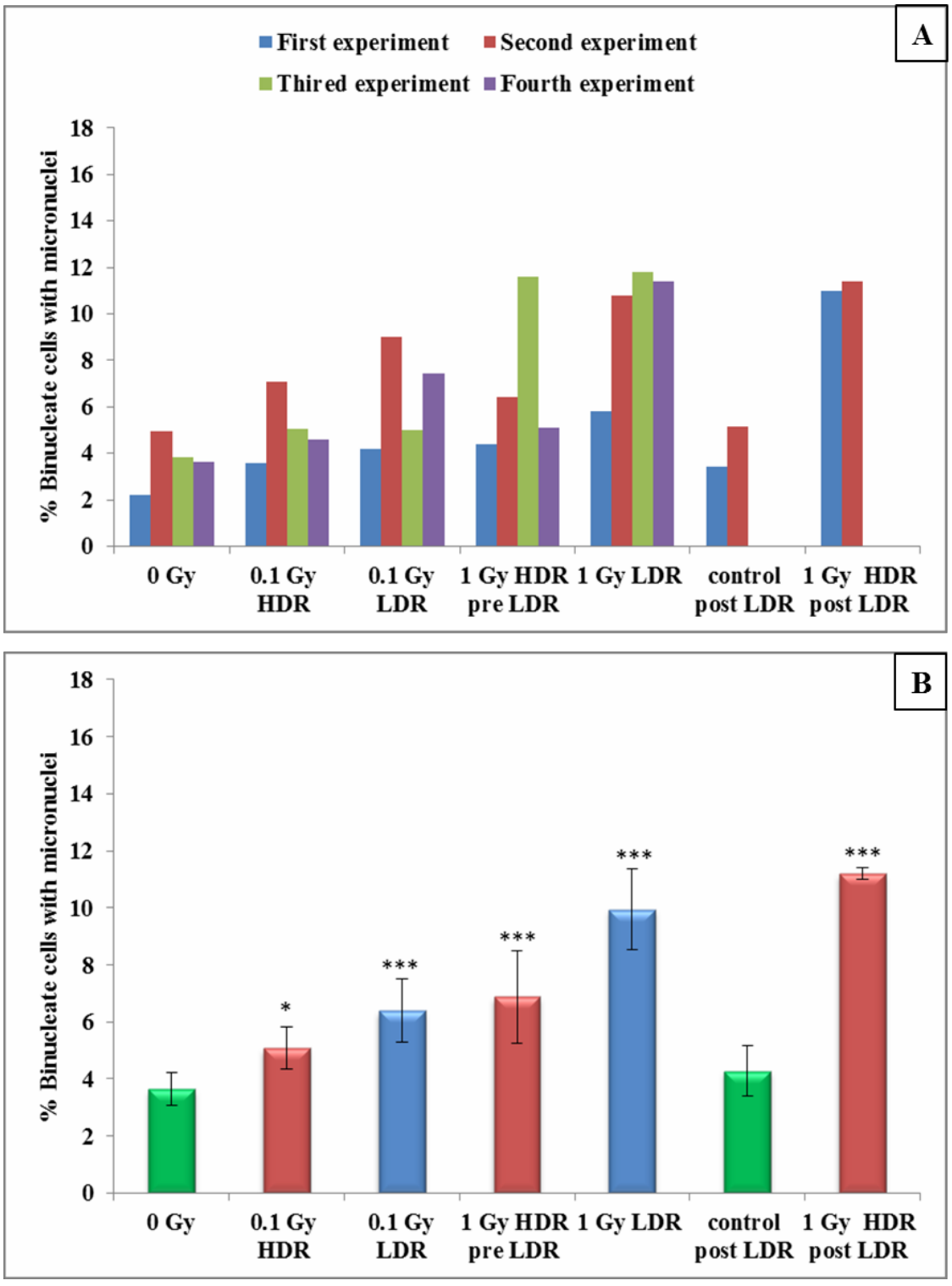


Figure 4.18: panel A and B: The percentage of binucleate cells (BN) with micronuclei ( MN) (%MN/BN) for high (0.42 Gy / min) and low (0.0031 Gy / min) dose rate at 0, 0.1 and 1 Gy immediately following irradiation, with addition of cytochalasin B immediately following irradiation (< 5 minutes). Panel A shows the data from the individual experiments from four parallel but separate experiments. Panel B represents the combined data of four independent but parallel experiments. Error bars represent the standard error of the mean of replicate experiments (SEM). * P < 0.05, ** P<0.01, *** P<0.001.

The results of the delayed cellular response at 10 population doublings following irradiation show an increase in micronuclei induction across all irradiated groups with the same trend between the separate two experiments except 1 Gy HDR (Figure 4.19 panel A).

For the combined data for the two independent experiments, the micronucleus induction of 0.1 and 1 Gy irradiated cells with both low and high dose rate remained significantly elevated. The results of both 0.1 and 1 Gy acute dose rate suggested greater micronucleus induction compared to their corresponding 0.1 and 1 Gy low dose rate as shown in Figure 4.19 panel B.

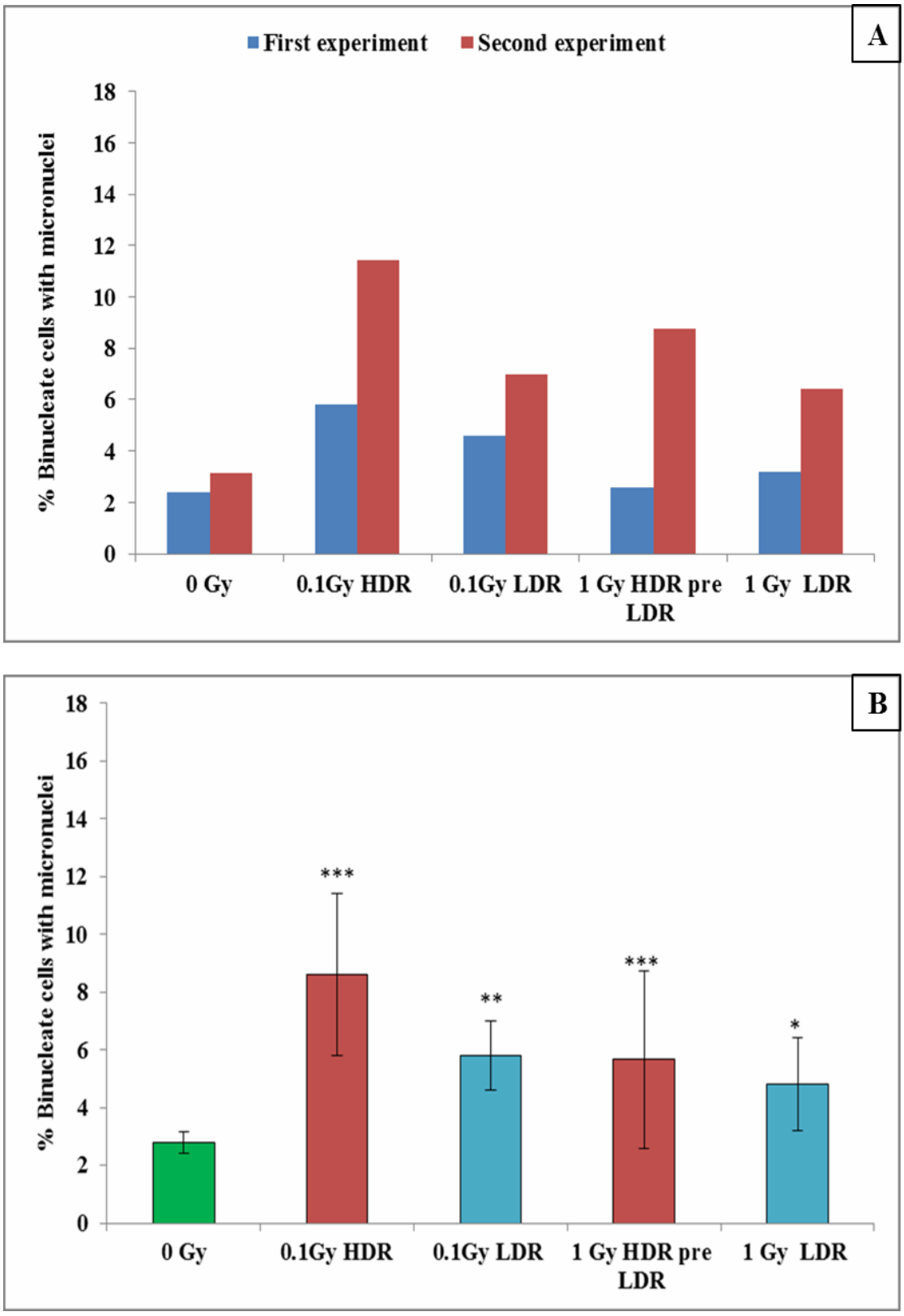


Figure 4.19: panel A and B: The percentage of binucleate cells (BN) with micronuclei ( MN) (%MN/BN) at high (0.42 Gy / min) and low (0.0031 Gy / min) dose rate at 0, 0.1 and 1 Gy at 10 population doublings post irradiation. Data from two independent experiments, error bars represent the standard error of the mean of replicate experiments (SEM). * P < 0.05, ** P<0.01, *** P<0.001.

The individual data sets from four independent experiments at 20 population doublings following irradiation showed a variation in the MN induction but with a similar trend between different radiation-level groups (Figure 4.20 panel A).

The data for the combined experiments showed a significant micronucleus formation over 20 population doublings, with an indication of an increase in MN formation after acute exposures compared to the corresponding doses at low dose rate. The induction of binucleate cells with micronuclei was significant with both 0.1 and 1 Gy high and low dose rate irradiation 13.573 ±0.312 % ($p \leq 0.001$), 10.858 ±0.282 % ($p \leq 0.001$), 8.367 ±0.27 % ($p \leq 0.001$) and 8.65 ±0.28 % ($p \leq 0.001$) respectively compared to their corresponding control (4.091± 0.198 %) as shown in Figure 4.20 panel B.

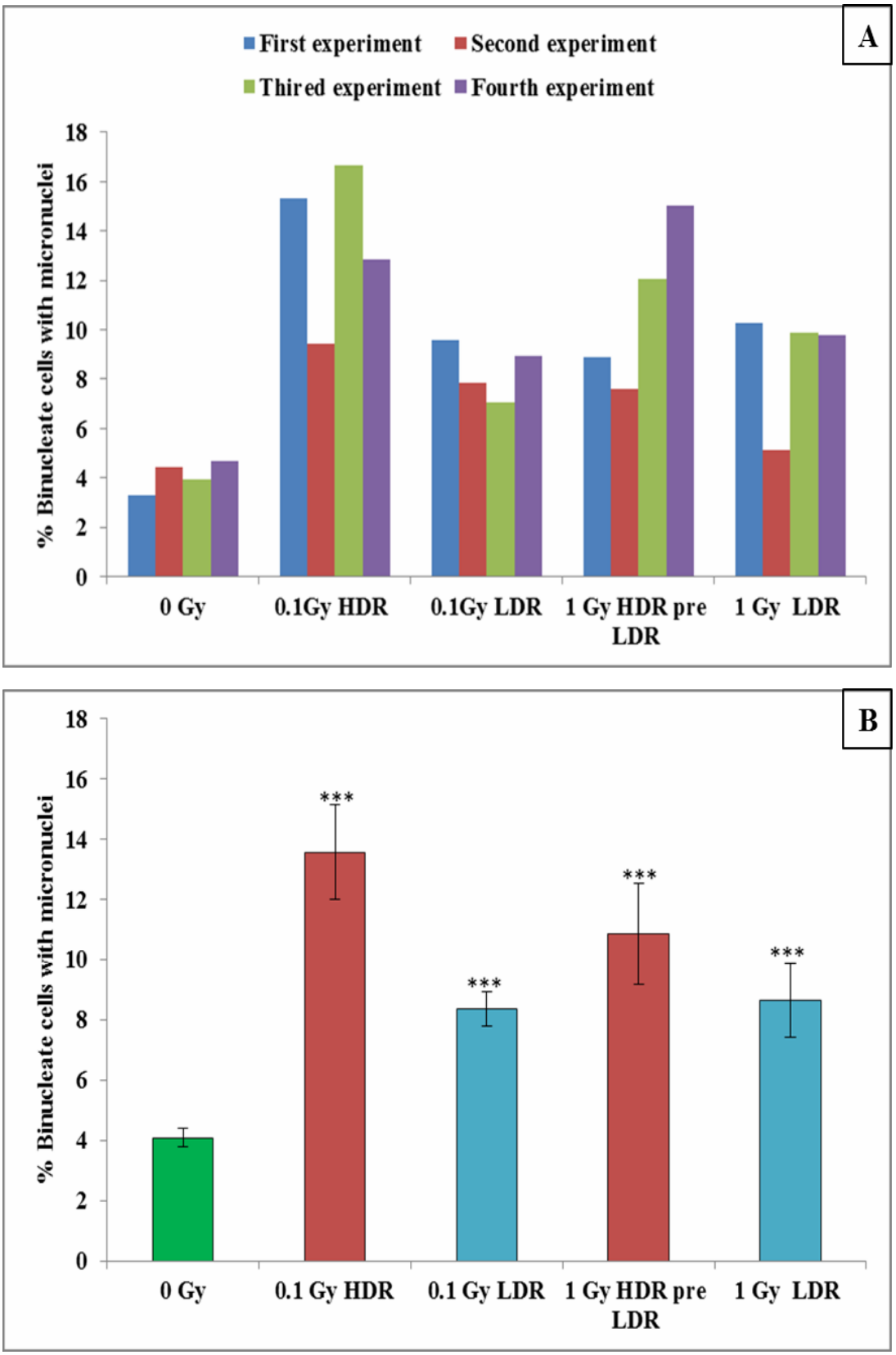


Figure 4.20: panel A and B: The percentage of binucleate cells (BN) with micronuclei (MN) (%MN/BN) at high (0.42 Gy / min) and low (0.0031 Gy / min) dose rate at 0, 0.1 and 1 Gy after 20 population doublings. Data from four independent experiments, error bars represent the standard error of the mean of replicate experiments (SEM). * $P < 0.05$, ** $P<0.01$, *** $P<0.001$.

## 4.3 Discussion

Genomic instability (GI) is characterised as the delayed biological responses/effects that occur in the descendants of irradiated cells many generations after the first radiation insult and manifest as delayed gene mutations, micronucleus formation, chromosomal damage and gene amplification (Kadhim *et al.*, 2013). This phenomenon is one of the well-known features of many cancers (Hanahan and Weinberg, 2011), although there are unanswered questions about the mechanistic understanding of these processes in relation to radiation biology (Kadhim and Hill, 2015).

Exposure to low doses both of high and low LET is able to induce GI (Smith *et al.*, 2003). For example, alpha-particles and x-rays are able to induce GI in primary human AG01522B fibroblasts in the form of an increase in apoptosis, micronucleus formation and delayed reproductive death as a delayed response following exposure (Belyakov *et al.*, 1999). The delayed induction of micronuclei was exhibited up to 30 population doublings following irradiation. However, this induction was more pronounced in the progeny of alpha-particle irradiated cells (0.5, 1.0 and 3 Gy) than the progeny of x-ray (1.0, 3.0 and 8.0 Gy) groups. The peak of micronucleus formation in the progeny of irradiated cells occurred at ≈ 3 days after 8 Gy x-ray irradiation and at 8 days after 3 Gy alpha-particle irradiation (Belyakov *et al.*, 1999). Moreover, exposure to LDR (1-3 Gy, 0.0004 Gy / minute) and HDR (1-3 Gy, 0.75 Gy / minute) gamma rays induced a significant increase in dicentric chromosomes in human lymphocytes at the first post-irradiation mitosis. However, the frequency of dicentric chromosomes per cell was significantly higher in the HDR than in both the LDR irradiated cultures. All irradiated cell cultures exhibited GI in human lymphocytes in the form of an increase in frequency of chromosome breaks and rearrangements at 11 days following irradiation (Holmberg *et al.*, 1998).

The immediate and delayed biological risks associated with low dose and low dose rate (LDR) radiation exposures are not yet well characterised (Turner *et al.*, 2015). However, the rationale or advantages for using LDR exposure in measuring cellular radiosensitivity of cells is that as damage and repair occur simultaneously during LDR exposures and the impact of different repair rates between cultures are therefore

boosted, which may lead to a greater difference in long-term repair rate (Geara *et al.*, 1992). This study aims to give a better understanding of low dose rate effects of radiation which has important implications for radiation protection as most environmental exposure tends to be at low dose rate rather than high dose rate (acute) (ICRP, 2007).

The susceptibility of primary human fibroblasts (HF19) was investigated for the induction of radiation-induced a range of cellular responses at early and late (10 and 20 population doublings) time-points following different doses of x-ray irradiation given at either high or low dose rates utilising cell viability assay, cell cycle measurement, micronucleus assay and comet assay. This project was thus established to investigate chromosomal damage associated with high and low dose rate irradiation and to investigate how the frequency of genomic instability varies with decreasing dose rate. The data clearly showed GI at different population doublings after exposure to x-rays, for low doses and low dose rate exposures, at levels similar to that observed for much higher doses delivered at a high dose rate.

The cell viability was examined at different times following irradiation with 1 Gy x-rays both at LDR and HDR. Results indicate a significant reduction in cell viability at 30 minutes and 8 hours following irradiation with HDR x-ray exposure compared to the control, while LDR showed only a slight decrease in cell viability at 30 minutes and 8 hours following the completion of irradiation, as shown in figure 4.1. This response could be due to the differences in time available for repair (Turner *et al*., 2015). Both dead and viable cells were differentially stained according to their permeability to the DNA-binding dyes in the kit's reagent (see chapter 2, section 2.2.4). The repair time (the time between the first radiation-induced lesions being formed and when the damage assay was performed) for the LDR exposure, was longer than for HDR exposures.

At 24 and 32 hours, results show a reduction in the percentage of viable cells for HDR and LDR irradiated cells compared to the control following 1 Gy x-ray irradiation. This matches the findings of Qiao *et al*. (2014) who showed that there is a significant decrease in cell viability in normal human fibroblast cells at 24 hours following exposure to 0 - 2.5 Gy x-ray irradiation (Qiao *et al.*, 2014). This also agrees with work published by Maierhofer *et al*. (2017) who noticed decreases in cell

viability in primary human fetal fibroblasts at 24 h following 2 Gy and 4 Gy x-ray irradiation (Maierhofer *et al.*, 2017). However, LDR irradiated cells displayed a lower level of cell viability at 24 and 32 hours following irradiation compared to their corresponding HDR irradiated cells, as shown in figure 4.1. This could be due to the higher micronucleus induction which was observed in LDR irradiated cells compared to their corresponding HDR irradiated cells following 0.1 and 1 Gy x-ray irradiation at the early time-point. Both showed a significant micronucleus formation compared to the controls, as shown in Figure 4.18. This is, to some extent, in agreement with findings observed in normal T-lymphocytes exposed to 0.5, 1 and 2 Gy x-ray irradiation which displayed an increase in chromosome aberration and a significant reduction of viability 3-4 days following exposure (Shiraishi *et al.*, 1976). It also agrees to some extent with the findings of Collis *et al*. (2004) who has observed that in normal human primary fibroblasts, there is a greater increase in cell death (reduced clonogenic capacity) post exposure to 2 Gy LDR (0.00156 Gy / min) irradiation (using $^{137}$Cs-gamma rays) than for the equivalent HDR (0.75 Gy / min) groups at 7-14 days following irradiation. This increase in cell death following LDR irradiation compared to the equivalent HDR irradiation was termed the "inverse dose rate effect". This phenomenon is well known to occur for many cell types but is poorly understood. This elevation in cell death of LDR groups was explained as a result of inefficient activation of the cellular signal for DNA damage (the DNA damage sensor ATM and its downstream target H2AX). Therefore, inefficient activation may demonstrate the evasion of cellular DNA damage repair mechanisms and therefore potential mutations (Collis *et al.*, 2004).

The dose-response curve for HDR irradiated HF19 cells obtained from micronucleus assay immediately following x-ray irradiation is presented in figure 4.4 (three biological replicates). All irradiated groups (0.5 - 4 Gy) showed a significant increase in micronucleus formation ($p \leq 0.001$) compared to the control. However, 1.5 Gy displayed lower induction of MN induction compared to 1 and 2 Gy irradiated groups. The 1.5 Gy irradiated groups might show other cellular responses such as dicentric chromosomes and reciprocal translocation which could not be detected using MN assay and would be detected using chromosomal analysis with the same timing of analysis. Another explanation could that this is due to that the cell cycle arrest in the G0/G1 cell cycle phase which could not be eventually manifested as

micronucleus formation in the new daughter nuclei at the end of telophase. Therefore, it is recommended to perform chromosomal analysis and cell cycle assay for 1.5 Gy group immediately following irradiation. However, a highly significant induction of MN was displayed by 1.5 irradiated group compared to control.

At 24 h following acute dose rate (HDR) x-ray irradiation, all experimental exposed groups (0.5, 1, 1.5, 2, 3 and 4 Gy) displayed a significant presence of micronuclei and this was observed at 10 population doublings for all groups, except for the progeny of 1 and 4 Gy cells. At LDR a similar trend was observed for all time-points for all experimental groups compared to control with most groups showing a significant induction of micronuclei with a few exceptions. However, at the early time-point, the LDR groups exhibited greater induction of micronuclei compared to the equivalent HDR irradiated groups, except 2.5 and 3 Gy groups, which could be due to the differences in time available for repair for both HDR and LDR groups (Turner *et al.*, 2015).

However, at the delayed time-point of 10 population doublings, the general trend was for HDR groups to show greater damage. At this delayed endpoint, the damage seen is not likely to be residual damage; however, the long term modulation of the background level of DNA damage could be the main source of the damage (Little, 2003). This damage is continually being produced and then repaired resulting in MN production.

For HDR irradiated cells, by the delayed time-point (20 population doublings), a significant induction of micronuclei compared to the control was observed for all groups with the exception of cells from the progeny of 0.1 and 0.5 Gy groups. The induction of MN in the progeny of 4 Gy LDR irradiated cells is in agreement with the results of Boreham *et al*. (2000) who observed a significant increase in the frequency of micronuclei induction in peripheral blood lymphocytes after 72, 96 and 120 hours following 4 Gy gamma ray irradiation at a similar low dose rate (0.0029 Gy / min). However, this induction was lower at LDR compared to the equivalent HDR (0.702 Gy/min) (Boreham *et al.*, 2000). There was no clear relationship between micronucleus induction of HDR and LDR groups at 20 population doublings across all irradiated groups in this study. This could be because a significant number

of damaged cells had been removed from the culture as results of mitotic catastrophe leaving healthy cells to continue to proliferate.

Total DNA damage results from the comet assay, as measured by comet tails, at the early time-point (24 hour following irradiation) demonstrated high levels of DNA damage in the majority of the experimental groups following x-ray irradiation with HDR at 0.1, 0.5, 1.5, 2, 2.5, 3 and 4 Gy with the exception of the 1 Gy irradiated cells which showed insignificant induction of DNA damage.

The DNA damage data observed at 10 population doublings additionally indicated that HF19 cells are susceptible to the induction of GI in the progeny of the irradiated cells. The percentage of DNA in the tail was significant across all groups 0.1, 0.5, 1, 1.5, 2, 2.5, 3 and 4 Gy HDR compared to the control. These data presented here, in part, agree with that of Guryev *et al*. (2009) who reported an increase in the degree of DNA fragmentation in CHO cells up to 21 days following HDR (1.5 Gy / min) for 1 Gy gamma-ray irradiation using the DNA neutral comet assay (DSBs) (Guryev *et al.*, 2009). At the delayed time point (20 population doublings), our current data showed a rise in DNA damage in the progeny of irradiated cells at 0.5, 1, 1.5, 2 and 2.5 Gy at HDR compared to control, whilst the DNA damage in 3 and 4 Gy irradiated HF19 cells was statistically insignificant.

Once again LDR irradiated cells showed a significant increase in the induction of DNA damage compared to control across almost all groups (0.1, 0.5, 1, 1.5, 2, 2.5, 3 and 4 Gy) at all time-points. Additionally, the pattern with respect to HDR was very similar to the pattern of induction of micronuclei with greater induction of DNA damage for LDR exposed cells at 24 h time-point for most groups, but was much greater induction of DNA damage at the delayed time-point of 10 population doublings for the HDR irradiated cells across almost all experimental groups. In agreement with the micronucleus assay, there was no clear pattern between LDR and HDR irradiated cell groups in terms of DNA damage at 20 population doublings following irradiation. Generally, an oscillation in response between the results obtained for LDR compared to HDR as a function of dose was observed at 10 and 20 population doublings in the single experiment performed with doses of 0.1, 0.5, 1, 1.5, 2, 2.5, 3 and 4 Gy x-ray irradiation. Therefore, a clearer understanding of x-ray

induced GI in HF19 cells may have been obtained if sufficient repeats had been performed.

Doses of 0.1 and 1 Gy are relevant to diagnostic and therapeutic uses of radiation and therefore it was considered these would be particularly relevant to analyse. Data clearly revealed an increase in the number of binucleate cells with MN (four biological replicates). This was observed in conjunction with reduced viability potentially following 1 Gy x-ray irradiation, suggesting that it is possible the increased levels of micronuclei are causing more cell death at 32 hours following irradiation. This explanation agrees with Shrivastava *et al*. (2006) who have reported that the predominant mode of cell death (mitotic death) which contributes to the loss of survival is linked with cytogenetic damage. This cytogenetic damage is displayed as chromosomal aberrations in metaphase which eventually manifest as micronucleus formation in the new daughter nuclei at the end of telophase (Shrivastava *et al.*, 2006). There was a greater expression of micronuclei in LDR at the early time-point compared to the equivalent HDR irradiated cells, which could be related to a concomitant increase in the percentage of cells arrested in G0/G1 cell cycle phase by HDR compared to LDR at 32 hours following irradiation.

Cell cycle arrest is a common and well known feature in mammalian cells following irradiation. The arrest of cells at different positions in the cell cycle as a response to DNA damage is controlled by molecular checkpoint genes. The three positions at which the checkpoints function are the $G_1$/S, S, and $G_2$/M checkpoints. However, the most important and radiosensitive checkpoint following radiation damage is the $G_2$/M at which cells pause to repair radiation-induced DNA damage prior to attempting mitosis (Hall and Giaccia, 2006). The results showed that the percentage of cell arrested in the G0/G1 phase early (1.5 h) following irradiation with 1 Gy at HDR was significantly high compared to the corresponding control. At 8 hours following irradiation the percentage of cells arrested in G0/G1 phase reduced to levels similar to those observed in the control cells, but levels in these 1 Gy irradiated cells further increased again significantly at the 24 and 32 hour time-points compared to their corresponding controls as shown in figure 4.2 panel A. Interestingly, at 32 hours following irradiation, the percentage of cells in G0/G1 phase reduced to similar levels observed in the control cells for 1 Gy LDR but the 1 Gy HDR cells remained

significantly higher. This suggests a greater proportion of HDR cells arrested in the G0/G1 stage, so fewer damaged cells reaching the point of forming binucleate cells, thus accounting for the greater numbers of micronuclei per binucleate cells at the early time point in LDR irradiated cells.

The arrest in G0/G1 phase in response to x-ray irradiation could be due to a transmitted signal via the p53 tumour suppressor protein in response to cellular damage. It is known that in the 1 - 2 hours following irradiation, the level of p53 protein increases and remains high for up to 72 hours (Kastan *et al.*, 1991). This increase is associated with a G1 arrest. Moreover, the arrest of G0/G1 in response to radiation and the degree of G0/G1 arrest depends on the level of p53 expressed (Kuerbitz *et al*., 1992). Additionally supporting this conclusion, diploid human skin fibroblasts showed transient arrest, re-entering the cell cycle at 24 h following irradiation with low (10 J / m2) UVC radiation (Gentile *et al.*, 2003). Also in support of this idea, Antoccia *et al*. (2009) demonstrated that normal human fibroblasts exhibited an inhibition of entry into S-phase following exposure to both high LET (protons) and low LET (X/gamma-rays) at doses of 1-4 Gy. This cell cycle arrest was believed to be initiated shortly following irradiation and remained for several days post exposure (Antoccia *et al*., 2009). One possible explanation is that at 24 h some cells might have gone through cell division post irradiation and experienced gross DNA damage potentially including chromosome rearrangements, which can cause slowing in S-phase entry. The duration of arrest (G1/S checkpoint) is dose dependent and is not fully initiated until several hours following exposure. For example, 1 Gy x-ray irradiation can activate G1/S arrest in all cells after 4–6 h leading to a slowing but not to complete inhibition of S-phase entry (Deckbar *et al.*, 2011).

The percentage of cells in S-phase in the 1 Gy cells was significantly lower at 0 and 24 hours post irradiation compared to the control for both HDR and LDR groups. The data at the latter time-point were lower however and not statistically significant. As a result of slowing of the DNA synthesis rate following irradiation, the S-phase was shown to have been delayed. Interestingly, the most radiosensitive cell cycle phase (G2/M) (Shen *et al.*, 2016) displayed a significant reduction the percentage of cells in G2/M for both 1 Gy LDR and 1 Gy HDR groups compared to the control after 24 hours. Recovery was observed for the LDR group by 32 hours following

irradiation, but not for the HDR group although the latter result was not statistically significant. This result would, however, support the hypothesis that cell arrest contributed to a greater formation of micronuclei in the LDR groups at the early time-point (see figure 4.2 panel C).

The significant reduction of the percentage of cells in G2/M 24 hours after x-ray irradiation could be due to chromatin compaction and poor repair competence (reduced enzyme access). Another possibility is that exposure to a relatively high dose of radiation could delay S and G2/M phases due to modulation in cyclin B1/p34cdc2 proteins working as a kinase complex which is required for passage through G2/M (Bernhard *et al.*, 1995).

The 1 Gy HDR group pre LDR (where HDR irradiation was performed before the LDR irradiation) suggested lower induction of micronuclei compared to the equivalent LDR group immediately following irradiation. This is probably due to the fact that the cells in each culture are in different cell cycle phases, so these go through division at different times. Additionally, the timing of adding Cytochalasin-B and subsequent time of collection is very different for the HDR and LDR exposures and therefore different collection efficiencies are more likely to be obtained as like is not being compared with like. It was therefore unsurprising to see different results and this was one of the reasons pre- and post-acute experiments were performed. However, the 1 Gy post-acute (HDR) irradiated group (where HDR irradiation was performed after the LDR irradiation) suggested greater induction of micronuclei compared to the equivalent LDR (Figure 4.18 panel B). This could be due to the expectation at a low dose rate of a separation of DNA damage lesions in time and therefore a decrease in the density of lesions that exist at any one time, as some would have been repaired before the production of later lesions. Therefore, the expected yield of damage (MN) at first mitosis would be lower with LDR compared to the equivalent HDR exposure. However, at high dose rate, the lesions produced could be closer together compared to low dose rate, resulting in interaction between lesions being more likely to occur. This lesion interaction could lead to misrepair that is detected as damage (MN) (Ruiz de Almodóvar *et al.*, 1994).

The general trend for 0.1 and 1 Gy progeny at 10 and 20 population doublings following irradiation suggested that HDR exposures induced a higher level of

micronucleus formation compared to LDR exposures. In accordance with data that showed different responses of GI between LDR and HDR, the findings suggest that HDR is associated with greater GI induction than LDR for the same doses of x-ray within human fibroblast HF19 cells. Work presented here agrees in part with that of Turner *et al.* (2015) who noticed that acute exposures induced a higher level of MN/BN compared to the equivalent LDR exposure in mouse lymphocytes 7 days after *in vivo* exposure to 0–4.45 Gy x-rays (Turner *et al.*, 2015). Interestingly, the micronucleus formation was higher in 0.1 Gy compared to the corresponding 1 Gy in the HDR group at both the delayed time-points. This could be due to the bystander effects as the change in gene expression occurs as early as 1 hour post radiation in doses as low as 0.05 Gy in bystander cells (Furlong *et al.*, 2013). Data suggest that exposure to low dose rate leads to a temporal separation of DNA damage lesions during the time of exposure and therefore a decrease in the density of lesions present at any one time (as some would have been repaired before the production of later lesions).The delayed induction of MN at 10 and 20 population doublings with low dose rate compared to the equivalent HDR exposure could be due to the potential change in the background level of damage. Zhang *et al.* (2016) found that exposure to a combined low dose rate neutron (0.028 mGy / h for 20 hours/day) and gamma ray (0.0167 Gy / h for 2 hours/day) radiation prompted a balance between the induction and repair of DSBs in T-cells of peripheral blood lymphocytes for 30 and 60 days following whole body irradiation. This was determined as there was no difference in the level of γ-H2AX protein expression in groups 30 and 60 days post irradiation (Zhang *et al.*, 2016).

Our findings of induction of GI instability at low dose (0.1 Gy) low LET x-ray irradiation in HF19 cells agree with the results of Kadhim (2003) who has observed that the delayed chromosomal aberrations were increased over controls in bone marrow cells from both CBA/H and C57BL/6 in bred strains following exposure to 0.1 (low) and 1 (high) Gy dose x-ray irradiation. However, the relationship between the percentage of chromosomal aberrations and dose was inverse between the strains. Additionally, an inverse relationship between apoptosis and chromosomal instability was shown in both strains at high doses (1 and 3 Gy) but there was no such clear relationship at the lowest dose (0.1 Gy). This inverse relationship between delayed

chromosomal instability and apoptosis may explicate the belief that there is no threshold dose for radiation-induced GI (Kadhim, 2003).

The comet and MN assay were performed once to measure the early, intermediate and delayed response (comet and MN assay) of HF19 to dose ranges (0,0.5,1,1.5,2,2.5,3,4) at high (0.42 Gy /minute) and low dose rates (0.0031 Gy / minute) of x-ray irradiation. Five hundred cells were analysed from one single experiment. These findings can be confirmed using further biological replicates, as measurement precision can be increased and biological variability decreased by testing other group of cells form the same batch of cells multiple times. However, reliability of data was higher for cell viability and cell cycle assay as they were collected from two separate but parallel experiments with small SEM. The cell response curve data are collected from three independent experiments with variation in the percentage of binucleate cells with micronuclei but with the same trend except for the 4 Gy group.

The MN assay was performed four different times to measure the induction of early and late micronucleus formation in HF19 cells following 0.1 and 1 Gy LDR and HDR x-ray exposure (doses relevant to diagnostic and therapeutic uses). At least 1500 binucleate cells were examined in each group. A similar trend was observed each time indicating that the results are replicable.

## 4.4 Conclusions

X-ray irradiation can induce early DNA damage in HF19 cells at both HDR and LDR at 0.1, 0.5, 1, 1.5, 2, 2.5, 3 and 4 Gy. The data suggested that the damage was higher at LDR compared to the equivalent HDR exposure at 0.1, 0.5, 1, 1.5, 2 and 4 Gy. The dose- response curve for micronucleus induction increased with dose until a plateau was reached and reduced slightly at the higher doses immediately following x-ray irradiation. Moreover, x-rays at 0.1 Gy (relevant diagnostic dose) and 1 Gy (relevant therapeutic dose) could induce DNA damage and micronucleus formation early after irradiation with both HDR and LDR. Furthermore, the LDR group displayed more damage compared to the corresponding HDR when investigated immediately after irradiation. However, the delayed damage was higher at HDR compared to the equivalent LDR x-ray irradiation. A relevant x-ray therapeutic dose

(1 Gy) is able to induce a significant reduction in cell viability after irradiation with HDR and LDR (30 minutes - 8 hours). This persists in cells exposed to 1 Gy LDR until 32 hours. Additionally, cell cycle arrest in G0/G1 was observed in 1 Gy x-ray irradiated cells (30 minutes - 24 hours) with both HDR and LDR exposure. This continued in cells exposed to 1 Gy HDR until 32 hours.

# Chapter 5.
# The molecular mechanisms involved in the induction of GI in HF19 cells following 0.1 and 1 Gy irradiation at high and low dose rate.

## 5.1 Introduction

Genomic instability is a factor which correlates closely with cancer risk, following exposure to ionising radiation (Moore *et al.*, 2005). An increase in reactive oxygen species (ROS) can drive a cycle of genomic instability resulting in DSBs and mutated repair, which can eventually lead to the acquisition of genomic changes (Sallmyr *et al.*, 2008). Natarajan *et al*. (2007) have also reported that Tumour Necrosis Factor (TNF-α) at certain concentrations which are not cytotoxic could play a role in the initiation of genomic instability through free radical generation following exposure to 0.1, 1 or 2 Gy low LET irradiation (Natarajan *et al.*, 2007). The cytokines secreted by irradiated cells such as Transforming Growth Factor beta 1 (TGF-β1) and other cytokine factors also play a role in the generation of genomic instability by working to increase intracellular levels of ROS in un-hit (un-irradiated) cells, which is one of the mechanisms for the bystander effect (Lehnert *et al.*, 1997; Narayanan *et al.*, 1997; Iyer *et al.*, 2000). This bystander effect can also lead to the induction of genomic instability within the progeny of bystander cells, comparable to that found within the progeny of directly irradiated cells (Bowler *et al.*, 2006). TGF-β1 signalling plays a role in initiation and integration of multiple cellular responses to IR, as well as to other biological damage (Barcellos-Hoff, 2005). Paradoxically, however, TGF-β1 also plays a crucial role in the cleansing of cells with genomic instability which process is mediated by p53 activation (Koukourakis, 2012).

As shown in chapter 4, 0.1 Gy (relevant diagnostic dose) and 1 Gy (relevant therapeutic dose) HDR and LDR x-ray irradiation-induced early DNA damage and micronucleus formation in HF19 cells. However, the results of the LDR groups suggested higher damage compared to the equivalent HDR groups. On the other hand, the data indicated that the delayed damage (GI) was higher with HDR compared to the corresponding LDR x-ray irradiation. Additionally, a relevant x-ray therapeutic dose (1 Gy) showed a significant reduction in cell viability after

irradiation with HDR and LDR (30 minutes and 8 hours). This reduction was maintained in the cells exposed to 1 Gy LDR until 32 hours following irradiation. Moreover, both HDR and LDR 1 Gy x-ray irradiation groups revealed a significant increase in the percentage of cells arrested in the G0/G1 phase at 30 minutes and 24 hours following irradiation. This arrest persisted in cells exposed to 1 Gy HDR until 32 hours following irradiation.

This study, therefore, focuses on the potential role of ROS, TNF-α and TGF-β1 in the initiation of processes that could lead to DNA damage and genomic instability in HF19 cells after 0.1 and 1 Gy HDR and LDR x-ray irradiation. Furthermore, the aim is to understand to what extent ROS, TNF-α and TGF-β1 could serve as a signalling mediator of the radiation-induced genomic instability of cells irradiated with HDR and LDR x-ray irradiation.

## 5.3 Results

Initially, we utilised the Oxidative Stress Assay (chapter 2, section 2.2.5) to assess the levels of ROS in the HF19 cells early (1.5 hours) and late (20 population doublings) following x-ray irradiation with 0, 0.1 and 1 Gy at high and low dose rate exposure.

### 5.3.1 Levels of ROS in HF19 cells at 1.5 h following x-ray irradiation at high and low dose rate exposure

Early at 1.5 hours following exposure, HF19 cells exposed to 0.1 Gy HDR showed a slight increase in cells exhibiting ROS (14.452 ± 1.114 %) compared to the control (13.648 ± 0.297 %). This increase, however, was not statistically significant. In contrast, the same dose at the same time end-point under LDR exposure revealed a highly significant increase in cells with ROS (20.492 ± 1.134 %) compared to the corresponding control. Interestingly, both the 0.1 Gy LDR and the 1 Gy HDR groups exhibited a similar level of cells with ROS (20.492 ± 1.134 % and 20.615 ± 0.572 % respectively). At high dose (1 Gy), both HDR and LDR groups displayed a highly significant increase in the level of cells with ROS (20.615 ± 0.572 %, 21.657 ± 1.060 % respectively) compared to the control. However, the level of ROS induction was

higher in the LDR group compared to the equivalent HDR group as shown in figure 5.1.

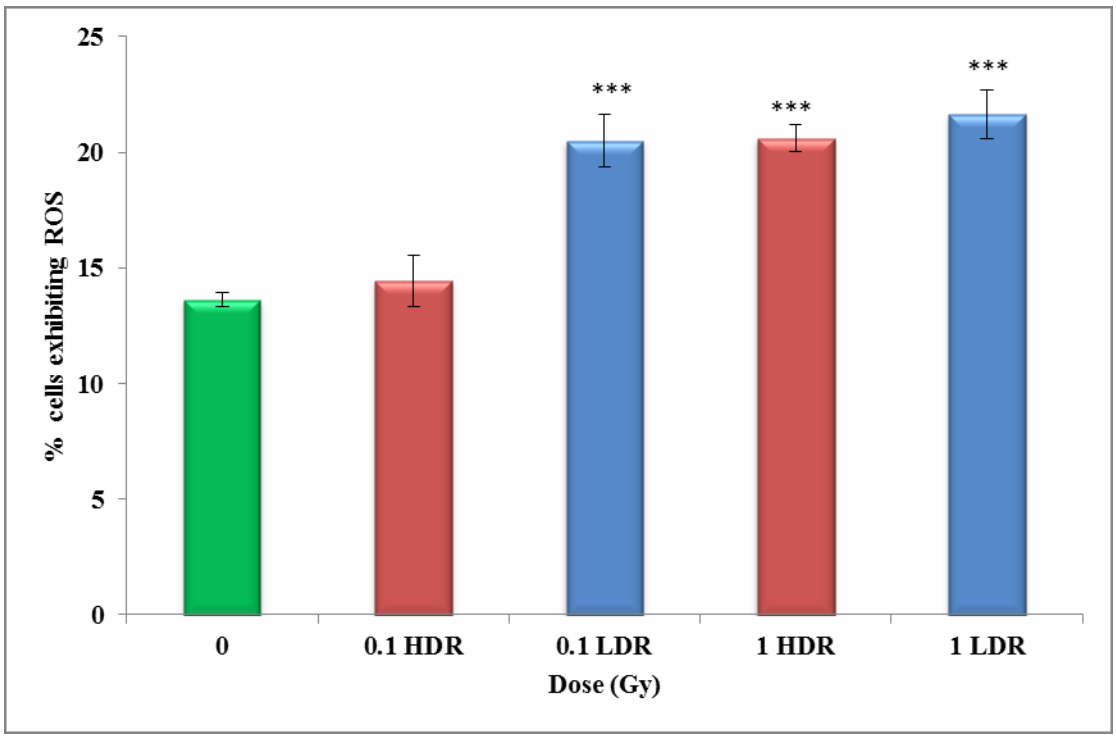


Figure 5.1: Percentage of HF19 cells with ROS+ at 1.5 hours following x-ray irradiation at 0.1 and 1 Gy HDR and LDR. Combined data from three independent experiments. Error bars represent the standard error of the mean of replicate experiments (SEM).* P < 0.05, ** P<0.01, *** P<0.001.

### 5.3.2 Levels of ROS in HF19 cells at 20 population doublings following x-ray irradiation at high and low dose rate exposure

At 10 passages, approximately 20 population doublings, following irradiation, the data clearly showed an increase in the level of cells with ROS as a delayed effect across all groups when compared to their corresponding control (0 Gy = 10.636 ± 1.054 %; 0.1 Gy HDR = 14.09 ± 2.288 %; 0.1 Gy LDR = 12.102 ± 1.639 %; 1 Gy HDR = 15.931 ± 1.2763 %; 1 Gy LDR = 15.185 ± 0.589 %). However, this increase was lower compared to the equivalent doses at 1.5 hours following irradiation. Cells irradiated at 0.1 Gy HDR and LDR demonstrated a slight increase in the level of ROS compared to the control, with a higher level at HDR compared to the corresponding LDR. This increase, however, was statistically insignificant. At high dose (1 Gy), both HDR and LDR groups displayed a highly significant ($P \leq 0.01$) induction of cells with ROS compared to the control. However, findings suggested that the HDR group

exhibited more formation of cells with ROS compared to the equivalent LDR irradiated group as shown in figure 5.2.

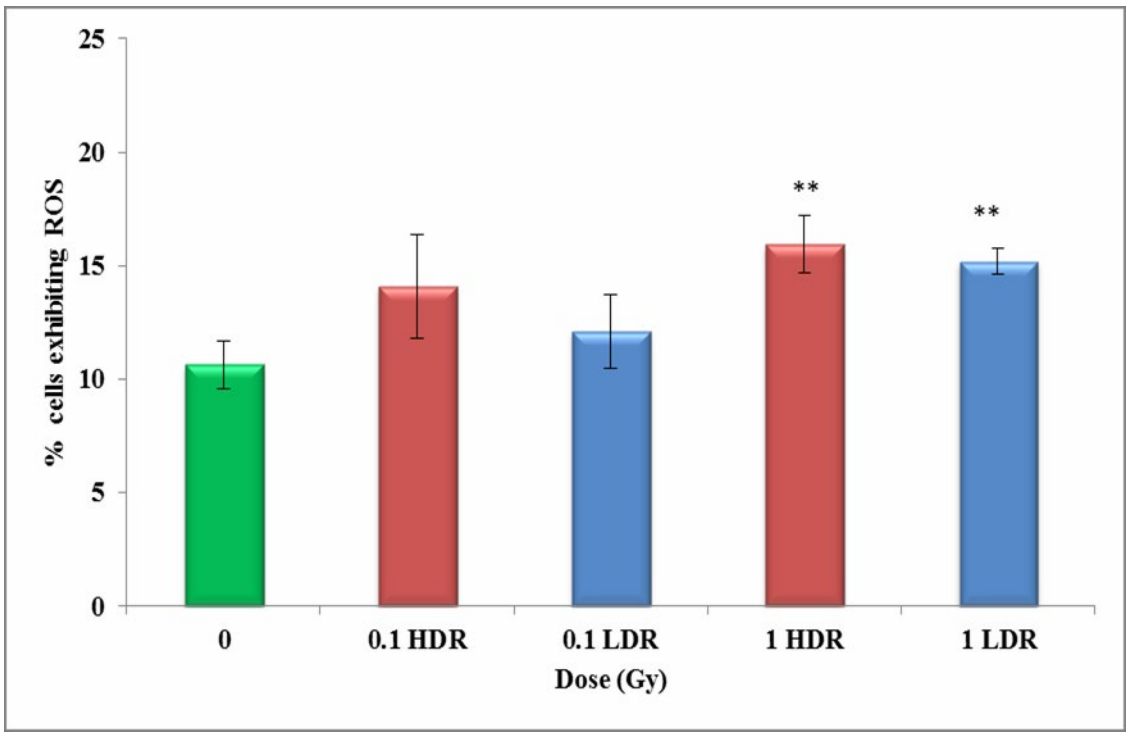


Figure 5.2: Percentage of HF19 cells with ROS+ at 20 population doublings following x-ray irradiation at 0.1 and 1 Gy HDR and LDR. Combined data from three independent experiments. Error bars represent the standard error of the mean of replicate experiments (SEM).* P < 0.05, ** P<0.01, *** P<0.001.

### 5.3.3 Investigating the potential role of Tumour Necrosis Factor α (TNF- α) and Transforming Growth Factor β1 (TGF-β1) in radiation-induced genomic instability in HF19 cells following x-ray irradiation at high and low dose rate exposure.

In HF19 cells, an increase in expression of TNF-α and TGF-β1 was observed at 1.5 hours following exposure to 0.1 and 1 Gy HDR and LDR with the exception of the 1 Gy LDR group for TGF-β1 expression. This increase, however, was not statistically significant compared to the control as shown in figure 5.3 panels A and B. The TNF-α expression in both the 0.1 and 1 Gy LDR groups was higher than the equivalent 0.1 and 1 Gy HDR group at 1.5 hours following x-ray irradiation. The same pattern was observed in TGF-β1 expression after 0.1 Gy HDR and 0.1 Gy LDR. However, 1 Gy

LDR irradiation-induced less TGF-β1 expression than the 1 Gy HDR group at 1.5h post x-ray irradiation.

After 20 population doublings following irradiation, an increase in TNF-α protein expression was shown by 0.1 Gy and 1 Gy at HDR and LDR compared to the control. This rise, however, was not statistically significant. A slight increase was shown at 0.1 and 1 Gy LDR compared to the HDR group as shown in figure 5.4 panel A. X-ray irradiation activated TGF-β1 expression at 0.1 Gy LDR and in both the 1 Gy HDR and LDR groups as a delayed effect. TGF-β1 expression at both 0.1 and 1 Gy LDR was higher compared the equivalent HDR groups as shown in figure 5.4 panel B.

The error bar of 1 LDR irradiate group is high which could be due to biological variation between the three biological replicates. The error bar of 1 LDR irradiated group is high which could either be due to biological variation between the three biological replicates or to unequal protein loading as it is hard to confirm the protein levels on the gel/blot without having loading controls.

Insignificant changes in TGF-β1 expression were observed in all groups compared to the control, which indicates that TGF-β1 was not implicated in the induction of genomic instability in HF19 cells following x-ray irradiation.

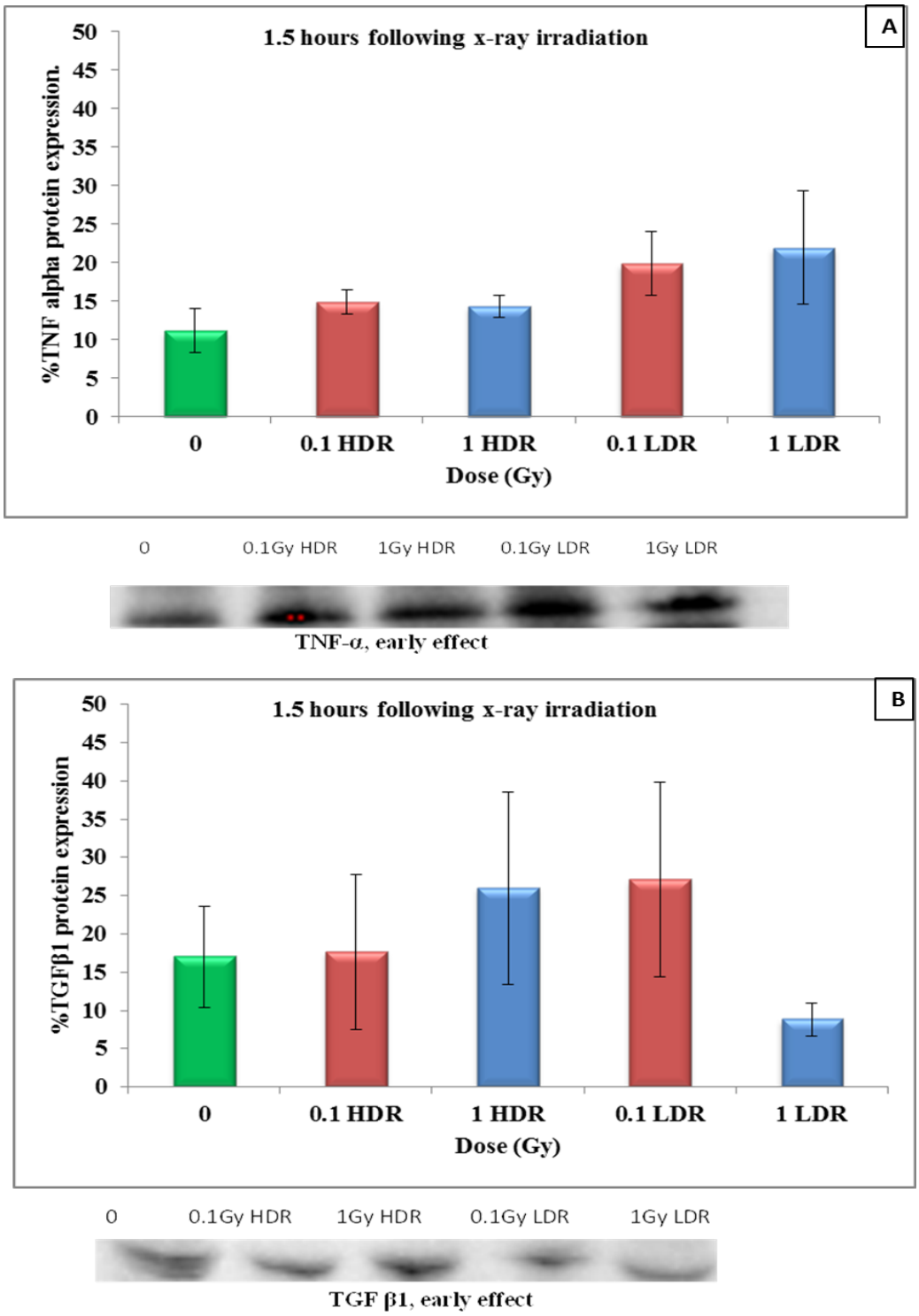


Figure 5.3: Western Blot Analysis of TNF-α and TGF-β1 expression levels in x-ray irradiated HF19 human fibroblasts cells at 1.5 hours following 0.1 and 1 Gy HDR and LDR exposure. Cells were exposed to 0.1 and 1 Gy HDR (0.42 Gy / minute) and LDR (0.00313 Gy / minute) x-ray irradiation. At 1.5 hours following irradiation, cells were subjected to Western Blot Assay to assess the TNF-α and TGF-β1 expression levels. Combined data from three independent experiments. Error bars represent the standard error of the mean of replicate experiments (SEM). * $P < 0.05$, ** $P<0.01$, *** $P<0.001$.

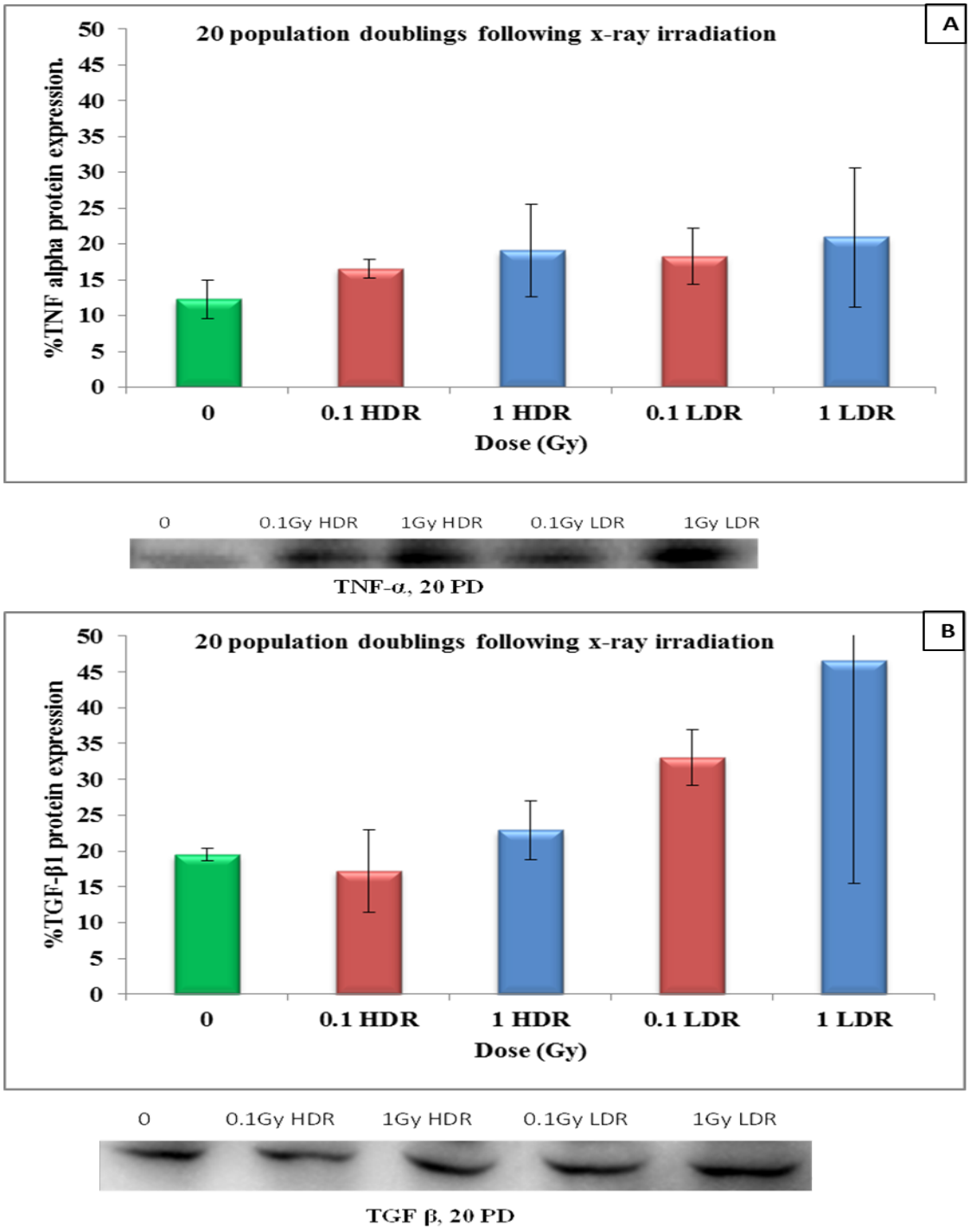


Figure 5.4: Western Blot Analysis of TNF-α and TGF-β1 expression levels in x-ray irradiated HF19 human fibroblasts cells at 20 population doublings following 0.1 and 1 Gy HDR and LDR exposure. Cells were exposed to 0.1 and 1 Gy HDR (0.42 Gy / minute) and LDR (0.00313 Gy / minute) x-ray irradiation. At 20 population doublings following irradiation, cells were subjected to Western Blot Assay to assess the TNF-α and TGF-β1 expression levels. Combined data from three independent experiments. Error bars represent the standard error of the mean of replicate experiments (SEM).* P < 0.05, ** P<0.01, *** P<0.001.

## 5.4 Discussion

Ionising radiation damages DNA directly by direct energy deposition and indirectly through induction of oxidative stress (radiolysis of water). At low doses, the predominant mechanism is indirect interaction. When this happens in the vicinity of DNA it contributes to oxidative stress in the form of ROS (Brigelius-Flohé and Maiorino, 2013). These reactive radicals can negatively affect the DNA repair process by affecting the function of proteins implicated in DNA repair (Hirayama *et al.*, 2009; Stadtman, 1993). These contribute greatly to the generation of degenerative diseases, ageing, and cancer when antioxidant defences are overwhelmed. Doudican *et al*. (2005) have observed that enhanced ROS production leads to a direct rise in oxidative mtDNA damage and mutagenesis. A profound genomic instability is caused by repair-deficient mutants subjected to oxidative stress conditions (Doudican *et al.*, 2005).

If ROS are not scavenged by the cells' antioxidants, they can work as a source of DNA damage, which is likely to result in mutations (Ragu *et al.,* 2007; Degtyareva *et al.,* 2008). These mutations directly participate in increasing genomic instability in HF19 cells. Reactive oxygen species such as hydroxyl radicals ($^{\cdot}OH$) can cause damage to all four nucleotide bases. Additionally, $^{1}O_2$ (singlet Oxygen, (ROS)) can interact with guanine resulting in carcinogenic alterations to DNA in the form of insertions, rearrangements, deletions, mismatched bases, and chromosomal translocations characteristic of cancer-driving chromosomal instability (Wiseman and Halliwell, 1996).

ROS can induce single or double-strand breaks of the DNA backbone, which may result in loss of fundamental genetic information if not properly repaired (Cooke *et al.*, 2003). Therefore, increase in ROS levels can induce DNA damage, which, if not repaired or mis-repaired, may contribute to genomic instability in HF19 cells.

The findings of this study demonstrated high early induction in ROS levels in the 0.1 and 1 Gy LDR and 1 Gy HDR groups in HF19 cells at 1.5 hours following irradiation. This is in agreement with previous findings of Doudican *et al*. (2005) who found that ROS induced by x-ray irradiation at 1.4 Gy / min in normal skin

fibroblasts generate primary lesions that may affect lipids and proteins. Carbonyl groups resulting from protein oxidation (ROS) can also induce polyunsaturated fatty acid peroxidation (Doudican *et al.*, 2005). The greater induction of ROS in the early LDR groups correlates to the higher induction of DNA damage in LDR compared to HDR as an early effect.

Doudican *et al*. (2005) also found that the damage was maintained over a long period of time after exposure. These findings agree with our results at 20 population doublings at 1 Gy for both HDR and LDR groups. There was a higher induction of ROS shown by both the HDR groups compared to the LDR groups as a late effect, which is in agreement to some extent with the findings of Tseng *et al*. (2013) who observed that the ROS levels displayed by LDR proton exposures over 2 days were lower compared to the corresponding HDR group in rodent cells (Tseng *et al.*, 2013). The higher induction of ROS levels in 0.1 and 1 Gy HDR groups compared to the equivalent LDR groups as a delayed effect also correlates with the observation of greater induction of DNA damage and micronucleus formation at the same doses, as reported previously in chapter 4. It can, therefore, be speculated that there is a link between ROS levels and DNA damage. This is supported by the observations of Azzam *et al*. (2012) who have reported that ≈2/3 of DNA damage is a result of indirect effects (linked to ROS) when irradiated with low LET ionising radiation, while 1/3 is due to direct interaction of DNA with radiation (Azzam *et al.*, 2012).

Additionally, at 20 population doublings, the ROS levels were uniformly higher across the 0.1 and 1 Gy HDR and LDR groups compared to the control. This concurs with Azzam *et al*. (2012) who have reported that ROS are generated for days and months following irradiation (Azzam *et al.*, 2012). The late DNA damage, therefore, which arises at 20 population doublings (micronuclei and whole DNA damage), further supports the idea that in HF19 cells GI may be due to the continuous emanation of ROS from some cells into a cell population following exposure.

The Tumour Necrosis Factor alpha (TNF-α) cytokine plays a paradoxical and complex role in cancer biology. It works as a cytotoxic agent to tumour cells under certain conditions; however, it also stimulates tumour angiogenesis and tumour-promoting inflammation (Tse *et al.*, 2012). The Transforming Growth Factor beta 1 (TGF-β1) signalling network has the same dichotomous role in carcinogenesis as it

has the potential to act either as a potent tumour suppressor early in carcinogenesis or a mediator of tumour progression at delayed time end-points in breast cancer cells (Tang *et al.*, 2003). Canney and Dean (1990) found that TGF-β1 activity may modify late post-radiation changes. The pathological changes of late radiation damage in non-tumour-bearing tissues were linked to the expression of TGF-β1 (Canney and Dean, 1990).

From the findings shown in figures 5.3 and 5.4 panels B and D, it can be inferred that x-ray irradiation activated the TNF-α and TGF-β1 expression for most of the irradiated groups early (at 1.5 hours) and late (at 20 population doublings). However, this increase was not statistically significant compared to the control.

In the light of our data, our interpretation of the relationship between TNF-α and TGF-β1 and radiation-induced genomic instability in HF19 cells is that TNF-α and TGF-β1 do not play a significant role in this relationship. The possible reason could be that TNF-α and TGF-β1 play different roles depending on the specific cell type of origin and the molecular aetiology of a tumour. For instance, Boerma *et al*. (2002) have found that cardiac fibroblasts and rat heart endothelial cells required different levels and durations of induced response and different doses to evoke significant changes in mRNA expression in the respective cell types. There was a significant increase in the average expression of TGF-β1 and mRNA observed between 4 and 48 hours in endothelial cells at 2 Gy, but in the fibroblasts, this was not observed until 8.5 Gy (Boerma *et al.*, 2002).

The intricacies of radiation effects mediated by TNF-α and TGF-β1 in HF19 cells will require further study to determine whether and under what circumstances TNF-α and TGF-β1 can accelerate or reduce RIGI.

Three independent but parallel experiments were performed to detect ROS and the increase in expression of TNF-α and TGF-β1 in cellular populations following 0.1 and 1Gy x-ray irradiation at high and low dose rate exposure. For ROS, a similar trend was observed each time with a small SEM of replicate experiments indicating that the results are replicable. However, the SEM for TNF-α and TGF-β1 is a bit high, in particular the 1Gy LDR TGF-β1 expression at 20 population doublings. This could be due to the biological variation between the three biological replicates or

unequal protein loading. An equal amount of loading protein can be demonstrated by loading controls, such as actin which is constitutively expressed by cells. Additionally, staining the gel using Coomassie blue dyes before transfer into the membrane or staining the plotted membrane using Ponceau-S Stain would each confirm the total protein loaded in each lane. Further approaches could be utilized to confirm these results such as qRT-PCR, sandwich enzyme linked immunosorbent assays (ELISA) and other quantitative immunohistochemistry techniques that may be more sensitive to assess the response of HF19 cells with regard to TNF-α across different doses and dose rates.

## 5.5 Conclusions

High dose rate (acute) and low dose rate (protracted) exposures to x-ray irradiation at 0.1 and 1 Gy trigger the induction of reactive oxygen species in HF19 cells at 1.5 h following irradiation. However, LDR x-ray exposure (0.1 and 1 Gy) suggested a greater level of oxidative stress in HF19 cells compared to the equivalent high dose rate at 1.5 h following irradiation, which correlates with the greater induction of DNA damage at LDR compared HDR as an early effect. At 20 population doublings (delayed effect), the production of ROS was high, which is generally linked to the induction of genomic instability as a late effect in HF19 cells. The results indicated that the damage was higher in the HDR group compared to the corresponding LDR group, as were the ROS levels observed. Genomic instability induction in HF19 cells (whether following exposure to HDR or LDR) is therefore strongly correlated with the induction of ROS levels. On the other hand, TNF-α and TGF-β1 are not implicated in early DNA damage in HF19 cells following either HDR or LDR x-ray irradiation. Therefore, it can be deduced that TNF-α and TGF-β1 are not linked to the induction of genomic instability in primary non-transformed human fibroblast HF19 cells following HDR or LDR x-ray irradiation. However, qRT-PCR, immunoblots or sandwich enzyme linked immunosorbent assays (ELISA) could be used to confirm this finding.

# Chapter 6.
# General Discussion

It has long been thought that the mechanisms of ionising radiation induced biological effects through direct and indirect interaction were well understood (Hall and Giaccia, 2006). However recently a paradigm shift has developed in our understanding of radiation induced damage namely the discovery of the non-targeted effect theory which highlights the vital role of intercellular signalling in the triggering of genomic instability (GI) and bystander effects (BE) (Kadhim *et al.*, 1992; Nagasawa and Little, 1992). Genomic instability can be defined as a high frequency of genomic alteration following an initial exposure to ionising radiation (IR), which can display as delayed effects in the progeny of the irradiated cells (Kadhim *et al.*, 2013). Many factors influence the induction of GI including genetic predisposition, cell type, radiation quality, and dose factors (Kadhim, 2003). Moreover, the rate at which a radiation dose is delivered to the cell or tissue is one of the vital factors affecting the biological effects of radiation (Hall and Giaccia, 2006).

This thesis was constructed to investigate the potential role of dose and dose rate as well as radiation quality on the induction of GI in HF19 cells (primary non-transformed human fibroblast cells). A further aim was to explore the potential role of Tumour Necrosis Factor alpha (TNF-α), Transforming Growth Factor β1 (TGF-β1), and Reactive Oxygen Species (ROS) in the initiation of processes that could lead to the induction of GI in HF19 cells following exposure to LDR and HDR x-ray doses associated with environmental and occupational exposures. This study was therefore set up as follows:

1. Initially, the susceptibility of HF19 cells to the induction of early DNA damage and GI was examined following exposure to 0.0001, 0.001, 0.01, 0.1, 0.5 and 1 Gy high LET alpha particle irradiation. Early and late DNA damage was assessed using micronucleus assay and comet assay.
2. The susceptibility of HF19 cells to the induction of early DNA damage and GI was examined following exposure to 0, 0.1, 0.5, 1, 1.5, 2, 2.4, 3 and 4 Gy at high (0.42 Gy / minute) and low dose rate (0.0031 Gy / minute) low LET x-ray irradiation. Micronucleus assay and comet assay were used to evaluate the

early and late DNA damage.

3. The 0.1 and 1 Gy LDR and HDR x-ray doses, similar to those that might be encountered in diagnostic and therapeutic uses of radiation in therapy-related health care respectively, were used to investigate the susceptibility of HF19 cells to the induction of initial DNA damage and GI. The DNA damage was assessed using micronucleus assay. Additionally, cell viability assay and cell cycle measurements were used to assess the percentages of both dead and viable cells and the percentage of cells arrested at different cell cycle phases respectively at different time endpoints: 30 minutes, 8, 24 and 32 hours following 1 Gy LDR and HDR x-ray irradiation.
4. The molecular mechanisms involved in the induction of GI in HF19 cells following 0.1 and 1 Gy x-ray irradiation at high and low dose rates were investigated by measuring the potential role of ROS, TNF-α and TGF-β1 in radiation-induced GI.

## 6.1 HF19 susceptibility to the induction of early DNA damage and GI following exposure to alpha particle irradiation.

One of our main aims has been addressed in the experimental findings of chapter 3 where early and late total DNA damage in HF19 cells following low and high doses of high LET (alpha particles) exposure was discussed. Initially, DNA damage was examined following exposure to different doses of alpha particles using comet assay and micronucleus assay. Our findings displayed a significant early (5 hours following irradiation) increase in micronucleus formation in HF19 cells following exposure to 0.0001, 0.001, 0.01, 0.1, 0.5 and 1 Gy high LET alpha particle irradiation. Significant induction of micronuclei was observed even with low doses (0.0001 and 0.001 Gy) where only 0.8 % and 7.72 % of cells and 0.097 % and ≈1 % of nuclei were traversed by alpha particles respectively. This micronucleus formation increases with an increasing percentage of cells traversed by alpha particles until ≈8 % where the level of response plateaus. Even though less than 10 % of the cells were irradiated a higher proportion showed micronuclei. We hypothesize that this is attributable to bystander signalling. These results are in agreement with Lin *et al*.

(2014) who have observed that CHO and L-1 cells displayed an increased induction of sister chromatid exchanges (SCE) following 0.0014 Gy alpha particle irradiation where only 0.8 % of the nuclei were hit. They explained the induction of damage as a result of bystander effects since the vast majority of the surviving cells expressing SCE happened in unirradiated bystander cells (Lin *et al.*, 2014). Additionally, the results of Azzam *et al*. support the same idea as a higher frequency of micronucleus induction was observed in AG1522 normal human-diploid skin fibroblasts following exposure to very low fluences of alpha-particles at 1–10 cGy. Azzam's study illustrated that the 3-fold increase in the induction of micronuclei following exposure to 1–3 cGy and the 4-fold increase after exposure to 10 cGy showed not only that radiation-traversed cells are responsible for the biological response or genetic damage, but also that the cells in a population in the vicinity of directly hit cells (bystander cells) can play a role (Azzam *et al.*, 2001)

As indicated above, the susceptibility of HF19 cells to the induction of GI following low and high doses of high LET (alpha particles) irradiation needed to be examined. HF19 cells were examined at 10 and 20 population doublings following irradiation. After 10 population doublings, a delayed effect, a high micronucleus formation, was observed across all doses (0.0001, 0.001, 0.01, 0.1, 0.5 and 1 Gy alpha particle irradiation) with the same trend as that of the data at 5 hours post exposure but with a slightly lower induction of MN/BN. At 20 population doublings, all irradiated groups displayed an increased induction of micronuclei; this was significant across all groups except 0.0001 and 0.1 Gy. It is possible that the same plateauing pattern would have been observed at 20 population doublings if sufficient repeats had been performed. These findings agree with previous results achieved by Kadhim *et al*. (1992) who observed that the progeny of haemopoietic cells displayed a high frequency of aberration following exposure to alpha particles at 0.2-0.8 Gy compared to the control (Kadhim *et al.*, 1992). The delayed results of high doses of alpha particles (0.5 and 1 Gy) where ≈100 % of nuclei were hit are in agreement with Kadhim's observations (2001), where GI was observed in immobilised human T-lymphocytes at 12-13 population doublings following high LET irradiation using microbeam technology with which each cell centre in a given population of cells was traversed by a single $^{3}He^{2+}$ particle (used as a surrogate alpha-particle). A significant increase in nonclonal chromosomal aberrations ($p<0.001$) with a high frequency of chromatid-

type was displayed by approximately 25 % of cells in the surviving progeny of irradiated cells at 12-13 population doublings following irradiation (Kadhim *et al*., 2001).

Early DNA damage (1 h following irradiation) was examined using comet assay following alpha particle irradiation, with the results showing an increase in DNA damage across all irradiated groups compared to the control. Interestingly, this induction was high even with low doses (0.0001 and 0.001 Gy where only 0.097 % and 0.97 % of the nuclei were traversed) which could be due to the induction of BE that cause DNA damage. According to the study of Zhang *et al*. (2009) BE required at least a 1-hour incubation with irradiated cells to generate a level of signals sufficient to produce the maximal level of mutations (Zhang *et al.*, 2009). Zhang *et al*. (2009) have observed that naïve WTK1 cells treated with irradiated WTK1 cells (2 Gy, gamma ray) for 0.5 hours displayed mutant fractions. However, the maximal level of mutations was displayed after 1-hour incubation (Zhang *et al.*, 2009). Lyng *et al*. (2011) have reported the first direct proof of membrane signalling in a human keratinocyte cell line within 30 seconds following the addition of irradiated cell conditioned medium using a live cell imaging approach (Lyng *et al.*, 2011).

The results of high doses of alpha particles (0.5 and 1 Gy) where ≈100 % of nuclei were traversed agree to some extent with Laurent *et al*. (2013) who found that normal human dermal fibroblasts exhibited an increase in DNA damage using comet assay at 3 hours following 2 and 6 Gy high LET carbon ion irradiation. This elevation in DNA damage was explained by the induction of new ROS production and secondary strand-breaks generated throughout the DNA repair process in which intermediate breaks are produced before ligation, or by DNA misrepair producing damage (Laurent *et al.*, 2013). Moreover, as high LET radiation produces clustered DNA damage which may be wrongly repaired, this hypothesis of the DNA damage misrepair producing damage should be preferred as the main cause of increasing DNA damage at this delayed endpoint (Laurent *et al.*, 2013). Our results showed that the significant increase in DNA damage measured using the comet assay at 1 hour following alpha particle irradiation is in agreement with DNA damage assessed using micronucleus assay.

The significant induction of DNA damage measured using comet assay compared to the control correlates with the significant induction of micronucleus formation. This enhancement of DNA damage may potentially be due to the differences in track structure with alpha particles which have high LET. This may not only produce clustering of damage on the nanometric scale but also a correlation of damage along its path through the cell, resulting in a very non-homogeneous dose within the hit cell.

The delayed effect of alpha particles at 10 population doublings showed a significant induction of DNA damage across all irradiated groups compared to the control. However, the amount of this induction was lower compared to the damage at 1-hour post irradiation.

At 20 population doublings, only 0.0001 and 0.01 Gy progeny with 0.8 % and 55.25 % of cells traversed respectively displayed significant DNA damage compared to the control. These findings are in agreement with Nagasawa and Little (1999) who stated that the mutation frequency per alpha particle track at low doses increased unexpectedly since both directly irradiated and bystander cells are prone to the formation of mutations (Nagasawa and Little, 1999). However, the progeny of the 0.001, 0.1, 0.5 and 1 Gy irradiated groups in which 100 % of cells were traversed showed different responses. The progeny of groups irradiated at 0.001, 0.1, 0.5 and 1 Gy displayed non-significant DNA damage. The results suggest that HF19 cells are susceptible to the induction of GI in the progeny of 0.0001 and 0.01 Gy at 20 population doublings (see chapter 3). This could be due to the removal of cells with high DNA damage by mitotic catastrophe leaving healthy cells to continue to proliferate.

Although the results do not show significant effects of the radiation at 0.001, 0.1, 0.5 and 1 Gy at 20 population doublings, these doses may have other detrimental effects when studying other endpoints such as chromosomal analysis and Gamma- H2AX. Additionally, in order to examine if alpha particles can induce GI with HF19 cells at 0.001, 0.1, 0.5 and 1 Gy, one suggestion might be that more time points may be required.

The sample size was measured using the G*Power program. The findings showed for MN assay that the number of binucleate cells examined in each group was more than sufficient, except with the 0.0001 Gy group, and for the comet assay data, the G*Power program showed the same trend of sample size. However, 0.1 and 0.01 Gy groups, which showed less induction of DNA damage compared to the equivalent irradiated groups, needed to be repeated at least one more time.

## 6.2 The susceptibility of HF19 cells to the induction of early DNA damage and GI following exposure to high (0.42 Gy / minute) and low dose rate (0.0031 Gy / minute) low LET x-ray irradiation.

A significant increase in micronucleus formation demonstrated the induction of DNA damage following exposure to 0.1, 0.5, 1, 1.5, 2, 2.5, 3 and 4 Gy at 24 hours following irradiation. However, the LDR x-ray irradiation groups indicated more damage compared to the corresponding HDR x-ray irradiated groups. It should be noted that due to time constraints this assay was performed once when comparing LDR and HDR x-ray exposure following exposure to the same range of doses. With 0.1 and 1 Gy x-ray doses, which can be considered relevant to diagnostic and therapeutic uses respectively, both LDR and HDR groups showed a significant increase in micronuclei compared to the control in four biological replicates. However, LDR x-ray irradiated groups suggested a greater induction of micronuclei compared to the equivalent HDR x-ray irradiated groups as an immediate effect in four biological replicates. This could be due to the difference in the timing of adding Cytochalasin-B and subsequent time of collection between the HDR and LDR x-ray irradiated groups, and therefore different collection efficiencies are more likely to be obtained as like is not being compared with like. Pre- and post-acute (HDR) experiments were consequently performed. Interestingly, the 1 Gy post-acute (HDR) irradiated group (on which the irradiation was performed after the LDR group) suggested greater induction of micronuclei compared to the equivalent LDR immediately following irradiation. This could result from the separation in time of DNA lesions for LDR irradiation, with some lesions being repaired before the production of later lesions during the irradiation period. However, at high dose rate

the lesions are produced closer together in time making it more likely that interactions between them happen (Ruiz de Almodóvar *et al.*, 1994). The experimental results of chapter 5 demonstrated that the higher induction of ROS following 0.1 and 1 Gy LDR and HDR x-ray irradiation was implicated in the induction of early DNA damage (1.5 h following irradiation) (figure 6.1). The ongoing generation of ROS and nitrogen species following the initial radiation exposure leads to oxidative changes which may continue to increase for days and months (Petkau, 1987). However, the ROS formation was greater in LDR groups as opposed to HDR x-ray irradiation.

HF19 cells were examined at 10 and 20 population doublings following irradiation. The general trend was a significant increase in the induction of micronuclei across all HDR irradiated groups except 1 and 4 Gy. There was an oscillation in response between the results obtained for LDR compared to HDR as a function of dose at 10 and 20 population doublings in the single experiment performed with 0.1, 0.5, 1, 1.5, 2, 2.5, 3 and 4 Gy dose x-ray irradiation. However, when the same experiment was performed four times with 0.1 and 1 Gy x-ray at 10 and 20 population doublings, the results showed a significant increase in micronucleus formation following 0.1 and 1 Gy LDR and HDR x-ray irradiation. The GI associated with HDR was greater compared to the equivalent LDR of x-ray within human fibroblast HF19 cells. The x-ray irradiation induced persistent induction of ROS was firstly described by Clutton *et al*. (1996) who observed that x-ray irradiated primary mouse bone marrow displayed an increase in ROS at 7 days following irradiation which correlated with DNA damage assessed by 8-hydroxy-2-deoxyguanine (Clutton *et al.*, 1996). Additionally, Rugo *et al.* (2002) have reported the persistence of ROS in normal diploid human cells for 2 weeks after exposure to 2, 4, and 6 Gy x-ray with a dose rate 0.72 Gy / min (Rugo *et al.*, 2002). The results of both Clutton *et al.* (1996) and Rugo *et al.* (2002) support the hypothesis that x-ray increases the delayed induction of ROS which are involved in the delayed DNA damage that could establish a phenotype of GI (Clutton *et al.*, 1996; Rugo *et al.*, 2002). As described in Chapter 5, the greater formation of ROS levels in 0.1 and 1 Gy groups at 10 and 20 population doublings compared to the corresponding LDR x-ray irradiated groups as a delayed effect correlates with the observation of higher induction of DNA damage and micronuclei at the same doses.

At 24 hours following LDR and HDR x-ray irradiation, DNA damage was observed using comet assay. The low LET x-ray irradiation at HDR showed a significant increase in DNA damage in HF19 cells at 0.1, 0.5, 1.5, 2, 2.5, 3 and 4 Gy compared to the control; these data were collected from one single experiment. In contrast, no significant induction of DNA damage was observed following 1 Gy x-ray irradiation within this experiment.

With x-ray irradiation at LDR, the exposure of HF19 cells to different doses demonstrated an early induction of DNA damage following irradiation, which was significant with 0.1, 0.5, 1, 2, 2.5 and 4 Gy x-ray irradiation compared to the control. However, there was no significant increase in DNA damage at 1.5 and 3 Gy compared to the control. No consistent difference was observed between the HDR and LDR experiments across the dose range. However, these data are limited due to their resulting from a single experiment.

The experiment also included analysis of DNA damage at 10 and 20 population doublings as a delayed effect. As expected there was a large induction of DNA damage in the progeny of 0.1, 0.5, 1, 1.5, 2, 2.5, 3 and 4 Gy HDR compared to the control at 10 population doublings. Although these data were collected from a single experiment, results showed, in part, an agreement with that of Guryev *et al*. (2009) who observed an increase in the degree of DNA fragmentation in CHO cells up to 21 days post 1 Gy gamma-ray irradiation (HDR, 1.5 Gy / min) using the DNA comet assay (Guryev *et al.*, 2009). With LDR, the progeny of 0.1, 0.5, 1, 1.5, 2, 2.5, 3 and 4 Gy irradiated cells showed a significant increase in the induction of DNA damage compared to the control. Moreover, the pattern with respect to HDR was very similar to the pattern of induction of micronuclei, with a greater induction of DNA damage for LDR exposed cells at 24 h time-point for most groups. However, a much greater induction of DNA damage was shown at the delayed 10 population doublings for the HDR irradiated cells across almost all experimental groups.

At 20 population doublings, the data illustrated an increase in DNA damage in the progeny of irradiated cells at 0.5, 1, 1.5, 2 and 2.5 Gy compared to control, whilst the DNA damage in 3 and 4 Gy irradiated HF19 cells was statistically insignificant. This could be due to most aberrations being lethal and having been removed from the cultures by 20 population doublings following x-ray irradiation (Kadhim *et al.*,

1998). In agreement with the micronucleus assay results, there was no clear pattern between LDR and HDR irradiated cell groups in terms of DNA damage at 20 population doublings following irradiation.

As an early effect, both low LET (x-ray, HDR (0.1, 0.5, 1.5, 2, 2.5, 3 and 4 Gy) and LDR (0.1, 0.5,1, 2, 2.5 and 4 Gy)) and high LET (alpha particle (0.0001, 0.001, 0.01, 0.1, 0.5 and 1 Gy)) showed a significant induction of DNA damage. Additionally, genomic instability was observed both following exposures to low (HDR 0.1, 0.5, 1, 1.5, 2, 2.5 and 4 Gy and LDR 0.5, 1, 1.5, 2, 2.5 and 4 Gy) and to high LET at 10 population doublings across all irradiated progeny groups. At 20 population doublings, fluctuations, perhaps oscillations, in the induction of GI across the spectrum of doses were observed following exposure to low and to high LET irradiation.

The reliability and precision of early, intermediate and delayed comet and MN data following exposure to (0, 0.5, 1, 1.5, 2, 2.5, 3, 4) at high (0.42 Gy / minute) and low dose rates (0.0031 Gy / minute) of x-ray irradiation were not high as the data were collected from one single experiment even with the analysis of five hundred cells. These reliability and precision can be increased and biological variability can be decreased by performing further biologicals replicates.

## 6.3 The susceptibility of HF19 cells to the induction of initial DNA damage and GI following LDR and HDR x-ray exposure in doses relevant to diagnostic and therapeutic uses and the potential molecular mechanisms involved in the induction of GI.

To further investigate the effect of dose and dose rate as well as the molecular mechanisms involved in the induction of GI in HF19 cells, experiments were performed where HF19 was irradiated with 0.1 and 1 Gy, doses relevant to diagnostic and therapeutic uses of radiation. The initial effect of 0.1 and 1 Gy LDR and HDR x-ray irradiation clearly suggested an increase in the number of binucleate cells with MN, with a higher level of induction at LDR compared to the equivalent

HDR pre LDR (where HDR irradiation was performed before the LDR irradiation) exposure. The micronucleus assay was performed following irradiation for four independent but parallel experiments. This is could be due to the fact that the cells in each culture are in different cell cycle phases, so these go through division at different times. Additionally, the difference between the HDR and LDR groups (under the same conditions of collection) in terms of the timing of adding Cytochalasin-B and the timing of the subsequent harvesting of cells can lead to different collection efficiencies as like is not being compared with like. It was therefore not too surprising to see different results and this was one of the reasons pre- and post-acute experiments were performed. Interestingly, the results of 1Gy post-acute (HDR) cells (where HDR irradiation was performed after the LDR irradiation) suggested a greater induction of micronuclei compared to the equivalent LDR cells. This reduction of micronuclei formation at LDR could be due to some fraction of the potential chromosomal damage that would have occurred as a result of the interaction of separate ionization tracks being repaired throughout the extended exposure to LDR irradiation (Ban *et al.*, 1991).

This observation correlates with the reduction of cell viability rate following 1 Gy LDR compared to 1Gy HDR at 32 hours post irradiation. Previously, Shrivastava *et al*. (2006) have stated that the predominant mode of cell death (mitotic death) which contributes to the loss of survival is correlated to cytogenetic damage. This cytogenetic damage is expressed as chromosomal aberrations in metaphase which eventually manifest as micronucleus formation in the new daughter nuclei at the end of telophase (Shrivastava *et al.*, 2006). Thus, the higher increase in micronucleus formation could lead to a rise in cell death (figure 6.2). The greater induction of micronucleus formation with 0.1 and 1 Gy HDR compared to LDR at the early time point is linked to the higher DNA damage observed with HDR irradiation using comet assay.

The previous study of Choi *et al*. (2007) has shown that when Jurkat T cells irradiated with 2.5 Gy $^{137}$Cs gamma-ray, both the mitochondria and Nox1 (gene encodes NADPH oxidase enzymes responsible for generating superoxide or hydrogen peroxide) were stimulated to generate ROS. Therefore, the results of chapter 5 showed that the significant increase in the cellular ROS level was accompanied by

an elevation in micronucleus formation. Thus, the ROS acted as signalling messengers that mediated the induction of micronuclei and regulated the cell viability (Choi *et al.*, 2007).

The results of this study suggested that the increase in ROS level in LDR compared to HDR was implicated in the higher induction of micronuclei in the 0.1 and 1 Gy LDR groups at 1.5 h following irradiation compared to the equivalent HDR (see chapter 5).

At 10 and 20 population doublings (delayed effects), micronucleus formation was examined to assess DNA damage in HF19 cells following exposure to 0.1 and 1 Gy x-ray irradiation at LDR and HDR. LDR and HDR groups all showed a significant induction of micronucleus formation which indicates that both LDR and HDR are capable of inducing GI at 10 and 20 population doublings. However, the results suggested that HDR is associated with greater GI induction than the equivalent LDR following exposure to x-ray within human fibroblast HF19 cells. This difference in the induction of DNA damage following HDR and LDR exposure was also observed using comet assay. The HDR progeny demonstrated more DNA damage compared to the corresponding LDR progeny following irradiation with 0.1 and 1 Gy x-ray at 10 and 20 population doublings. These findings agree with the data reported by Turner *et al*. (2015) where the exposure to HDR showed a greater induction of MN compared to the equivalent LDR exposure in mouse lymphocytes at 24 hours and 7 days after *in vivo* exposure to 0–4.45 Gy x-ray irradiation (Turner *et al.* 2015).

At least 1500 binucleate cells were analysed in each irradiated group for MN assay from four biological replicates. The data showed similar trend each time indicating replicability of the results.

The higher induction of ROS across 0.1 and 1 Gy HDR and LDR at 20 population doublings supports the idea that the induction of GI (micronuclei and whole DNA damage) in HF19 cells is due to the continuous higher induction of ROS across 0.1 and 1 Gy of ROS from some cells into a cell population following exposure (see chapter 5). Previously, Petkau (1987) has stated that ROS are produced for days and months following irradiation (Petkau, 1987). However, this induction of ROS was higher in HDR groups compared to the equivalent LDR groups, which could have led

to more micronucleus formation in HDR progeny compared to the corresponding LDR progeny as illustrated in chapter 4 section 4.2.5.

In light of our data, early DNA damage (1.5 h following irradiation) and GI induction in HF19 cells are strongly correlated with the induction of higher ROS levels at 0.1 and 1 Gy x-ray irradiation. However, TNF-α and TGF-β1 did not play a significant role in radiation-induced DNA damage and GI induction in HF19 following exposure to 0.1 and 1 Gy HDR and LDR (see chapter 5).

The ROS findings suggested replicability since they were collected from three biological replicates performed on different days with small SEM. However, the TNF-α and TGF-β1 data showed high SEM which was most obvious in the 1Gy LDR TGF-β1 expression at 20 population doublings, even though three separate but parallel experiments had been used to collect these data. This biological variation could be reduced by analysing an increased number of biological replicates. Furthermore, confirmation of the TNF-α and TGF-β1 data can be achieved using different methods such as qRT-PCR, sandwich enzyme linked immunosorbent assays (ELISA) and other quantitative immunohistochemistry. These approaches could be more sensitive for investigating the potential role of TNF-α and TGF-β1 in radiation-induced genomic instability in HF19 cells following x-ray irradiation at high and low dose rate exposure.

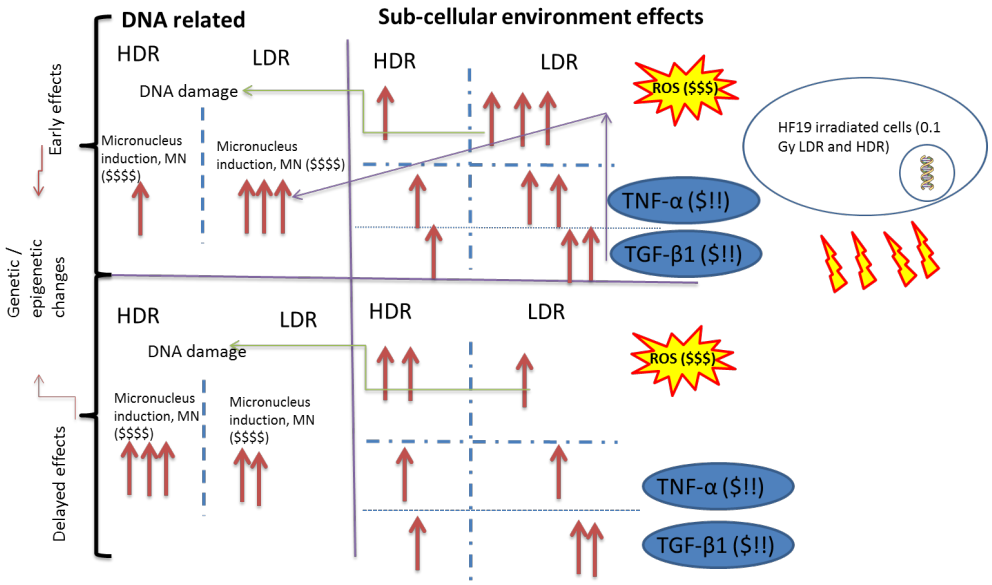


| Measuring damage | Biological replicates | Measuring damage | Biological replicates | Measuring damage | Biological replicates |
|---|---|---|---|---|---|
| MN ($$$$) | Four times | TNF-α and TGF-β1 ($!!) | Three times, requested clarification by another approach | ROS ($$$) | Three times |

Figure 6.1: A schematic of possible mechanistic interactions between DNA, ROS, TNF-α and TGF-β1 in the induction of GI post exposure to 0.1 Gy HDR and LDR x-ray irradiation.

Radiation can induce ROS, which in turn can cause DNA damage. As well as ROS influencing TGF-β1 signalling, TGF-β1 signalling can control ROS generation (Krstić *et al.*, 2015), despite the low level of TGF-β1. Low induction of TNF-α often induces intracellular ROS formation (Chen *et al.*, 2008). LDR x-ray exposure elicits ROS in HF19 cells at a greater level compared to the equivalent HDR as an early effect post irradiation, which is linked to the greater induction of DNA damage at LDR compared HDR as an early effect. As time progresses, cells were suggested to undergo genetic and epigenetic changes which could lead to the effects observed in the progeny of the irradiated cells that were seen at 20 population doublings. At 20 PD, the production of ROS were higher in HDR progeny compared to LDR progeny, which correlates to the induction of genomic instability as a late effect in HF19 cells.

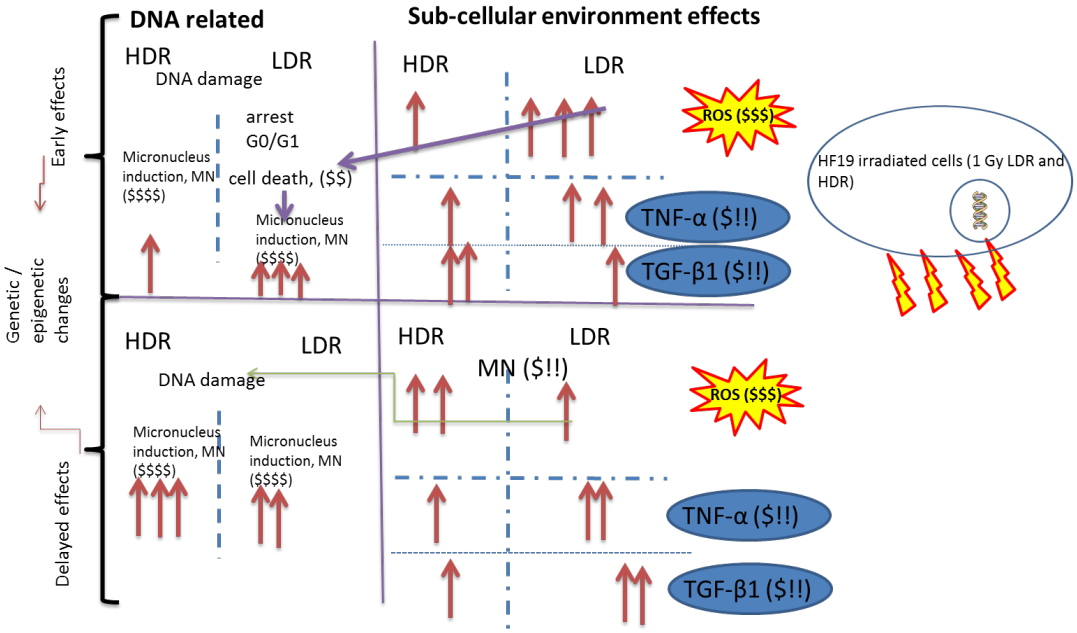


| Measuring damage | Biological replicates | Measuring damage | Biological replicates |
|---|---|---|---|
| MN ($$$$) | Four times | TNF-α and TGF-β1 ($!!) | Three times, requested clarification by another approach |
| ROS ($$$) | Three times | Cell death($$) | Two times (replicable) |

Figure 6.2: A schematic of possible mechanistic interactions between DNA, ROS, TNF-α and TGF-β1 in the induction of GI post exposure to 1 Gy HDR and LDR x-ray irradiation.

LDR x-ray exposure elicits ROS in HF19 cells at a greater level compared to the equivalent HDR as an early effect post 1 Gy x-ray irradiation. This is linked to the greater induction of chromosomal aberrations in the metaphase, which eventually manifest as micronucleus formation in the new daughter nuclei at the end of telophase. The greater initial induction of micronuclei in LDR group compared to the equivalent HDR could also be due to the concomitant increase in the percentage of cells arrested in the G0/G1 cell cycle phase by HDR compared to LDR. TGF-β1 signalling can control the ROS generation (Krstić *et al.*, 2015), despite the low level of TGF-β. Low induction of TNF-α often induces intracellular ROS formation (Chen *et al.*, 2008). As time progresses, cells were suggested to undergo genetic and epigenetic changes which could lead to the effects observed in the progeny of the irradiated cells that were seen at 20 population doublings. At 20 PD, the production of ROS were higher in HDR progeny compared to LDR progeny, which correlates to the higher induction of GI in HDR compared to the equivalent LDR as a late effect in HF19 cells.

## 6.4 Future work

As shown in chapter 4, 0.1 and 1 Gy LDR and HDR x-ray irradiation of HF19 cells lead to an increase in GI with a higher induction in HDR compared to the equivalent LDR x-ray irradiation. The MN data were collected from four independent parallel experiments showing a similar trend which demonstrates the replicability of the results. More investigations, therefore, on different cell lines/cell types would be valuable for evaluating radiation protection, radiation damage, and medical diagnosis and treatment of radiation exposure. However, in chapter 3, although 1000 cells were examined for comet and MN assays, the recommended sample size was calculated using G*Power since only two biological replicates were used. The G*Power results for the MN assay data showed that a sufficient number of binucleate cells was analysed in each irradiated group for a powerful statistical analysis except with the 0.0001 Gy group. Additionally, the same trend of sample size was observed with the comet assay results. However, the G*Power results for 0.1 and 0.01 Gy groups recommended repeating the comet assay at least one more time.

This work has shown that ROS is correlated to the induction of GI in HF19 cells following HDR or LDR x-ray irradiation. This, therefore, poses the question what the other cellular components are that are responsible for the stimulation of the signalling that leads to the induction of GI in HF19 cells and if the extracellular signal-related kinase (ERK), mitogen-activated protein kinase (MAPK), Ataxia telangiectasia-mutated (ATM) and protein 53 (P53) pathways could be involved the induction of GI in HF19 following exposure to x-ray and alpha particle irradiation. A better understanding of how radiation dose rate affects the molecular mechanisms involved in the induction of GI would contribute to the evaluation of radiation protection, radiation damage, and medical diagnosis and treatment for radiation exposure. Despite our best efforts of optimizing quantification approaches of immunoblot data, we believe that qRT-PCR, sandwich enzyme linked immunosorbent assays (ELISA) and other quantitative immunohistochemistry may be more suitable to assess the response of HF19 cells with regard to TNF-α and TGF-β1 across different doses and dose rates.

Furthermore, more studies are needed to study the role of bystander signalling in the induction of GI following exposure to x-ray and alpha particle irradiation using media transfer or using co-culture dishes (so separating out irradiated and un-irradiated cells). Some recent studies reported by Kadhim's group suggested that genomic instability can be instigated due to alterations in telomeric metabolism induced by both proteins and RNAs of exosomes in epithelial cancer cells following x-ray irradiation (Al-Mayah et al., 2016). Moreover, another experiment potentially worth doing is attempting to inhibit or enhance various pathways by adding components in excess to see how this modulates the response with and without radiation. For example, the relative importance of the superoxide radical pathways could be investigated by using various inhibitors such as superoxide dismutase (SOD), polyethylene glycol (PEG)-SOD (Luo *et al.,* 2009).

Another interesting point moving forward could be the investigation of the induction of GI in lung cells in in vivo-like situations. One technique that could be used involves using three-dimensional in vivo-like dense colonies of normal primary human fibroblast to investigate the induction of GI in lung cells in a 96-well plate format; this would be applicable for high-throughput screening. However, the *in vivo* situation may not be as simple as that found in the *in vitro* system as a result of the contribution from other systems in the biological body. Additionally, further studies using different cell types of different origins are needed to address the general effect of radiation quality and radiation dose rate in the induction of GI following exposure to x-ray and alpha particle irradiation.

# References


Al-Mayah, A.H.J., Irons, S.L., Pink, R.C., Carter, D.R.F., Kadhim, M.A. (2012) Possible role of exosomes containing RNA in mediating nontargeted effect of ionizing radiation. *Radiation Research*. 177(5), 539–545.

Al-Mayah, A., Bright, S., Chapman, K., Irons, S., Luo, P., Carter, D., Goodwin, E., Kadhim, M. (2015) The non-targeted effects of radiation are perpetuated by exosomes. *Mutation Research*. 772, 38–45.

Al-Mayah, A.H.J., Bright, S.J., Bowler, D.A., Slijepcevic, P., Goodwin, E., Kadhim, M.A. (2016) Exosome-Mediated Telomere Instability in Human Breast Epithelial Cancer Cells after X Irradiation. *Radiation Research*. 187(1), 98–106.

Antoccia, A., Sgura, A., Berardinelli, F., Cavinato, M., Cherubini, R., Gerardi, S., Tanzarella, C. (2009) Cell cycle perturbations and genotoxic effects in human primary fibroblasts induced by low-energy protons and X/gamma-rays. *Journal of Radiation Research*. 50(5), 457–468.

Asaithamby, A., Hu, B., Chen, D.J. (2011) Unrepaired clustered DNA lesions induce chromosome breakage in human cells. *Proceedings of the National Academy of Sciences of the United States of America*. 108(20), 8293–8298.

Aypar, U., Morgan, W.F., Baulch, J.E. (2011) Radiation-induced epigenetic alterations after low and high LET irradiations. *Mutation Research*. 707(1-2), 24–33.

Azzam, E.I., de Toledo, S.M., Gooding, T., Little, J.B. (1998) Intercellular communication is involved in the bystander regulation of gene xpression in human cells exposed to very low fluences of alpha particles. *Radiat. Res.* 150, 497–504.

Azzam, E. I., de Toledo, S.M., Little, J.B. (2001) Direct evidence for the participation of gap junction-mediated intercellular communication in the transmission of damage signals from alpha -particle irradiated to nonirradiated cells. *Proceedings of the National Academy of Sciences of the United States of America*. 98(2), 473–478.

Azzam, E.I., Toledo, S.M. de, Spitz, D.R., Little, J.B. (2002) Oxidative Metabolism Modulates Signal Transduction and Micronucleus Formation in Bystander Cells from α-Particle-irradiated Normal Human Fibroblast Cultures. *Cancer Research*. 62(19), 5436–5442.

Azzam, E.I., Jay-Gerin, J.-P., Pain, D. (2012) Ionizing radiation-induced metabolic oxidative stress and prolonged cell injury. *Cancer letters*. 327(0), 48–60.

Ban, S., Donovan, M.P., Cologne, J.B., Sawada, S. (1991) Gamma-ray- and fission neutron-induced micronuclei in PHA stimulated and unstimulated human lymphocytes. *Journal of Radiation Research*. 32(1), 13–22.

Banaz-Yasar, F., Lennartz, K., Winterhager, E., Gellhaus, A. (2008) Radiation-induced bystander effects in malignant trophoblast cells are independent from gap junctional communication. *Cell Biochem.* 103, 149–161.

Barcellos-Hoff, M.H. (2005) How tissues respond to damage at the cellular level: orchestration by transforming growth factor-β (TGF-β). *The British Journal of Radiology*. Supplement_27(1), 123–127.

Baverstock, K. (2000) Radiation-induced genomic instability: a paradigm-breaking phenomenon and its relevance to environmentally induced cancer. *Mutation research*. 454(1-2), 89–109.

BEIR VI (1999) *Health effects of exposure to Radon*. Washington DC: The National Academies Press.

BEIR VII (2005) *Health Risks from Exposure to Low Levels of Ionizing Radiation: BEIR VII Phase 2*. Washington DC: The National Academies Press.

Belyakov, O.V., Prise, K.M., Trott, K.R., Michael, B.D. (1999) Delayed lethality, apoptosis and micronucleus formation in human fibroblasts irradiated with X-rays or alpha-particles. *International Journal of Radiation Biology*. 75(8), 985–993.

Ben-Hur, E., Elkind, M.M. (1974) Thermally enhanced radioresponse of cultured Chinese hamster cells: damage and repair of single-stranded DNA and a DNA complex. *Radiation Research*. 59(2), 484–495.

BER (2010) Office of biological and environmental research, Office of Science, U.S. Department of energy. Available at:. https://www.science.doe.gov/ober/. (Accessed: 25th September 2017).

Bernhard, E.J., Maity, A., Muschel, R.J., McKenna, W.G. (1995) Effects of ionizing radiation on cell cycle progression. A review. *Radiation and Environmental Biophysics*. 34(2), 79–83.

Bindokas, V.P., Jordán, J., Lee, C.C., Miller, R.J. (1996) Superoxide production in rat hippocampal neurons: selective imaging with hydroethidine. *The Journal of Neuroscience: The Official Journal of the Society for Neuroscience*. 16(4), 1324–1336.

Birben E., Sahiner U., Sackesen C., Erzurum S., Kalayci O. (2012) Oxidative Stress and Antioxidant Defense. *World Allergy Organ J* . 5, 9 – 19.

Boerma, M., Bart, C.I., Wondergem, J. (2002) Effects of ionizing radiation on gene expression in cultured rat heart cells. *International Journal of Radiation Biology*. 78(3), 219–225.

Bohm, F., Hendry, J., Hill, R., Le Heron, J., Mishra, K., Trott, K., Wondergem, J. (2010) *Radiation Biology*. Vienna, Austria: IAEA-TCS-42.

Boreham, D.R., Dolling, J.A., Maves, S.R., Siwarungsun, N., Mitchel, R.E. (2000) Dose-rate effects for apoptosis and micronucleus formation in gamma-irradiated human lymphocytes. *Radiation Research*. 153(5 Pt 1), 579–586.

Bowler, D.A., Moore, S.R., Macdonald, D.A., Smyth, S.H., Clapham, P., Kadhim, M.A. (2006) Bystander-mediated genomic instability after high LET radiation in murine primary haemopoietic stem cells. *Mutation research*. 597(1-2), 50–61.

Boyd, M., Ross, S.C., Dorrens, J., Fullerton, N.E., Tan, K.W., Zalutsky, M.R., Mairs, R.J. (2006) Radiation-induced biologic bystander effect elicited in vitro by targeted diopharmaceuticals labeled with alpha-, beta-, and augerelectron-emitting adionuclides,. *Nucl. Med.* 47, 1007–1015.

Brenner, D.J. (2012) Exploring two two-edged swords. *Radiation Research*. 178(1), 7–16.

Brigelius-Flohé, R., Maiorino, M. (2013) Glutathione peroxidases. *Biochimica Et Biophysica Acta*. 1830(5), 3289–3303.

Butterworth, K.T., McGarry, C.K., Trainor, C., O'Sullivan, J.M., Hounsell, A.R., Prise, K.M. (2011) Out-of-field cell survival following exposure to intensity-modulated radiation fields. *Radiat. Oncol. Biol. Phys*. 79, 1516–1522.

Canney, P.A., Dean, S. (1990) Transforming growth factor beta: a promotor of late connective tissue injury following radiotherapy? *The British Journal of Radiology*. 63(752), 620–623.

Chen, X., Andresen1, B.T., Hill, M., Zhang, J., Booth, F., Zhang, C. (2008) Role of Reactive Oxygen Species in Tumor Necrosis Factor-alpha Induced Endothelial Dysfunction. *Current Hypertension Reviews*. 4(4), 245–255.

Chen, H., Wang, B., Wang, C., Cao, W., Zhang, J., Ma, Y., Hong, Y., Fu, S., Wu, F., Ying, W. (2016) Dose-rate plays a significant role in synchrotron radiation X-ray-induced damage of rodent testes. *International Journal of Physiology, Pathophysiology and Pharmacology*. 8(4), 140–145.

Cho, Y.H., Kim, S.Y., Woo, H.D., Kim, Y.J., Ha, S.W., Chung, H.W. (2015) Delayed Numerical Chromosome Aberrations in Human Fibroblasts by Low Dose of Radiation. *International Journal of Environmental Research and Public Health*. 12(12), 15162–15172.

Choi, K.-M., Kang, C.-M., Cho, E.S., Kang, S.M., Lee, S.B., Um, H.-D. (2007) Ionizing radiation-induced micronucleus formation is mediated by reactive oxygen species that are produced in a manner dependent on mitochondria, Nox1, and JNK. *Oncology Reports*. 17(5), 1183–1188.

Cimini, D., Degrassi, F. (2005) Aneuploidy: a matter of bad connections. *Trends in Cell Biology*. 15(8), 442–451.

Clutton, S.M., Townsend, K.M., Walker, C., Ansell, J.D., Wright, E.G. (1996) Radiation-induced genomic instability and persisting oxidative stress in primary bone marrow cultures. *Carcinogenesis*. 17(8), 1633–1639.

Collis, S.J., Schwaninger, J.M., Ntambi, A.J., Keller, T.W., Nelson, W.G., Dillehay, L.E., Deweese, T.L. (2004) Evasion of early cellular response mechanisms following low level radiation-induced DNA damage. *The Journal of Biological Chemistry*. 279(48), 49624–49632.

Luo, Z., Chen, Y., Chen, S., Welch, WJ., Andresen, BT., Jose, PA., Wilcox, CS. (2009) Comparison of inhibitors of superoxide generation in vascular smooth muscle cells. *British Journal of Pharmacology*,157, 935–943.

Cooke, M.S., Evans, M.D., Dizdaroglu, M., Lunec, J. (2003) Oxidative DNA damage: mechanisms, mutation, and disease. *FASEB journal: official publication of the Federation of American Societies for Experimental Biology*. 17(10), 1195–1214.

Cox, R., Masson, W.. (1975) *X-ray survival curves of cultured human diploid fibroblasts*. In Alper, T. (ed.), in Cell Survival after Proceedings of the 6th L. H. Gray Conference. London: Institute of Physics/Chichester: John Wiley.

Curwen, G.B., Tawn, E.J., Cadwell, K.K., Guyatt, L., Thompson, J., Hill, M.A. (2012) mFISH analysis of chromosome aberrations induced in vitro by α-particle radiation: examination of dose-response relationships. *Radiation Research*. 178(5), 414–424.

Darby, S., Hill, D., Auvinen, A., Barros-Dios, J.M., Baysson, H., Bochicchio, F., Deo, H., Falk, R., Forastiere, F., Hakama, M., Heid, I., Kreienbrock, L., Kreuzer, M., Lagarde, F., Mäkeläinen, I., Muirhead, C., Oberaigner, W., Pershagen, G., Ruano-Ravina, A., Ruosteenoja, E., Rosario, A.S., Tirmarche, M., Tomásek, L., Whitley, E., Wichmann, H.-E., Doll, R. (2005) Radon in homes and risk of lung cancer: collaborative analysis of individual data from 13 European case-control studies. *BMJ (Clinical research ed.)*. 330(7485), 223.

Deckbar, D., Jeggo, P.A., Lobrich, M. (2011) Understanding the limitations ofradiation-induced cell cycle checkpoints. *Critical Reviews in Biochemistry and Molecular Biology*. 46(4), 271–283.

Degtyareva, N.P., Chen, L., Mieczkowski, P., Petes, T.D., Doetsch, P.W. (2008) Chronic Oxidative DNA Damage Due to DNA Repair Defects Causes Chromosomal Instability in Saccharomyces cerevisiae. Molecular and Cellular Biology. 28(17), 5432–5445.

Delara, C.M., Jenner, T.J., Townsend, K.M., Marsden, S.J., O'Neill, P. (1995) The effect of dimethyl sulfoxide on the induction of DNA double-strand breaks in V79-4 mammalian cells by alpha particles. *Radiation Research*. 144(1), 43–49.

Di Giorgio, M., Kreiner, A.J., Schuff, J.A., Vallerga, M.B., Taja, M.R., Lopez, F.O., Alvarez, D.E., Saint Martin, G., Burton, A., Debray, M.E., Kesque, J.M., Somacal, H., Stoliar, P., Valda, A., Davidson, J., Davidson, M., Ozafran, M.J., Vazquez, M.E. (2004) Evaluation through comet assay of DNA damage induced in human lymphocytes by alpha particles. Comparison with protons and Co-60 gamma rays. 11th International Congress of the International Radiation Protection Association, 23-28 May 2004, Madrid. Spain: Full paper.

Dillehay, L.E. (1990) A Model of Cell Killing by Low-Dose-Rate Radiation Including Repair of Sublethal Damage, G2 Block, and Cell Division. *Radiation Research*. 124(2), 201–207.

Dionian, J., Muirhead, C.R., Wan, S.L., Wrixon, A.D. (1986) *The risks of leukaemia and other cancers in Thurso from radiation exposure*. Chilton: National Radiological Protection Board.

Dodge, J.E., Okano, M., Dick, F., Tsujimoto, N., Chen, T., Wang, S., Ueda, Y., Dyson, N., Li, E. (2005) Inactivation of Dnmt3b in mouse embryonic fibroblasts results in DNA hypomethylation, chromosomal instability, and spontaneous immortalization. *The Journal of Biological Chemistry*. 280(18), 17986–17991.

Doudican, N.A., Song, B., Shadel, G.S., Doetsch, P.W. (2005) Oxidative DNA damage causes mitochondrial genomic instability in Saccharomyces cerevisiae. *Molecular and Cellular Biology*. 25(12), 5196–5204.

Dubrova, Y.E. (2003) Radiation-induced transgenerational instability. *Oncogene*. 22(45), 7087–7093.

Fearon, E., Vogelstein, B. (1990) A genetic model for colorectal cancer tumorigenesis.

*Cell*. 61, 759–767.

Feinendegen, L., Muehlensiepen, H., Lindberg, C., Marx, J., Porschen, W., Booz, J. (1983) *Acute effect of very low dose in mouse bone marrow cells: A physiological response to background radiation. In International symposium on the effects of low-level radiation with special regard to stochastic and non-stochastic effects.* In International symposium on the effects of low-level radiation with special regard to stochastic and non-stochastic effects; Venice, pp. 459–471.

Feinendegen, L.E. (2002) Reactive oxygen species in cell responses to toxic agents.

*Human & Experimental Toxicology*. 21(2), 85–90.

Fenech, M. (2006) Cytokinesis-block micronucleus assay evolves into a 'cytome' assay of chromosomal instability, mitotic dysfunction and cell death. *Mutation Research*. 600(1-2), 58–66.

Fenech, M. (2007) Cytokinesis-block micronucleus cytome assay. *Nature Protocols*. 2(5), 1084–1104.

Fenech, M., Kirsch-Volders, M., Natarajan, A.T., Surralles, J., Crott, J.W., Parry, J., Norppa, H., Eastmond, D.A., Tucker, J.D., Thomas, P. (2011) Molecular mechanisms of micronucleus, nucleoplasmic bridge and nuclear bud formation in mammalian and human cells. *Mutagenesis*. 26(1), 125–132.

Filkowski, J.N., Ilnytskyy, Y., Tamminga, J., Koturbash, I., Golubov, A., Bagnyukova, T., Pogribny, I.P., Kovalchuk, O. (2010) Hypomethylation and genome instability in the germline of exposed parents and their progeny is associated with altered miRNA expression. *Carcinogenesis*. 31(6), 1110–1115.

Frankenberg-Schwager, M., Frankenberg, D., Blöcher, D., Adamczyk, C. (1981) Effect of dose rate on the induction of DNA double-strand breaks in eucaryotic cells. *Radiation Research*. 87(3), 710–717.

Furlong, H., Mothersill, C., Lyng, F.M., Howe, O. (2013) Apoptosis is signalled early by low doses of ionising radiation in a radiation-induced bystander effect. *Mutation Research*. 741-742, 35–43.

Gaudet, F., Hodgson, J.G., Eden, A., Jackson-Grusby, L., Dausman, J., Gray, J.W., Leonhardt, H., Jaenisch, R. (2003) Induction of tumors in mice by genomic hypomethylation. *Science (New York, N.Y.)*. 300(5618), 489–492.

Geara, F.B., Peters, L.J., Ang, K.K., Wike, J.L., Sivon, S.S., Guttenberger, R., Callender, D.L., Malaise, E.P., Brock, W.A. (1992) Intrinsic radiosensitivity of normal human fibroblasts and lymphocytes after high- and low-dose-rate irradiation. *Cancer Research*. 52(22), 6348–6352.

Gentile, M., Latonen, L., Laiho, M. (2003) Cell cycle arrest and apoptosis provoked by UV radiation-induced DNA damage are transcriptionally highly divergent responses. *Nucleic Acids Research*. 31(16), 4779–4790.

Ghandhi, S.A., Yaghoubian, B., Amundson, S.A. (2008) Global gene expression analyses of bystander and alpha particle irradiated normal human lung fibroblasts: synchronous and differential responses. *BMC medical genomics*. 1, 63.

Ghandhi, S.A., Smilenov, L.B., Elliston, C.D., Chowdhury, M., Amundson, S.A. (2015) Radiation dose-rate effects on gene expression for human biodosimetry. *BMC medical genomics*. 8, 22.

Goodhead, D.T. (1994) Initial events in the cellular effects of ionizing radiations: clustered damage in DNA. *Int J Radiat Biol*. 65(1), 7–17.

Goodhead, D.T. (1999) Mechanisms for the biological effectiveness of high-LET radiations. *Journal of Radiation Research*. 40 Suppl, 1–13.

Goodhead, D.T. (2009) Understanding and characterisation of the risks to human health from exposure to low levels of radiation. *Radiation Protection Dosimetry*. 137(1-2), 109–117.

Goodhead, D.T. (2010) New radiobiological, radiation risk and radiation protection paradigms. *Mutation Research*. 687, 13–16.

Goodhead, D.T., Bance, D.A., Stretch, A., Wilkinson, R.E. (1991) A versatile plutonium-238 irradiator for radiobiological studies with alpha-particles. *International Journal of Radiation Biology*. 59(1), 195–210.

Goodhead, D.T, Nikjoo, H. (1997) Clustered damage in DNA: estimates from track-structure simulations. *Radiation Research*. 148, 485–486.

Graupner, A, Eide, D., Instanes, C., Andersen, J., Brede, D., Lind, O., Brandt-Kjelsen, A., Dertinger, S., Lind, O., Brandt-Kjelsen, A., Bjerke, H., Salbu, B., Oughton, D., Brunborg, G., Olsen, A. (2016) Gamma radiation at a human relevant low dose rate is genotoxic in mice. *Scientific Reports.* (2016) Sep 6;6:32977. doi: 10.1038/srep32977

Grygoryev, D., Moskalenko, O., Hinton, T.G., Zimbrick, J.D. (2013) DNA damage caused by chronic transgenerational exposure to low dose gamma radiation in Medaka fish ( Oryzias latipes ). *Radiation Research*. 180(3), 235–246.

Gudkov, A.V., Gurova, K.V., Komarova, E.A. (2011) Inflammation and p53. *Genes & Cancer*. 2(4), 503–516.

Guryev, D.V., Osipov, A.N., Lizunova, E.Y., Vorobyeva, N.Y., Boeva, O.V. (2009) Ionizing radiation-induced genomic instability in CHO cells is followed by selection of radioresistant cell clones. *Bulletin of Experimental Biology and Medicine*. 147(5), 596-598.

Hagelstrom, R.T., Askin, K.F., Williams, A.J., Ramaiah, L., Desaintes, C., Goodwin, E.H., Ullrich, R.L., Bailey, S.M. (2008) DNA-PKcs and ATM influence generation of ionizing radiation-induced bystander signals. *Oncogene*. 27, 6761–6769.

Hall, E.J. (1972) Radiation dose-rate: a factor of importance in radiobiology and radiotherapy. *The British Journal of Radiology*. 45(530), 81–97.

Hall, E.J., Bedford, J.S. (1964) Dose rate: its effect on the survival of HELA cells irradiated with gamma rays. *Radiation Research*. 22, 305–315.

Hall, E.J., Brenner, D.J. (1991) The dose-rate effect revisited: radiobiological considerations of importance in radiotherapy. *International Journal of Radiation Oncology, Biology, Physics*. 21(6), 1403–1414.

Hall, E.J., Hei, T.K. (2003) Genomic instability and bystander effects induced by high-LET radiation. *Oncogene*. 22(45), 7034–7042.

Hall, Eric J., Giaccia, A.J. (2006) *Radiobiology for the Radiologist*. Lippincott: Williams & Wilkins.

Hall, E. J., & Giaccia, A. J. (2011). Radiobiology for the radiologist (7th ed.). Philadelphia: Lippincott Williams & Wilkins.

Hanahan, D., Weinberg, R.A. (2011) Hallmarks of cancer: the next generation. *Cell*. 144(5), 646–674.

Hartlerode, A.J., Scully, R. (2009) Mechanisms of double-strand break repair in somatic mammalian cells. *The Biochemical Journal*. 423(2), 157–168.

Hei, T.K., Zhou, H., Chai, Y., Ponnaiya, B., Ivanov, V.N.. (2011) Radiation induced nontargeted response: mechanism and potential clinical implications. *Curr. Mol. Pharmacol.* 4, 96–105.

Hill, M.A., Herdman, M.T., Stevens, D.L., Jones, N.J., Thacker, J., Goodhead, D.T. (2004) Relative sensitivities of repair-deficient mammalian cells for clonogenic survival after alpha-particle irradiation. *Radiation Research*. 162(6), 667–676.

Hintzsche, H., Hemmann, U., Poth, A., Utesch, D., Lott, J., Stopper, H., Working Group 'In vitro micronucleus test', Gesellschaft für Umwelt-Mutationsforschung (GUM, German-speaking section of the European Environmental Mutagenesis and Genomics Society EEMGS) (2017) Fate of micronuclei and micronucleated cells. *Mutation Research*. 771, 85–98.

Hirayama, R., Ito, A., Tomita, M., Tsukada, T., Yatagai, F., Noguchi, M., Matsumoto, Y., Kase, Y., Ando, K., Okayasu, R., Furusawa, Y. (2009) Contributions of direct and indirect actions in cell killing by high-LET radiations. *Radiation Research*. 171(2), 212–218.

Holm, K., Staaf, J., Lauss, M., Aine, M., Lindgren, D., Bendahl, P.-O., Vallon-Christersson, J., Barkardottir, R.B., Höglund, M., Borg, Å., Jönsson, G., Ringnér, M. (2016) An integrated genomics analysis of epigenetic subtypes in human breast tumors links DNA methylation patterns to chromatin states in normal mammary cells. *Breast Cancer Research*. 18, 27.

Holmberg, K., Meijer, A.E., Harms-Ringdahl, M., Lambert, B. (1998) Chromosomal instability in human lymphocytes after low dose rate gamma-irradiation and delayed mitogen stimulation. *International Journal of Radiation Biology*. 73(1), 21–34.

Hughes, J.S., Watson, S.J., Jones, A.L., Oatway, W.B. (2005) Review of the radiation exposure of the UK population. *Journal of Radiological Protection: Official Journal of the Society for Radiological Protection*. 25(4), 493–496.

ICRP (2007) The 2007 Recommendations of the International Commission on Radiological Protection. ICRP publication 103. *Annals of the ICRP*. 37(2-4), 1–332.

Iyer, R., Lehnert, B.E., Svensson, R. (2000) Factors underlying the cell growth-related bystander responses to alpha particles. *Cancer Research*. 60(5), 1290–1298.

Jaiswal, M., LaRusso, N.F., Burgart, L.J., Gores, G.J. (2000) Inflammatory cytokines induce DNA damage and inhibit DNA repair in cholangiocarcinoma cells by a nitric oxide-dependent mechanism. *Cancer Research*. 60(1), 184–190.

Jella, K.K., Rani, S., O'Driscoll, L., McClean, B., Byrne, H.J., Lyng, F.M. (2014) Exosomes are involved in mediating radiation induced bystander signaling in human keratinocyte cells. *Radiation Research*. 181(2), 138–145.

Joo, H.M., Nam, S.Y., Yang, K.H., Kim, C.S., Jin, Y.W., Kim, J.Y. (2012) The effects of low-dose ionizing radiation in the activated rat basophilic leukemia (RBL-2H3) mast cells. *The Journal of Biological Chemistry*. 287(33), 27789–27795.

Kadhim, M.A. (2003) Role of genetic background in induced instability. *Oncogene*. 22(45), 6994–6999.

Kadhim, M. A., Macdonald, D.A., Goodhead, D.T., Lorimore, S.A., Marsden, S.J., Wright, E.G. (1992) Transmission of chromosomal instability after plutonium alpha-particle irradiation. *Nature*. 355(6362), 738–740.

Kadhim, M.A., Lorimore, S.A., Hepburn, M.D., Goodhead, D.T., Buckle, V.J., Wright, E.G. (1994) Alpha-particle-induced chromosomal instability in human bone marrow cells. *Lancet*. 344(8928), 987–8.

Kadhim, M., Marsden, S., Wright, E. (1998) Radiation-induced chromosomal instability in human fibroblasts: temporal effects and influence of radiation quality. *Int. J. Radiat. Biol.*73, 143–148.

Kadhim, M.A., Wright, E.G. (1998) Radiation-induced transmissable chromosomal instability in haemopoietic stem cells. *Advances in space research: the official journal of the Committee on Space Research (COSPAR)*. 22(4), 587–596.

Kadhim, M.A., Marsden, S.J., Goodhead, D.T., Malcolmson, A.M., Folkard, M., Prise, K.M., Michael, B.D. (2001) Long-term genomic instability in human lymphocytes induced by single-particle irradiation. *Radiation Research*. 155(1 Pt 1), 122–126.

Kadhim, M.A., Hill, M.A., Moore, S.R. (2006) Genomic instability and the role of radiation quality. *Radiation Protection Dosimetry*. 122(1-4), 221–227.

Kadhim, M., Salomaa, S., Wright, E., Hildebrandt, G., Belyakov, O., Prise, K., Little, M. (2013) Non-targeted effects of ionising radiation-Implications for low dose risk. *Mutation Research*. 752(2), 84–98.

Kadhim, M.A., Hill, M.A. (2015) Non-targeted effects of radiation exposure: recent advances and implications. *Radiation Protection Dosimetry*. 166(1-4), 118–124.

Karaman, A., Binici, D.N., Kabalar, M.E., Çalıkuşu, Z. (2008) Micronucleus analysis in patients with colorectal adenocarcinoma and colorectal polyps. *World Journal of Gastroenterology: WJG*. 14(44), 6835–6839.

Kashino, G., Prise, K.M., Suzuki, K., Matsuda, N., Kodama, S., Suzuki, M., Nagata, K., Kinashi, Y., Masunaga, S., Ono, K., Watanabe, M. (2007) Effective suppression of bystander effects by DMSO treatment of irradiated CHO cells. *Radiat. Res*. 48, 327– 333.

Kastan, M.B., Onyekwere, O., Sidransky, D., Vogelstein, B., Craig, R.W. (1991) Participation of p53 protein in the cellular response to DNA damage. *Cancer Research*. 51(23 Pt 1), 6304–6311.

Kaup, S., Grandjean, V., Mukherjee, R., Kapoor, A., Keyes, E., Seymour, C.B., Mothersill, C.E., Schofield, P.N. (2006) Radiation-induced genomic instability is associated with DNA methylation changes in cultured human keratinocytes. *Mutation Research/Fundamental and Molecular Mechanisms of Mutagenesis*. 597(1–2), 87–97.

Kennedy, C.H., Mitchell, C.E., Fukushima, N.H., Neft, R.E., Lechner, J.F. (1996) Induction of genomic instability in normal human bronchial epithelial cells by 238Pu alpha-particles. *Carcinogenesis*. 17(8), 1671–1676.

Koturbash, I., Baker, M., Loree, J., Kutanzi, K., Hudson, D., Pogribny, I., Sedelnikova, O., Bonner, W., Kovalchuk, O. (2006) Epigenetic dysregulation underlies radiation-induced transgenerational genome instability in vivo. *International Journal of Radiation Oncology, Biology, Physics*. 66(2), 327–330.

Koukourakis, M.I. (2012) Radiation damage and radioprotectants: new concepts in the era of molecular medicine. *The British Journal of Radiology*. 85(1012), 313–330.

Kovalchuk, O., Burke, P., Besplug, J., Slovack, M., Filkowski, J., Pogribny, I. (2004) Methylation changes in muscle and liver tissues of male and female mice exposed to acute and chronic low-dose X-ray-irradiation. *Mutation Research*. 548(1-2), 75–84.

Kovalchuk, O., Baulch, J.E. (2008) Epigenetic changes and nontargeted radiation effects- is there a link? *Environmental and Molecular Mutagenesis*. 49(1), 16–25.

Krstić, J., Trivanović, D., Mojsilović, S., Santibanez, J.F. (2015) Transforming Growth Factor-Beta and Oxidative Stress Interplay: Implications in Tumorigenesis and Cancer Progression. *Oxidative Medicine and Cellular Longevity*. (2015):654594. doi: 10.1155/2015/654594.

Kuerbitz, S.J., Plunkett, B.S., Walsh, W.V., Kastan, M.B. (1992) Wild-type p53 is a cell cycle checkpoint determinant following irradiation. *Proceedings of the National Academy of Sciences of the United States of America*. 89(16), 7491–7495.

.Lam, R.K.K., Fung, Y.K., Han, W., Yu, K.N. (2015) Rescue Effects: Irradiated Cells Helped by Unirradiated Bystander Cells. *International Journal of Molecular Sciences*. 16(2), 2591

Laurent, C., Leduc, A., Pottier, I., Prévost, V., Sichel, F., Lefaix, J.-L. (2013) Dramatic increase in oxidative stress in carbon-irradiated normal human skin fibroblasts. *PloS One*. 8(12), e85158.

Lehnert, B.E., Goodwin, E.H., Deshpande, A. (1997) Extracellular factor(s) following exposure to alpha particles can cause sister chromatid exchanges in normal human cells. *Cancer Res.* 57, 2164–2171.

Lehnert, B.E., Iyer, R. (2002) Exposure to low-level chemicals and ionizing radiation: reactive oxygen species and cellular pathways. *Human and Experimental Toxicology*. 21, 65–69.

Liao, W., McNutt, M.A., Zhu, W.-G. (2009) The comet assay: a sensitive method for detecting DNA damage in individual cells. Methods (San Diego, Calif.). 48(1), 46–53.

Limoli, C.L., Kaplan, M.I., Phillips, J.W., Adair, G.M., Morgan, W.F. (1997) Differential Induction of Chromosomal Instability by DNA Strand-breaking Agents. *Cancer Research*. 57(18), 4048–4056.

Limoli, C.L., Giedzinski, E. (2003) Induction of Chromosomal Instability by Chronic Oxidative Stress. *Neoplasia (New York, N.Y.)*. 5(4), 339–346.

Limoli, C.L., Giedzinski, E., Morgan, W.F., Swarts, S.G., Jones, G.D.D., Hyun, W. (2003) Persistent oxidative stress in chromosomally unstable cells. *Cancer Research*. 63(12), 3107–3111.

Lin, Y.-F., Nagasawa, H., Little, J.B., Kato, T.A., Shih, H.-Y., Xie, X.-J., Wilson, P.F., Brogan, J.R., Kurimasa, A., Chen, D.J., Bedford, J.S., Chen, B.P.C. (2014) Differential radiosensitivity phenotypes of DNA-PKcs mutations affecting NHEJ and HRR systems following irradiation with gamma-rays or very low fluences of alpha particles. *PloS One*. 9(4), e93579.

Lindahl, T. (1993) Instability and decay of the primary structure of DNA. *Nature*. 362(6422), 709–715.

Little, J.B. (2000) Radiation carcinogenesis. *Carcinogenesis*. 21, 397–404. Little, J.B. (2003) Genomic instability and radiation. *J Radiol Prot.* . 23(2).

Little, M.P., Wakeford, R., Tawn, E.J., Bouffler, S.D., Berrington de Gonzalez, A. (2009) Risks Associated with Low Doses and Low Dose Rates of Ionizing Radiation: Why Linearity May Be (Almost) the Best We Can Do. *Radiology*. 251(1), 6–12.

Liu, Y.-C., Ma, W.-H., Ge, Y.-L., Xue, M.-L., Zhang, Z., Zhang, J.-Y., Hou, L., Mu, R.(2016) RNAi-mediated gene silencing of vascular endothelial growth factor C suppresses growth and induces apoptosis in mouse breast cancer in vitro and in vivo. *Oncology Letters*. 12(5), 3896–3904.

Lorimore, S.A., Kadhim, M.A., Pocock, D.A., Papworth, D., Stevens, D.L., Goodhead, D.T., Wright, E.G. (1998) Chromosomal instability in the descendants of unirradiated surviving cells after alpha-particle irradiation. *Proc Natl Acad Sci U S A*. 95, 5730–3.

Lorimore, S.A., Coates, P.J., Wright, E.G. (2003) Radiation-induced genomic instability and bystander effects: inter-related nontargeted effects of exposure to ionizing radiation. *Oncogene*. 22, 7058–69.

Lorimore, S.A., Chrystal, J.A., Robinson, J.I., Coates, P.J., Wright, E.G. (2008) Chromosomal instability in unirradiated hemaopoietic cells induced by macrophages exposed in vivo to ionizing radiation. *Cancer Research*. 68(19), 8122–8126.

Lorimore, S.A., Mukherjee, D., Robinson, J.I., Chrystal, J.A., Wright, E.G. (2011) Long-lived Inflammatory Signaling in Irradiated Bone Marrow Is Genome Dependent. *Cancer Research*. 71(20), 6485–6491.

Luzhna, L., Kathiria, P., Kovalchuk, O. (2013) Micronuclei in genotoxicity assessment: from genetics to epigenetics and beyond. *Frontiers in Genetics*. 4. Doi: 10.3389/fgene.2013.00131.

Lyng, F.M., Seymour, C.B., Mothersill, C. (2000) Production of a signal by irradiated cells which leads to a response in unirradiated cells characteristic of initiation of apoptosis. *Br. J. Cancer*. 83, 1223–1230.

Lyng, F.M., Howe, O.L., McClean, B. (2011) Reactive oxygen species-induced release of signalling factors in irradiated cells triggers membrane signalling and calcium influx in bystander cells. *International Journal of Radiation Biology*. 87(7), 683–695.

Lyulko, O.V., Garty, G., Randers-Pehrson, G., Turner, H.C., Szolc, B., Brenner, D.J. (2014) Fast Image Analysis for the Micronucleus Assay in a Fully Automated High-Throughput Biodosimetry System. *Radiation research*. 181(2), 146–161.

Maierhofer, A., Flunkert, J., Dittrich, M., Müller, T., Schindler, D., Nanda, I., Haaf, T. (2017) Analysis of global DNA methylation changes in primary human fibroblasts inthe early phase following X-ray irradiation. *PLOS ONE*. 12(5), e0177442.

Marín, A., Martín, M., Liñán, O., Alvarenga, F., López, M., Fernández, L., Büchser, D., Cerezo, L. (2014) Bystander effects and radiotherapy. *Reports of Practical Oncology and Radiotherapy*. 20(1), 12–21.

Mauro, M., Caradonna, F., Klein, C.B. (2016) Dysregulation of DNA methylation induced by past arsenic treatment causes persistent genomic instability in mammalian cells. *Environmental and Molecular Mutagenesis*. 57(2), 137–150.

McConnell, A.M., Konda, B., Kirsch, D.G., Stripp, B.R. (2016) Distal airway epithelial progenitor cells are radiosensitive to High-LET radiation. *Scientific Reports*. 6. DOI: 10.1038/srep33455

Meng, H., Cao, Y., Qin, J., Song, X., Zhang, Q., Shi, Y., Cao, L. (2015) DNA

Methylation, Its Mediators and Genome Integrity. *International Journal of Biological Sciences*. 11(5), 604–617.

Miller, A.C., Brooks, K., Stewart, M., Anderson, B., Shi, L., McClain, D., Page, N. (2003) Genomic instability in human osteoblast cells after exposure to depleted uranium: delayed lethality and micronuclei formation. *Journal of Environmental Radioactivity*. 64(2-3), 247–259.

Millipore (2013) MuseTM Cell Cycle Kit User‘s Guide. Available at: ’http: //www.icms.qmul.ac.uk/flowcytometry/uses/musekits/protocols/MCH1001064600-3387MAN [B] MUSE CELL CYCLE KIT USER’S GUIDE.pdf". (Accessed: 25th April 2016).

Milner, J., Shrubsole, C., Das, P., Jones, B., Ridley, I., Chalabi, Z., Hamilton, I., Armstrong, B., Davies, M., Wilkinson, P. (2014) Home energy efficiency and radon related risk of lung cancer: modelling study. *BMJ (Clinical research ed.)*. 348, f7493.

Moore, S.R., Marsden, S., Macdonald, D., Mitchell, S., Folkard, M., Michael, B., Goodhead, D.T., Prise, K.M., Kadhim, M.A. (2005) Genomic instability in human lymphocytes irradiated with individual charged particles: involvement of tumor necrosis factor alpha in irradiated cells but not bystander cells. *Radiation research*. 163(2), 183–190.

Morgan, W.F., Day, J.P., Kaplan, M.I., McGhee, E.M. (1996) Genomic instability induced by ionizing radiation. *Radiation research*. 146, 247–258.

Morgan, W.F. (2003) Non-targeted and delayed effects of exposure to ionizing radiation: Radiation-induced genomic instability and bystander effects in vitro. *Radiation Research*. 159(5), 567–580.

Morgan, W.F. (2012) Non-targeted and Delayed Effects of Exposure to Ionizing Radiation: I. Radiation-Induced Genomic Instability and Bystander Effects In Vitro. *Radiation Research*. 178, AV223–AV236.

Mothersill, C., Seymour, C. (1997) Medium from irradiated human epithelial cells but not human fibroblasts reduces the clonogenic survival of unirradiated cells. *Radiat. Biol.* 71, 421–427.

Mothersill, C., Seymour, C.B. (1998) Cell-cell contact during gamma irradiation is not required to induce a bystander effect in normal human keratinocytes: evidence for release during irradiation of a signal controlling survival into the medium. *Radiat. Res.* 149, 256–262.

Mukherjee, D., Coates, P.J., Rastogi, S., Lorimore, S.A., Wright, E.G. (2013) Radiation-induced bone marrow apoptosis, inflammatory bystander-type signaling and tissue cytotoxicity. *International Journal of Radiation Biology*. 89(3), 139–146.

Nagasawa, H., Little, J.B. (1992) Induction of sister chromatid exchanges by extremely low doses of alpha-particles. *Cancer Research*. 52(22), 6394–6396.

Nagasawa, H., Little, J.B. (1999) Unexpected sensitivity to the induction of mutations by very low doses of alpha-particle radiation: evidence for a bystander effect. *Radiation Research*. 152(5), 552–557.

Nais, A.H.W. (1998) *An Introduction to Radiobiology*. 2nd edition. Chichester: Wiley.

Nakajima, T., Wang, B., Ono, T., Uehara, Y., Nakamura, S., Ichinohe, K., Braga-Tanaka, I., Tanaka, S., Tanaka, K., Nenoi, M. (2017) Differences in sustained alterations in protein expression between livers of mice exposed to high-dose-rate and low-dose-rate radiation. *Journal of Radiation Research*. 1;58(4) 1–9.

Narayanan, P.K., Goodwin, E.H., Lehnert, B.E. (1997) Alpha particles initiate biological production of superoxide anions and hydrogen peroxide in human cells. *Cancer Research*. 57(18), 3963–3971.

Natarajan, M., Gibbons, C.F., Mohan, S., Moore, S., Kadhim, M.A. (2007) Oxidative stress signalling: a potential mediator of tumour necrosis factor alpha-induced genomic instability in primary vascular endothelial cells. *The British Journal of Radiology*. 80, 13–22.

Nikjoo, H., O'Neill, P., Terrissol, M., Goodhead, D.T. (1994) Modelling of radiation-induced DNA damage: the early physical and chemical event. *Int J Radiat Biol*. 66(5), 453–7.

Niwa, O., Barcellos-Hoff, M.H., Globus, R.K., Harrison, J.D., Hendry, J.H., Jacob, P., Martin, M.T., Seed, T.M., Shay, J.W., Story, M.D., Suzuki, K., Yamashita, S., ICRP (2015) ICRP Publication 131: Stem Cell Biology with Respect to Carcinogenesis Aspects of Radiological Protection. *Annals of the ICRP*. 44(3-4), 7–357.

O'Donovan, P.J., Livingston, D.M. (2010) BRCA1 and BRCA2: breast/ovarian cancer susceptibility gene products and participants in DNA double-strand break repair. *Carcinogenesis*. 31(6), 961–967.

Olive, P.L., Banath, J.P. (2006) The comet assay: a method to measure DNA damage in individual cells : Article : Nature Protocols. *Nat. Protocols*. 1(1), 23–29.

Olive, P.L. (2009) Impact of the comet assay in radiobiology. *Mutation Research*. 681(1), 13–23.

Petkau, A. (1987) Role of superoxide dismutase in modification of radiation injury. *The British Journal of Cancer. Supplement*. 8, 87–95.

Pham-Huy, L.A., He, H., Pham-Huy, C. (2008) Free Radicals, Antioxidants in Disease and Health. *International Journal of Biomedical Science: IJBS*. 4(2), 89–96.

Pichierri, P., Franchitto, A., Palitti, F. (2000) Predisposition to cancer and radiosensitivity. *Genetics and Molecular Biology*. 23(4), 1101–1105.

Pollycove, M., Feinendegen, L.E. (2001) Biologic responses to low doses of ionizing radiation: Detriment versus hormesis. Part 2. Dose responses of organisms. *Journal of Nuclear Medicine: Official Publication, Society of Nuclear Medicine*. 42(9), 26N–32N, 37N.

Ponnaiya, B., Cornforth, M.N., Ullrich, R.L. (1997) Radiation-induced chromosomal instability in BALB/c and C57BL/6 mice: the difference is as clear as black and white. *Radiation Research*. 147(2), 121–125.

Portess, D.I., Bauer, G., Hill, M.A., O'Neill, P. (2007) Low-dose irradiation of nontransformed cells stimulates the selective removal of precancerous cells via intercellular induction of apoptosis. *Cancer Research*. 67(3), 1246–1253.

Qiao, Y., Zhang, P., Wang, C., Ma, L., Su, M. (2014) Reducing X-Ray Induced Oxidative Damages in Fibroblasts with Graphene Oxide. *Nanomaterials*. 4(2), 522–534.

Ragu, S., Faye, G., Iraqui, I., Masurel-Heneman, A., Kolodner, R.D., Huang, M.-E. (2007) Oxygen metabolism and reactive oxygen species cause chromosomal rearrangements and cell death. Proceedings of the National Academy of Sciences of the United States of America. 104(23), 9747–9752.

Roots, R., Okada, S. (1975) Estimation of life times and diffusion distances of radicals involved in x-ray-induced DNA strand breaks of killing of mammalian cells. *Radiation Research*. 64(2), 306–320.

Rössler, U., Hornhardt, S., Seidl, C., Müller-Laue, E., Walsh, L., Panzer, W., Schmid, E., Senekowitsch-Schmidtke, R., Gomolka, M. (2006) The sensitivity of the alkaline comet assay in detecting DNA lesions induced by X rays, gamma rays and alpha particles. Radiation Protection Dosimetry. 122(1-4), 154–159.

Rugo, R.E., Secretan, M.B., Schiestl, R.H. (2002) X Radiation Causes a Persistent Induction of Reactive Oxygen Species and a Delayed Reinduction of TP53 in Normal Human Diploid Fibroblasts. *Radiation Research*. 158(2), 210–219.

Rühm, W., Woloschak, G.E., Shore, R.E., Azizova, T.V., Grosche, B., Niwa, O., Akiba, S., Ono, T., Suzuki, K., Iwasaki, T., Ban, N., Kai, M., Clement, C.H., Bouffler, S., Toma, H., Hamada, N. (2015) Dose and dose-rate effects of ionizing radiation: a discussion in the light of radiological protection. *Radiation and Environmental Biophysics*. 54(4), 379–401.

Ruiz de Almodóvar, J.M., Bush, C., Peacock, J.H., Steel, G.G., Whitaker, S.J., McMillan, T.J. (1994) Dose-rate effect for DNA damage induced by ionizing radiation in human tumor cells. *Radiation Research*. 138(1 Suppl), S93–96.

Salkind, N.J. (2010) *Statistics for people who (think they) hate statistics Statistics for People Who (Think They) Hate Statistics.* 3rd ed. London: SAGE Publications Ltd.

Sallmyr, A., Fan, J., Rassool, F.V. (2008) Genomic instability in myeloid malignancies: increased reactive oxygen species (ROS), DNA double strand breaks (DSBs) and error-prone repair. *Cancer Letters*. 270(1), 1–9.

Salomaa, S., Holmberg, K., Lindholm, C., Mustonen, R., Tekkel, M., Veidebaum, T., Lambert, B. (1998) Chromosomal instability in in vivo radiation exposed subjects. *International Journal of Radiation Biology*. 74(6), 771–779.

Sartor, O., Maalouf, B.N., Hauck, C.R., Macklis, R.M. (2012) Targeted use of Alpha Particles: Current Status in Cancer Therapeutics. *Journal of Nuclear Medicine & Radiation Therapy*. 3(4). Doi:10.4172/2155-9619.1000136

Savage, J.R.K. (2002) Reflections and meditations upon complex chromosomal exchanges. *Mutation Research*. 512(2-3), 93–109.

Sawant, S., Zheng, W., Hopkins, K., Randers-Pehrson, G., Lieberman, H., Hall, E. (2002) The radiation-induced bystander effect for clonogenic survival. *Radiat Res*. 157, 361–64.

Scully, R., Xie, A. (2013) Double strand break repair functions of histone H2AX. *Mutation Research*. 750(1-2), 5–14.

Seth, I., Schwartz, J.L., Stewart, R.D., Emery, R., Joiner, M.C., Tucker, J.D. (2014) Neutron exposures in human cells: bystander effect and relative biological effectiveness. *PloS One*. 9(6), e98947.

Shao, C., Lyng, F.M., Folkard, M., Prise, K.M. (2006) Calcium fluxes modulate the radiationinduced bystander responses in targeted glioma and fibroblast cells. *Radiat. Res*. 166, 479–487.

Shen, H., Tsoli, M., Chang, C., Chitranjan, A., Liu, J., Hau, E., Kankean, A., Ehteda, A., Franshaw, L., Valvi, S., Ziegler, D. (2016) Hg-04dichloroacetate and metformin combine to modulate glucose metabolism and potently sensitise dipg cells to radiation therapy. *Neuro-Oncology*. 18(Suppl 3), iii48.

Shikazono, N., Noguchi, M., Fujii, K., Urushibara, A., Yokoya, A. (2009) The yield, processing, and biological consequences of clustered DNA damage induced by ionizing radiation. Journal of Radiation Research. 50(1), 27–36.

Shimura, T., Sasatani, M., Kamiya, K., Kawai, H., Inaba, Y., Kunugita, N. (2016) Mitochondrial reactive oxygen species perturb AKT/cyclin D1 cell cycle signaling via oxidative inactivation of PP2A in lowdose irradiated human fibroblasts. *Oncotarget*. 7(3), 3559–3570.

Shiraishi, Y., Minowada, J., Sandberg, A.A. (1976) Differential Sensitivity to X-Ray of Chromosomes of Blood T-Lymphocytes and B- and T-Cell Lines. *In Vitro*. 12(7), 495–509.

Shirsath, K., Bhat, N., Anjaria, K., Desai, U., Balakrishnan, S. (2014) Cytokinesis blocked micron ucleus (CB-MN) assay for biodosimetry of high dose accidental exposure. *Interrnational Journal of Radiation Research*. 12(3), 211–215.

Shrivastava, V., Mishra, A.K., Dwarakanath, B.S., Ravindranath, T. (2006) Enhancement of radionuclide induced cytotoxicity by 2-deoxy-D-glucose in human tumor cell lines. *Journal of Cancer Research and Therapeutics*. 2(2), 57–64.

Shuryak, I. (2016) Mechanistic Modeling of Dose and Dose Rate Dependences of Radiation-Induced DNA Double Strand Break Rejoining Kinetics in Saccharomyces cerevisiae. *PLoS ONE*. 11(1). Doi: 10.1371/journal.pone.0146407

Smith, L.E., Nagar, S., Kim, G.J., Morgan, W.F. (2003) Radiation-induced genomic instability: radiation quality and dose response. *Health Physics*. 85(1), 23–29.

Stadtman, E.R. (1993) Oxidation of free amino acids and amino acid residues inproteins by radiolysis and by metal-catalyzed reactions. *Annual Review of Biochemistry*. 62, 797–821.

Strauss, H.W., Mariani, G., Volterrani, D., Larson, S.M. eds. (2012) *Nuclear Oncology: Pathophysiology and Clinical Applications*. 2012 edition. New York: Springer.

Streffer, C. (2000) Genomic Instability Induced by Ionizing Radiation. In the 10th international radiation protection association. Universitaetsklinikum, Essen Germany, pp. 1–5. Available at: http://www.irpa.net/irpa10/cdrom/01314.pdf (Accessed: 23/09/2017)

Suman, S., Kumar, S., Moon, B.-H., Fornace, A.J., Kallakury, B.V.S., Datta, K. (2017) Increased Transgenerational Intestinal Tumorigenesis in Offspring of Ionizing Radiation Exposed Parent APC1638N/+ Mice. *Journal of Cancer*. 8(10), 1769–1773.

Sumption, N., Goodhead, D.T., Anderson, R.M. (2015) Alpha-Particle-Induced Complex Chromosome Exchanges Transmitted through Extra-Thymic Lymphopoiesis In Vitro Show Evidence of Emerging Genomic Instability. *PloS One*. 10(8), e0134046.

Tanaka, K., Kohda, A., Toyokawa, T., Ichinohe, K., Oghiso, Y. (2008) Chromosome aberration frequencies and chromosome instability in mice after long-term exposure to low-dose-rate gamma-irradiation. *Mutation Research*. 657(1), 19–25.

Tang, B., Vu, M., Booker, T., Santner, S.J., Miller, F.R., Anver, M.R., Wakefield, L.M. (2003) TGF-β switches from tumor suppressor to prometastatic factor in a model of breast cancer progression. *Journal of Clinical Investigation*. 112(7), 1116–1124.

Tang, F.R., Loke, W.K. (2015) Molecular mechanisms of low dose ionizing radiation-induced hormesis, adaptive responses, radioresistance, bystander effects, and genomic instability. *International Journal of Radiation Biology*. 91(1), 13–27.

Tang, F.R., Loke, W.K., Khoo, B.C. (2017) Low-dose or low-dose-rate ionizing radiation–induced bioeffects in animal models. *Journal of Radiation Research*. 58(2), 165–182.

Thomas, P., Umegaki, K., Fenech, M. (2003) Nucleoplasmic bridges are a sensitive measure of chromosome rearrangement in the cytokinesis-block micronucleus assay. *Mutagenesis*. 18(2), 187–194.

De Toledo, S.M., Buonanno, M., Harris, A.L., Azzam, E.I. (2017) Genomic instability induced in distant progeny of bystander cells depends on the connexins expressed in the irradiated cells. *International Journal of Radiation Biology*, (Jun 15),1–13. Doi: 10.1080/09553002.2017

Trott, K.R., Jamali, M., Manti, L., Teibe, A. (1998) Manifestations and mechanisms of radiation-induced genomic instability in V-79 Chinese hamster cells. *International Journal of Radiation Biology*. 74(6), 787–791.

Trzeciak, A.R., Barnes, J., Evans, M.K. (2008) A Modified Alkaline Comet Assay for Measuring DNA Repair Capacity in Human Populations. *Radiation research*. 169(1), 110–121.

Tse, B.W.C., Scott, K.F., Russell, P.J. (2012) Paradoxical Roles of Tumour Necrosis Factor-Alpha in Prostate Cancer Biology. *Prostate Cancer*. 2012, e128965.

Tseng, B.P., Lan, M.L., Tran, K.K., Acharya, M.M., Giedzinski, E., Limoli, C.L. (2013) Characterizing low dose and dose rate effects in rodent and human neural stem cells exposed to proton and gamma irradiation. *Redox Biology*. 1(1), 153–162.

Turner, H.C., Shuryak, I., Taveras, M., Bertucci, A., Perrier, J.R., Chen, C., Elliston, C.D., Johnson, G.W., Smilenov, L.B., Amundson, S.A., Brenner, D.J. (2015) Effect of dose rate on residual γ-H2AX levels and frequency of micronuclei in X-irradiated mouse lymphocytes. *Radiation Research*. 183(3), 315–324.

UNSCEAR (1986) *Genetic and Somatic Effects of Ionizing Radiation: 1986 Report to the General Assembly, with Annexes*. New York: United Nations.

Usman, M., Tewfik, I., Volpi, E. (2017) Genome instability in childhood obesity: A conceptual framework for an assessment, intervention and monitoring programme of inflammation and DNA damage in paediatric obesity. *International Journal of Food, Nutrition and Public Health*. 9(1), 1–12.

Vaiserman, A.M. (2010) Radiation Hormesis: Historical Perspective and Implications for Low-Dose Cancer Risk Assessment. *Dose-Response*. 8(2), 172–191.

Vral, A., Fenech, M., Thierens, H. (2011) The micronucleus assay as a biological dosimeter of in vivo ionising radiation exposure. *Mutagenesis*. 26(1), 11–17.

Ward, J. (1999) New paradigms for low-dose radiation response. In Proceedings of the American Statistical Association Conference on Radiation and Health. *Radiat Res.* 151, 92–117.

Ward, J. (2002) The radiation-induced lesions which trigger the bystander effect. *Mutat Res Fundam Mol Mech Mutag*. 499, 151–54.

Watson, G.E., Lorimore, S.A., Clutton, S.M., Kadhim, M.A., Wright, E.G. (1997) Genetic factors influencing alpha-particle-induced chromosomal instability. *International Journal of Radiation Biology*. 71(5), 497–503.

Watson, G., Lorimore, S., Macdonald, D., Wright, E. (2000) Chromosomal instability in unirradiated cells induced in vivo by a bystander effect of ionizing radiation. *Cancer Res.* 60(20), 5608–11.

Watson, G.E., Pocock, D.A., Papworth, D., Lorimore, S.A., Wright, E.G. (2001) In vivo chromosomal instability and transmissible aberrations in the progeny of haemopoietic stem cells induced by high- and low-LET radiations. *International Journal of Radiation Biology*. 77(4), 409–417.

Wei, S., Eksioglu, E.A., Chen, X., Cluzeau, T., Basiorka, A., Burnette, A., Wei, M., McGraw, K.L., Padron, E., List, A.F. (2015) Inflammaging-Associated Metabolic Alterations Foster Development of the MDS Genotype. *Blood*. 126(23), 144–144.

Werner, E., Wang, H., Doetsch, P.W. (2014) Opposite roles for p38MAPK-driven responses and reactive oxygen species in the persistence and resolution of radiation-induced genomic instability. *PloS One*. 9(10), e108234.

Werner, E., Wang, Y., Doetsch, P.W. (2017) A Single Exposure to Low- or High-LET Radiation Induces Persistent Genomic Damage in Mouse Epithelial Cells In Vitro and in Lung Tissue. *Radiation Research*. Doi: 10.1667/RR14685.1

Widel, M. (2016) Radiation Induced Bystander Effect: From in Vitro Studies to Clinical Application. *International Journal of Medical Physics, Clinical Engineering and Radiation Oncology*. 05(01), 1.

Widel, M. (2017) Radionuclides in radiation-induced bystander effect; may it share in radionuclide therapy? *Neoplasma*. 64(5):641-654

Wilkins, R.C., Ng, C.E., Raaphorst, G.P. (1998) Comparison of high dose rate, low dose rate, and high dose rate fractionated radiation for optimizing differences in radiosensitivities in vitro. *Radiation Oncology Investigations*. 6(5), 209–215.

Wilkins, R.C., Rodrigues, M.A., Beaton-Green, L.A. (2017) The Application ofImaging Flow Cytometry to High-Throughput Biodosimetry. *Genome Integrity*. 8, 7.

Wiseman, H., Halliwell, B. (1996) Damage to DNA by reactive oxygen and nitrogen species: role in inflammatory disease and progression to cancer. *The Biochemical Journal*. 313 ( Pt 1), 17–29.

Wolff, H.A., Hennies, S., Herrmann, M.K.A., Rave-Fränk, M., Eickelmann, D., Virsik, P., Jung, K., Schirmer, M., Ghadimi, M., Hess, C.F., Hermann, R.M., Christiansen, H. (2011) Comparison of the micronucleus and chromosome aberration techniques for the documentation of cytogenetic damage in radiochemotherapy-treated patients with rectal cancer. *Strahlentherapie Und Onkologie: Organ Der Deutschen Röntgengesellschaft ... [et Al]*. 187(1), 52–58.

Wong, T.P.W., Law, Y.L., Tse, A.K.W., Fong, W.F., Yu, K.N. (2010) Influence of Magnolol on the bystander effect induced by alpha-particle irradiation. Applied Radiation and Isotopes: Including Data, Instrumentation and Methods for Use in Agriculture, Industry and Medicine. 68(4-5), 718–721.

Wright, E.G. (1998) Radiation-induced genomic instabilityin haemopoietic cells. *Radiat Biol*. 74, 681–687.

Wuttke, K., Müller, W.-U., Streffer, C. (1998) The sensitivity of the in vitrocytokinesis-blocked micronucleus assay in lymphocytes for different and combined radiation qualities. *Strahlentherapie und Onkologie*. 174(5), 262–268.

Yang, Y., Ma, H. (2009) Western Blotting and ELISA Techniques. *Researcher.*

2009;1(2):67-86

Yoshikawa, T., Naito, Y. (2002) What Is Oxidative Stress? *JMAJ* .45(7): 271–276, 2002

Zeman, E.M. (2017) Review of Jennifer Yu and Mohamed Abazeed: Radiobiology Self-Assessment Guide. *International Journal of Radiation Biology*. 93((7)), 1–2.

Zhang, Y., Zhou, J., Baldwin, J., Held, K.D., Prise, K.M., Redmond, R.W., Liber, H.L. (2009) Ionizing radiation-induced bystander mutagenesis and adaptation: Quantitative and temporal aspects. *Mutation research*. 671(1-2), 20–25.

Zhang, J., He, Y., Shen, X., Jiang, D., Wang, Q., Liu, Q., Fang, W. (2016) γ-H2AX responds to DNA damage induced by long-term exposure to combined low-dose-rate neutron and γ-ray radiation. *Mutation Research. Genetic Toxicology and Environmental Mutagenesis*. 795, 36–40.

Zhao, Y., de Toledo, S.M., Hu, G., Hei, T.K., Azzam, E.I. (2014) Connexins and cyclooxygenase-2 crosstalk in the expression of radiation-induced bystander effects. *British Journal of Cancer*. 111(1), 125–131.

Zhou, H., Ivanov, V.N., Gillespie, J., Geard, C.R., Amundson, S.A., Brenner, D.J., Yu, Z., Lieberman, H.B., Hei, T.K. (2005) Mechanism of radiation-induced bystandereffect: role of the cyclooxygenase-2 signaling pathway. *Proceedings of the National Academy of Sciences of the United States of America*. 102(41), 14641–14646.

# Presentations and posters

2017. Presentation to department of Biological and Medical Sciences at Oxford Brookes University: Radiation-induced chromosome instability and intercellular communication: the role of dose rate and implications for carcinogenesis.

2016. Poster presentation to Association for Radiation Research meeting, University of Leicester: Radiation-induced chromosome instability: the role of dose and dose rate.

2015. Poster presentation to the annual Postgraduate Research Student Symposium at Oxford Brookes University: Chromosomal instability in α-particle irradiated normal human lung fibroblasts.

2014. Presentation to the annual Postgraduate Research Student Symposium at Oxford Brookes University: Radiation-induced chromosome instability and intercellular communication: the role of dose rate and implications for carcinogenesis.